DYNAMIC COMBINATORIAL CHEMISTRY OF ESTERS AND BENZOINS: DISTILLATIVE SELF-SORTING AND MACROCYCLIZATION

A Dissertation Presented to

the Faculty of the Department of Chemistry

University of Houston

In Partial Fulfillment

of the Requirement for the Degree

Doctor of Philosophy

By

Qing Ji

August 2015

DYNAMIC COMBINATORIAL CHEMISTRY OF ESTERS AND BENZOINS:

DISTILLATIVE SELF-SORTING AND MACROCYCLIZATION

_____

Qing Ji

APPROVED:

_____

Dr. Ognjen Š. Miljanić, Chairman

_____

Dr. Olafs Daugulis

_____

Dr. Jeremy May

_____

Dr. David Hoffman

_____

Dr. Gila Stein

_____

Dean, College of Natural Sciences and Mathematics

DYNAMIC COMBINATORIAL CHEMISTRY OF ESTERS AND BENZOINS:

DISTILLATIVE SELF-SORTING AND MACROCYCLIZATION

An Abstract of a Dissertation Presented to

the Faculty of the Department of Chemistry

University of Houston

In Partial Fulfillment

of the Requirement for the Degree

Doctor of Philosophy

By

Qing Ji

August 2015

ACKNOWLEDGEMENT

The PhD program from UH chemistry department adds an unique experience to my life after my five years' study in organic chemistry. The very first person I want to mention is Professor Ognjen Miljanić. It was my exceptional pleasure to be accepted in and study in Professor Ognjen Miljanić's laboratory for five years, from where I was taught how to appraoch and solve scientific problems systematically and where I was encouraged to create new chemistry ideas under large extent of freedom. He supported me generously to attend domestic and international chemistry conferences in New Orleans, Dallas, Shanghai, and San Francisco from where I obtained my opportunities to learn cutting-edge chemistries and to obtain industrial interviews. I enjoyed the devoted teaching from Professor Olafs Daugulis and Professor Jeremy May that their classes always gave me great movitation to learn more about the unknowns. Originating from these outstanding principle investigators, I started to meet extraodinary people from University of Houston.

It is my research group members who provided me the opportunity to learn different people from diverse cultures. Dr. Jaebum Lim as the senior colleague shared with me his experiences and techniques in organic chemistry wholeheartedly, which facilitated my latter independent project management capability. Dr. Teng-hao Chen's tough and inspirational personality indeed influenced me on my way to approach chemistry problems. I enjoyed my time to work with Chia-Wei Hsu and Dr. Ilja Popovs

along with their dedicated attitude and knowledgable synthetic skills. During our once-in-a-lifetime party to celebrate the tenure of Professor Ognjen Miljanić, Ha Le, Jennifer Nguyen, and Mohamed Hashim gave me an unforgettable company in the course of 'Houston–San Francisco' round-way road trip. We enjoyed nature's magnificent craftsmanship from the Grand Canyon to the Delicate Arch. I appreciated Hao-Chuan Zhou to offer accomodations on our first day of arrival in San Francisco at 3 am and his company for an adventurous hiking in Yosemite National Park on the next day for 16 miles.

My undergraduate student Nadia El-Hamdi helped me to accomplish my "scent transmutation" project very effectively during the summer of 2013. In the early 2015, she took the responsibility as the coach and assembled our group as a team to do workout in the gym every day. Undoubtedly, her patience and skills of leadership are influential to me and it will make her a great medical school student and an outstanding professional as a doctor. For the whole sweating team members: Jennifer Nguyen, Ha Le, María Márquez, Allen Chen, Jonathan Nguyen, and Ljubodrag Vujisić, your irreplaceable companies made us the best team.

It was a memorable time to spend with high school friend Guang-Yan Qin and Feng-Chi Wu in Denver during the Christmas in 2013. You overestimated my skiiing skills and brought me to the blue lanes in the mountain that my performance was like a "rolling cheese". During the Christmas of 2014 and July 4th of 2015, I enjoyed my road

trip with Ronald Besandre, Jiun-Le Shih, and Yi-Yin Kuo to visit Dr. Santa Jansone-Popova and Dr. Ilja Popovs in Knoxville.

I also want to give my acknowledgement to a very inspirational friend Hao-chuan Zhou from San Francisco for his absolute support since we knew each other from 1996. To my old friends Xing Li, Su-Jie Li and Cheng-Yan Ni from Singapore, without your original support, I even would not apply for this PhD program. As a student from Nankai high school, it is her name Nankai to drive me to work harder and to be a better person. Lastly, I want to acknowledge my family members for their absolute support spiritually and physically; specifically it was my parents who introduced calligraphy, painting, and classical guitar to me, which later enriched my PhD life as I was solving scientific problems.

ABSTRACT

Dynamic combinatorial libraries (DCLs) are collections of structurally related compounds that can interconvert through reversible chemical reaction(s). Such reversibility endows DCLs with adaptability to external stimuli, as rapid interconversion allows quick expression of those DCL components, which best respond to the disturbing stimulus. Chapter one focuses on the comparison between thermodynamically and kinetically controlled phenomena that occur within DCLs. Specifically, it will describe self-sorting under the influence of reversible and irreversible chemical and physical stimuli.

Metal alkoxides, such as NaO*t*-Bu or $Ti(OBu)_4$, can initiate acyl exchange within complex ester libraries. Reactive distillation of such DCLs isolates the most volatile ester at the expense of the less volatile library members that share a constituent with it. This process can be iteratively repeated to yield up to four industrially relevant esters as pure products from a single reaction setup.

Esters are also volatile and pleasantly smelling compounds, commonly used as food additives. Using $Ti(OBu)_4$-catalyzed acyl exchange, we demonstrate a scent transmutation experiment, in which two fragrant esters swap their acyl and alkoxy substituents and are, during the course of a reactive distillation, quantitatively converted into two different esters with distinct fragrance properties. We view this simple and appealing experiment as highly suitable for instructional use, since it can be used to teach

the concepts of chemical equilibrium, distillation, transesterifcation, dynamic combinatorial chemistry, and the industrially relevant process of reactive distillation.

Using cyanide-assisted benzoin condensation of isophthaldehyde terephthalaldehyde, we first prepared cyclotribenzoin and cyclotetrabenzoin. Cyclotribenzoin is a cone-shaped macrocycle whose three benzene rings define a cuplike cavity, while six of its C–H bonds convergently point in the opposite direction. This combination of convergently oriented cation- and anion-binding groups, coupled with an exceedingly simple synthesis, promises to make cyclotribenzoin an appealing platform for supramolecular chemistry studies. Cyclotetrabenzoin is a square shape-persistent macrocycle ornamented with four α-hydroxyketone functionalities pointing away from the central cavity, whose dimensions are 6.9×6.9 Å. In the solid state, these functional groups extensively hydrogen bond, resulting in a microporous three-dimensional organic framework with one-dimensional nanotube channels. This material exhibits permanent porosity, with a Langmuir surface area of 52 m^2g^{-1}.

TABLE OF CONTENTS

ACKNOWLEDGEMENT iv

ABSTRACT vii

TABLE OF CONTENTS ix

LIST OF FIGURES xv

LIST OF SCHEMES xxii

LIST OF TABLES xxv

Chapter One Self-Sorting Phenomena in Dynamic Combinatorial Chemistry

1.1 Introduction 1

1.2 Early Concepts in Self-Sorting 4

1.2.1 Small Molecules 4

1.2.2 Copolymers and Surfaces 8

1.3 Comparison between Thermodynamic and Kinetic Self-Sorting 12

1.3.1 Thermodynamic Control of Self-Sorting 12

1.3.1.1 Self-Assembly of Metal-Oligopyridine Helicates 12

1.3.1.2 Macrocyclization of Esters 15

1.3.1.3 Self-Sorting of Copper-Imine Complexes 21

1.3.2 Kinetic Control of Self-Sorting..... 25

1.3.2.1 Dynamic Chiral Resolution of Esters 25

1.3.2.2 Oxidative Self-Sorting of Imines 28

1.3.2.3 Distillative Self-Sorting of Imines 32

1.4 Conclusion 35

1.5 Referencs..... 36

Chapter Two Iterative Ester Reactive Distillation: Experimental Design and Characterization

2.1 Introduction..... 45

2.2 Results and Discussion 50

2.3 Conclusions and Outlook..... 55

2.4 Experimental Section..... 56

2.4.1 General Methods 56

2.4.2 Synthesis of Ester Starting Materials 58

2.4.3 Reactive Distillations of [2×2] Ester Libraries 62

2.4.3.1 Ethyl Acetate (**93**) and Benzyl Benzoate (**105**) 62

2.4.3.2 Ethyl Butyrate (**98**) and Benzyl Benzoate (**105**) 66

2.4.3.3 Ethyl Acetate (**93**) and Butyl Butyrate (**99**) 69

2.4.3.4 Ethyl Acetate (**93**) and Octyl Octanoate (**108**) 72

2.4.3.5 Butyl Butyrate (**99**) and Octyl Octanoate (**108**) 77

2.4.4 Reactive Distillations of [3×3] Ester Libraries 83

2.4.4.1 Ethyl Acetate (**93**), Butyl Butyrate (**99**), and Benzyl Benzoate (**105**) ... 83

2.4.4.2 Ethyl Acetate (**93**), Butyl Butyrate (**99**), and Octyl Octanoate (**108**) 88

2.4.5 Reactive Distillations of [4×4] Ester Libraries 93

2.4.5.1 Ethyl Acetate (**93**), Butyl Butyrate (**99**), Octyl Octanoate (**108**), and Cetyl Palmitate (**113**) 93

2.4.6 Reactive Distillations of [2×3] Ester Libraries 102

2.4.6.1 Ethyl Acetate (**93**), Ethyl Butyrate (**98**), and Benzyl Benzoate (**105**) . 102

2.5 References 107

Chapter Three Scent Transmutation: A New Way to Teach on Chemical Equilibrium, Distillation, and Dynamic Combinatorial Chemistry

3.1 Introduction 113

3.2 Results and Discussion 117

3.3 Conclusions and Outlook 121

3.4 Experimental Section 122

3.4.1 General Methods 122

3.4.2 Ethyl Acetate (**93**) and Octyl Octanoate (**108**) 126

3.4.3 Ethyl Acetate (**93**) and Phenylethyl Phenylacetate (**116**) 130

3.4.4 Methyl Acetate (**118**) and Phenylethyl Cinnamate (**119**) 134

3.4.5 Ethyl Isovalerate (**121**) and Phenylethyl Phenylacetate (**116**) 137

3.4.6 Isoamyl Acetate (**123**) and Phenylethyl Isovalerate (**124**) 141

3.4.7 Ethyl Acetate (**93**) and Isoamyl Isovalerate (**122**) 145

3.5 References 148

Chapter Four Cyclotribenzoin and Cyclotetrabenzoin: Synthesis and Gas Adsorption Studies

4.1 Introduction 150

4.2 Results and Discussion 152

4.2.1 Synthesis of Compounds **127**, **128**, and **129** 152

4.2.2 X-Ray Crystal Structure Analysis of Compound **127** 154

4.2.3 X-Ray Crystal Structure Analysis of Compound **129** 157

4.2.4 Thermogravimetric Analysis of Compound **129** 162

4.2.5 Gas Adsorption Analysis of Compound **129** 162

4.3 Conclusions and Outlook 162

4.4 Experimental Section 163

4.4.1 General Methods 163

4.4.2 Synthesis of Compound **127**, **128**, and **129** 164

4.4.2.1 Synthesis of Compound **127** 164

4.4.2.2 Synthesis of Compound **128** 165

4.4.2.3 Synthesis of Compound **129** 166

4.4.3 Thermogravimetric Analysis of Compound **129** 168

4.4.4 Powder X-Ray Diffraction Patterns of Compound **129** 169

4.4.5 Gas Adsorption Isotherm of Compound **129** 170

4.4.6 Crystal Data for Compound **127** 170

4.4.7 Crystal Data for Compound **129** 172

4.5 References 173

LIST OF FIGURES

Figure 1.1 Structures of **1**, **2**, (±)-**3**, and (±)-**4.** 6

Figure 1.2 Structures of compounds **5**–**13**. 7

Figure 1.3 Schematic representation of a solvent dependant noncovalently functionalized triblock copolymer (top); selective self-assembly and disassembly in 85:15 mixture of chloroform:dioxane. 11

Figure 1.4 Functionalization of cholic acid methyl ester **33** with different substitutions before macrocyclization. 18

Figure 2.1 General setups used for the ester self-sorting reactions 58

Figure 2.2 ^{1}H NMR spectra of the starting mixture (bottom) of esters **93**, **95**, **103**, and **105**, and the distillate (middle) and distillation residue (top) obtained after the reactive distillation of that mixture. 65

Figure 2.3 ^{1}H NMR spectra of the starting mixture (bottom) of esters **98**, **100**, **103**, and **105**, and the distillate (middle) and distillation residue (top) obtained after the reactive distillation of that mixture. 68

Figure 2.4 ^{1}H NMR spectra of the starting mixture (bottom) of esters **93**, **94**, **98**, and **99**, and the distillate (middle) and distillation residue (top) obtained after the reactive distillation of that mixture. 71

Figure 2.5 ^{1}H NMR spectra of the starting mixture (bottom) of esters **93**, **96**, **106**, and **108**, and the distillate (middle) and distillation residue (top) obtained after the reactive distillation of that mixture..... 75

Figure 2.6 Gas chromatogram of the distillation residue from the reactive distillation of an equimolar mixture of **93**, **96**, **106**, and **108**, with internal standard (dodecane) added for calibration. THF was used as the solvent. 77

Figure 2.7 Gas chromatogram of the distillate from the reactive distillation of a mixture of **99**, **101**, **107**, and **108**, with internal standard (dodecane) added for calibration. THF was used as the solvent. 80

Figure 2.8 Gas chromatogram of the distillation residue from the reactive distillation of a mixture of **99**, **101**, **107**, and **108**, with internal standard (dodecane) added for calibration. THF was used as the solvent..... 81

Figure 2.9 ^{1}H NMR spectra of the starting mixture (bottom) of esters **99**, **101**, **107**, and **108**, and the distillate (middle) and distillation residue (top) obtained after the reactive distillation of that mixture..... 82

Figure 2.10 ^{1}H NMR spectra of the starting mixture (bottom) of esters **93–105**, and the two distillates (middle) and distillation residue (top) obtained after the reactive distillation of that mixture..... 87

Figure 2.11 Gas chromatogram of the distillation residue from the reactive distillation of an equimolar mixture of **93**, **94**, **96**, **98**, **99**, **101**, **106**, **107**, and **108**, with internal standard (dodecane) added for calibration. THF was used as the solvent..... 91

Figure 2.12 ^{1}H NMR spectra of the starting mixture (bottom) of esters **93**, **94**, **96**, **98**, **99**, **101**, **106**, **107**, and **108**, and the two distillates (middle) and distillation residue (top) obtained after the reactive distillation of that mixture. 92

Figure 2.13 ^{1}H NMR spectra of the three distillates and the distillation residue resulting from the reactive distillation of an equimolar mixture of esters **93**, **94**, **96**, **97**, **98**, **99**, **101**, **102**, **106**, **107**, **108**, **109**, **110**, **111**, **112**, and **113**. 98

Figure 2.14 Gas chromatogram of the second distillate from the reactive distillation of an equimolar mixture of **93**, **94**, **96**, **97**, **98**, **99**, **101**, **102**, **106**, **107**, **108**, **109**, **110**, **111**, **112**, and **113**, with internal standard (dodecane) added for calibration. THF was used as the solvent. 99

Figure 2.15 Gas chromatogram of the third distillate from the reactive distillation of an equimolar mixture of **93**, **94**, **96**, **97**, **98**, **99**, **101**, **102**, **106**, **107**, **108**, **109**, **110**, **111**, **112**, and **113**, with internal standard (dodecane) added for calibration. THF was used as the solvent. 100

Figure 2.16 Gas chromatogram of the distillation residue from the reactive distillation of an equimolar mixture of **93**, **94**, **96**, **97**, **98**, **99**, **101**, **102**, **106**, **107**, **108**, **109**, **110**, **111**,

112, and **113**, with internal standard (dodecane) added for calibration. THF was used as the solvent. 101

Figure 2.17 ^{1}H NMR spectra of the starting mixture (bottom) of esters **93**, **95**, **98**, **100**, **103** (2 equivalent), and **105**, and the two distillates (middle) and distillation residue (top) obtained after the reactive distillation of that mixture. 106

Figure 3.1 General setup used for the scent transmutation reactions..... 125

Figure 3.2 ^{1}H NMR spectra of the starting mixture (bottom) of esters **96** and **106**, and the distillate (middle) and distillation residue (top) after the scent transmutation of that mixture. 128

Figure 3.3 Gas chromatogram of the distillation residue from the scent transmutation of an equimolar mixture of **96** and **106**, with internal standard (dodecane) added for calibration. THF was used as the solvent..... 129

Figure 3.4 ^{1}H NMR spectra of the starting mixture (bottom) of esters **114** and **115**, and the distillate (middle) and distillation residue (top) after the scent transmutation of that mixture. 132

Figure 3.5 Gas chromatogram of the distillation residue from the scent transmutation of an equimolar mixture of **114** and **115**, with internal standard (dodecane) added for calibration. THF was used as the solvent..... 133

Figure 3.6 ^{1}H NMR spectra of the starting mixture (bottom) of esters **114** and **117**, and the distillate (middle) and distillation residue (top) after the scent transmutation of that mixture. 136

Figure 3.7 ^{1}H NMR spectra of the starting mixture (bottom) of esters **120** and **115**, and the distillate (middle) and distillation residue (top) after the scent transmutation. 139

Figure 3.8 Gas chromatogram of the distillation residue from the scent transmutation of an equimolar mixture of **120** and **115**, with internal standard (dodecane) added for calibration. THF was used as the solvent..... 140

Figure 3.9 Gas chromatogram of the distillation distillate from the scent transmutation of an equimolar mixture of **114** and **122**, with internal standard (dodecane) added for calibration. THF was used as the solvent..... 143

Figure 3.10 Gas chromatogram of the distillation residue from the scent transmutation of an equimolar mixture of **114** and **122**, with internal standard (dodecane) added for calibration. THF was used as the solvent..... 144

Figure 3.11 ^{1}H NMR spectra of the starting mixture (bottom) of esters **123** and **121**, and the distillate (middle) and distillation residue (top) after the scent transmutation of that mixture. 147

Figure 3.12 Gas chromatogram of the distillation residue from the scent transmutation of an equimolar mixture of **123** and **121**, with internal standard (dodecane) added for calibration. THF was used as the solvent..... 148

Figure 4.1 X-ray crystal structure of **127**. On the left, a side view showing convergent positioning of six C–H bonds in a conical structure. On the right, a top down view of the macrocycle. Disordered THF molecules were removed for clarity. Thermal ellipsoids shown at 50% probability. 155

Figure 4.2 Segment of a crystal packing diagram of **127**, viewed along the crystallographic *c* axis. Hydrogen atoms and disordered THF molecules were removed for clarity..... 156

Figure 4.3 X-ray crystal structure of **129**. A top-down view of the tetramer, showing all α-hydroxyketone functional groups pointing away from the macrocycle cavity (left). A side view showing the twisted orientation of the benzene rings on the opposite sides of the square tetramer (right). Thermal ellipsoids shown at 50% probability. Element colors: C—gray, O—red, H—white. 158

Figure 4.4 Crystal packing of **129**. **A**: Two parallel columns of molecules of **129** establish an infinite tape of hydrogen bonds, highlighted in green. Molecules on the left are colored by element, those on the right are colored to highlight separate nanotubes. **B**: Segment of the extended crystal structure of **129**, viewed along the crystallographic *c* axis. This view of the structure shows the arrays of hydrogen bonded nanotubes, and the intrinsic pores of **129**. Element colors: C—gray, O—red, H—white..... 159

Figure 4.5 The crystal structure packing of compound **129** superimposes the satellite image of Eixample. 161

Figure 4.6 TGA of compound **129**..... 168

Figure 4.7 Comparison of PXRD patterns of compound **129**: simulated from single-crystal X-ray data (top) and measured from a freshly recrystallized sample of **126** (bottom)..... 169

Figure 4.8 Adsorption (●) and desorption (○) of N_2 gas within the pores of **129**, measured at 77 K. 170

LIST OF SCHEMES

Scheme 1.1 Imine-based macrocycle synthesis templated by $ZnCl_2$ (left) and Fe(II)-templated synthesis of phthalocyanine (right). 3

Scheme 1.2 The general polymer backbone synthesis. 8

Scheme 1.3 Noncovalent universal polymer backbone functionalization strategies. 9

Scheme 1.4 Self-recognition in the self-assembly of the double helicates **21^2H –24^2H** from a mixture of the oligobipyridine strands **21^2H –24^2H** and CuI ions (BF_4^- or PF_6^- anions omitted)..... 13

Scheme 1.5 Self-recognition in the self-assembly of the double helicate **$22a^2$H** and the triple helicate **25^3H** from a mixture of the oligobipyridine strands **25** and **22a** and of Cu(II) and Ni(II) ions (ClO_4^- anions omitted). 15

Scheme 1.6 a). TBDMSCl, Et_3N, DMAP, DMF, room temperature; b). 1.5 equiv BH_3•THF, diglyme, 0 °C, Me_3NO, 100 °C; c). Jones reagent, acetone, room temperature; d). MeOH, $HCl_{conc.}$, room temperature; e). TBAF, THF, room temperature..... 16

Scheme 1.7 Reaction condition: KOMe, [18]crown-6, toluene, reflux..... 17

Scheme 1.8 Macrocyclization of cholic acid methyl ester under thermodynamic control. Cyclization condition: KOMe, Dicyclohexyl-18-crown-6, toluene. 19

Scheme 1.9 The Cu(I)-templated formation of structures **43**–**46** from amines **38** and **39** together with aldehydes **40**, **41**, and **42**..... 22

Scheme 1.10 Compounds **39**, **40**, and **41** might only be used to construct the precursors of **43** and **44**. 23

Scheme 1.11 Compounds **43**, **44**, and **45** are all individually allowed, but only **43** and **45** are observed in this system for the given stoichiometry. 24

Scheme 1.12 Generation of a dynamic nitroaldol library and lipase-mediated asymmetric resolution..... 26

Scheme 1.13 Synthesis of benzazoles by oxidative cyclization of directly (Route A) and indirectly (Route B) prepared imines. 29

Scheme 1.14 Oxidative self-sorting of a [2×2] mixture of imines. 30

Scheme 1.15 Oxidative self-sorting of a [3×3] mixture of imines. 31

Scheme 1.16 Simplification of a [2×2] mixture of imines during the course of a vacuum distillation. 33

Scheme 1.17 Simplification of a [3×3] mixture of imines during the course of a vacuum distillation. 34

Scheme 2.1 Self-sorting of dynamic [2×2] ester libraries during reactive distillation (all of the starting esters were mixed in equimolar amounts). 51

Scheme 2.2 Self-sorting of dynamic [3×3] ester libraries during reactive distillation..... 52

Scheme 2.3 Self-sorting of dynamic [4×4] ester libraries during reactive distillation..... 54

Scheme 2.4 Self-sorting of dynamic [2×3] ester libraries during reactive distillation..... 55

Scheme 3.1 Ester transmutation transforms two moderate volatility esters into the highly volatile ester that is distilled away (shown in red) and the low-volatility ester that remains in the distillation residue (shown in blue)..... 115

Scheme 3.2 Ester Transmutation Experiments Performed in this Study (organoleptic properties of selected compounds are given next to their structures)..... 118

Scheme 4.1 Synthesis of cyclotribenzoin **127** and its silylated derivative **128**. Both enantiomers of **127** and **128** are produced. 153

Scheme 4.2 Synthesis of cyclotetrabenzoin **129**. 154

LIST OF TABLES

Table 2.1 Calculated compositions of three ester libraries before and after iterative reactive distillation: an equimolar [4×4] library (top), an equimolar [3×5] library (middle), and a non-equimolar [4×4] library (bottom and numbers in the table indicate the stoichiometry of esters). 48

Table 2.2 Compound codes for esters examined in this study. 49

Table 4.1 Crystallographic Data of Compound **127** 170

Table 4.2 Crystallographic Data of Compound **129** 172

Chapter One Self-Sorting Phenomena in Dynamic Combinatorial Chemistry

1.1 Introduction

Dynamic combinatorial chemistry (DCC)[1] points out an chemical environment under thermodynamic control, which is applied for the effective construction of a new molecule out of a chemical library using reversible reactions. Individual library members can be amplified if they respond well to the distorting influence of external stimuli. A dynamic combinatorial library (DCL) is generated from a blend of library members, which can react with each other to achieve interconversion through specific non-covalent or reversible covalent interactions via functionalization of library members. Once the library interchange is triggered, the distribution of library members is dependent on the thermodynamic minimum of the whole system through equilibrium. The concentration of each library member is dependent on their stability relative to other library members and that may vary upon the introduction of external stimuli. An individual component in a library based on non-covalent interactions might be amplified if template is added; this amplification shifts the equilibrium of the system towards the most stabilized product at the expense of other species.

Developed in the 1990s, the basic principle of DCC proceeded from the realization that it is very difficult to fullfill the task of constructing effective receptors capable of specific molecular recognition by using a straightforward synthetic design

approach. A newer, more efficient and general approach which was characteristic of combinatoriality, selectivity, and amplificability was later introduced to solve this problem. The guest molecule is allowed to select its own host, effectively "choosing" the most effective host from a mixture of potential candidates. Accordingly, selection will lead to the shift of equilibrium distribution in the DCL, which further amplifies the most stable host-guest combination. For chemical complex characteristic of molecular recognition ability, this approach could be considered as the intersection of two existing approaches to synthesis: thermodynamically controlled template synthesis and combinatorial chemistry.

In thermodynamically controlled chemical reactions, such as esterification, acetalization, and imination, the target products could be amplified by shifting the equilibrium to the product's side via removal of the water, temperature control, or stoichiometry control. Templates could also be used in thermodynamically controlled syntheses to enhance product formation. As early as 1900's, Emil Fischer's study on carbohydrate and Werner's study on coordination complexes showed evidence of the use thermodynamic control in synthesis.[2] In 1953, Watson and Crick discovered the DNA double helix and the templated synthesis during the DNA replication was also reported accordingly.[3] In 1926, the metal ion-templated synthesis of a imine macrocycle had been achieved by Seidel in the reaction between 2-aminobenzaldehyde and $ZnCl_2$,[4] although it was identified as such only much later (Scheme 1.1, left).[5] A few years later, Linstead reported another unexpected iron-templated macrocyclization reaction between phthalic anhydride and ammonia (Scheme 1.1 right).[6] In the 1960s, templated synthesis

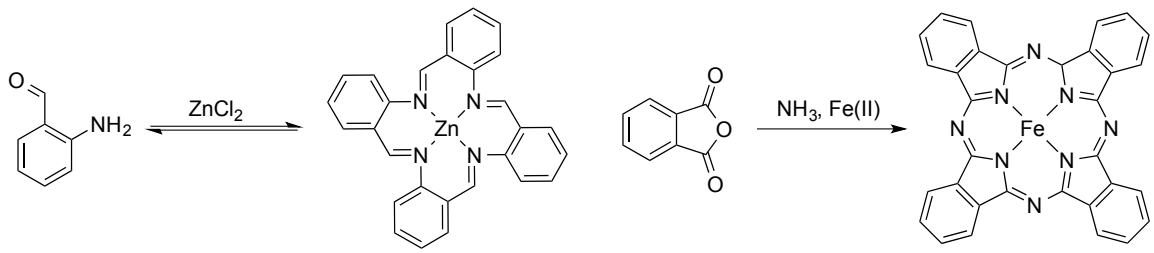

Scheme 1.1 Imine-based macrocycle synthesis templated by $ZnCl_2$ (left) and Fe(II)-templated synthesis of phthalocyanine (right).

was clarified and developed by Busch in his pioneering work on both kinetic and thermodynamic controlled synthesis.[7] The Ni(II)-templated bis-imine macrocycle synthesis expressing the role of a template in stabilizing a desired product from a complex equilibrating mixture is probably the first reported example.[8]

In 1995, Hamilton *et al.* reported one of the first example of synthetic recepters using reversible coordination of metal ions through combinatorial approach.[9] Harding *at al.*, in the same year, reported the guest-induced amplification of a metallo-macrocycle and metallo-[2]catenane from a mixture.[10] The concept of DCC was first introduced into literature in the mid-1990s by both Sanders and Lehn groups independently. Early studies in Sanders group involved base-catalyzed transesterification to generate macrocycles formed from steroid-based building blocks.[11] It was demonstrated that modest amplification of specific macrocycles could be achieved upon addition of different alkali metal ions. Lehn group's development of the DCC concept was a result from his metal helicates, showing that the major product in the DCL is dependent on the nature of the counterion which binds in the center of the helicates.[12]

In order to acquire a diverse range of products, the concept of design in DCC is compromised so that it allows the possibility of generating unexpected structures with unanticipated properties. Reversible chemistry is chosen to set up DCLs and to design suitable building blocks. The design of building blocks involves incorporating suitable functional groups at one or multiple positions, which are able to react reversibly when combined with other building blocks. The rest of the molecule is designed to cooperate with the purpose of a specific DCL, while not interupting the exchange reactions. Common features for design of building blocks are: (1) inclusion of functionalities to assist molecular recognition; (2) the overall shapes of building blocks are taken into consideration; (3) incorporation of solubilizing functionalities, chromophores, or other reporter groups. The common type of exchange reactions such as disulfides, imines, and alkene metathesis for different applications are extensively discussed in recent reviews and exploration of novel reversible reactions fitting for use in DCLs is in progress.[13]

1.2 Early Concepts in Self-Sorting

1.2.1 Small Molecules

The very early concepts of self-sorting came from research on biological polymers. In order to generate a faithful replication and transcription of genetic information stored in DNA, the complete control over the composition of and the precise positioning of functionalities in this biopolymer are obligatory. Nature applied the

combination of enzymatic catalysis, molecular recognition and non-equilibrium proofreading process to achieve the required level of fidelity. Since the application of non-equilibrium proofreading process in synthetic polymers still remains a challenge, the use of molecular recognition is dominantly exercised to direct the the composition of self-assembled polymer systems. These self-assembly strategies are based on internal stimuli that bias polymer compositions instead of using templates that stands for the external stimulus in DCC.

Self-sorting represents the ability to distinguish self and nonself. Nature shows this phenomenon from the replication of DNA and recrystallization of racemates into conglomerates. Self-sorting also exists in even very simple examples like phase separation of oil and water. Isaacs group has investigated the strength of self-sorting in mixture of several synthetic host-guest complexes in organic solvent and water.[14] In 2002, they reported that molecular clips undergo heterochiral aggregation and self-sorting.[14d] In this report, compounds **1**, **2**, (±)-**3**, and (±)-**4** form tightly self-associated dimers in $CDCl_3$ driven by the simultaneous formation of π–π interactions and two hydrogen bonds (Figure 1.1). The individual ^1H NMR spectra of **1**, **2**, (±)-**3**, and (±)-**4** showed two sets of resonances amide NH groups and the protons on substituted *o*-xylylene side-walls. These observations suggested that the kinetic and thermodynamic stable dimeric aggregates are formed in $CDCl_3$. The X-ray crystal structure obtained for **1** and (±)-**4** also provided evidences for the dimerization of these four compounds and gave reasonable geometries of their aggregates in $CDCl_3$. Two C=O···HN hydrogen bonds were found in each

molecular clip that contributed significantly to the dimerization.[15] Their high thermodynamic stability also arose from π–π interactions of four aromatic rings

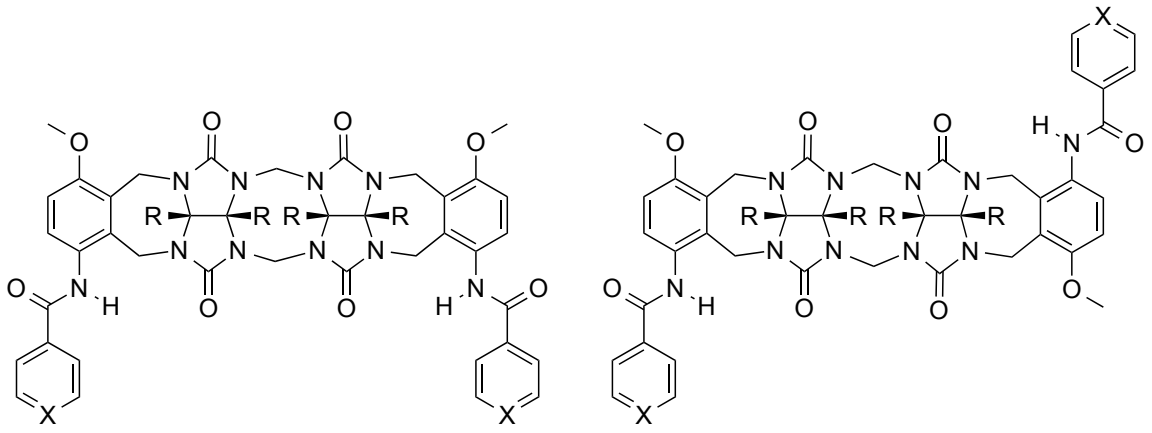

1 X = CH; R = CO_2Et
2 X = N; R = CO_2Et

(±)-**3** X = CH; R = CO_2Et
(±)-**4** X = N; R = CO_2Et

Figure 1.1 Structures of **1**, **2**, (±)-**3**, and (±)-**4.**

penetrating into clefts of the opposite molecular clip.[16] In summary, this study developed one of the earliest examples displaying self-sorting phenomenon driven by H-bonding and π–π interactions. In 2003, Isaacs group reported another set of examples, showing that the self-sorting in synthetic systems is more likely to be a general phenomenon rather than an exceptional behavior.[17] Compounds **5**–**13** are well-known for their self-assembled aggregates shown in Figure 1.2; their self-assembly behavior in a complex mixture was re-examined by ^{1}H NMR spectroscopy in an organic solvent with barium picrate additive. Structures observed were $\mathbf{5}_{10}$•Ba^{2+}+2Pic^-,[18a] $\mathbf{6}_{16}$•2Ba^{2+}•4Pic^-,[18a] $\mathbf{7}_2$,[18b] $\mathbf{8}_3$•$\mathbf{9}_6$,[18c] $\mathbf{10}_2$,[18d] $\mathbf{11}_2$,[18e, 18f] $\mathbf{12}_2$, and $\mathbf{13}_2$ in $CDCl_3$ solution; H-bonding within the region (8.0–14.5 ppm) was examined. According to literature reports, each of these molecules undergoes self-assembly to generate well-defined aggregates. A mixture of **5**–**13** in $CDCl_3$ were also

prepared later with the extraction of barium picrate from water. The ^{1}H NMR spectra of the mixture are nearly the superposition of of the spectra of the individual aggregates. This study indicates that the self-sorting happened in the solution solely based on thermodynamic preferences of molecular assembly rather than kinetically controlled aggregations.

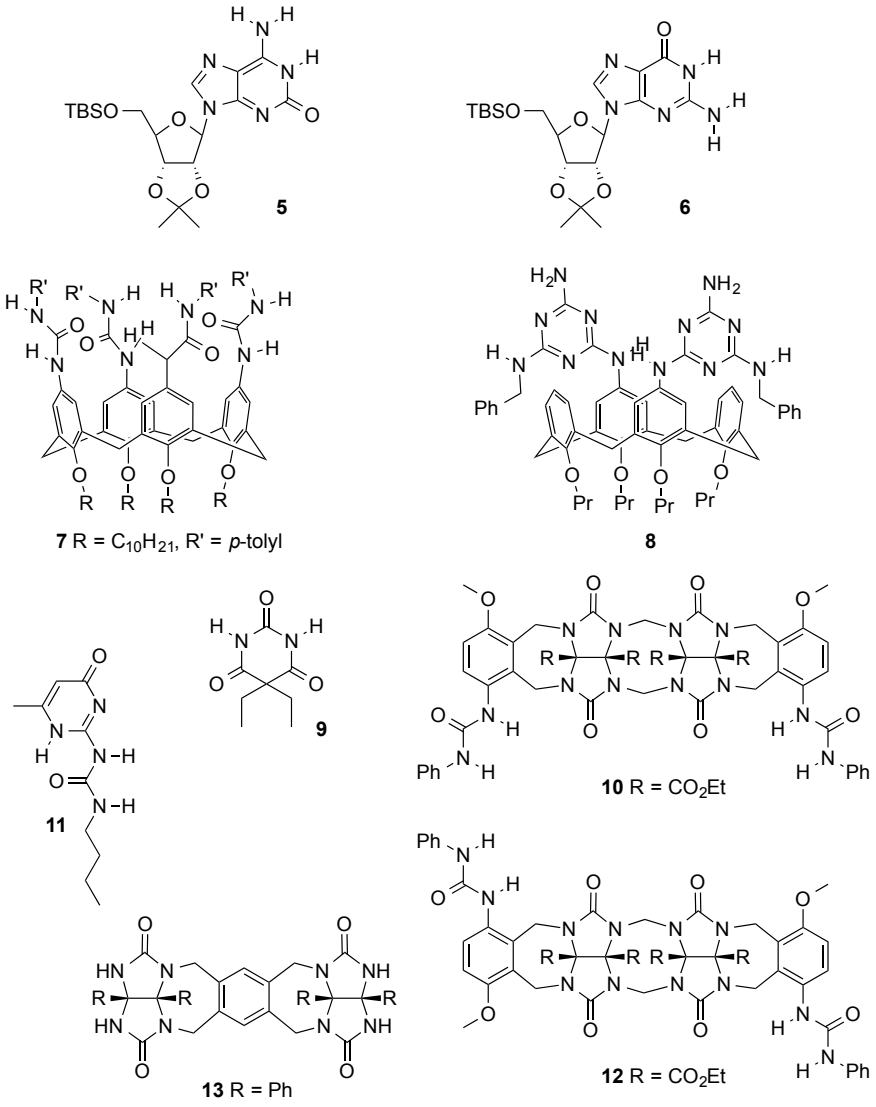

Figure 1.2 Structures of compounds **5**–**13**.

1.2.2 Copolymers and Surfaces

While Isaacs group focused on the studies of self-sorting in small molecule systems, other research groups have extended this concept to copolymers and onto surfaces.[19] Weck's group reported polymers with norborene-based backbones and two functionalities as the host groups; it was able to bind different guest molecules based on metal-ligand interactions, hydrogen bonding, or ionic complexes.[20] The copolymers designed in the Weck group are based on two monomers containing terminal metal-coordination or hydrogen bonding recognition moiety (Scheme 1.2).[21] Both monomers

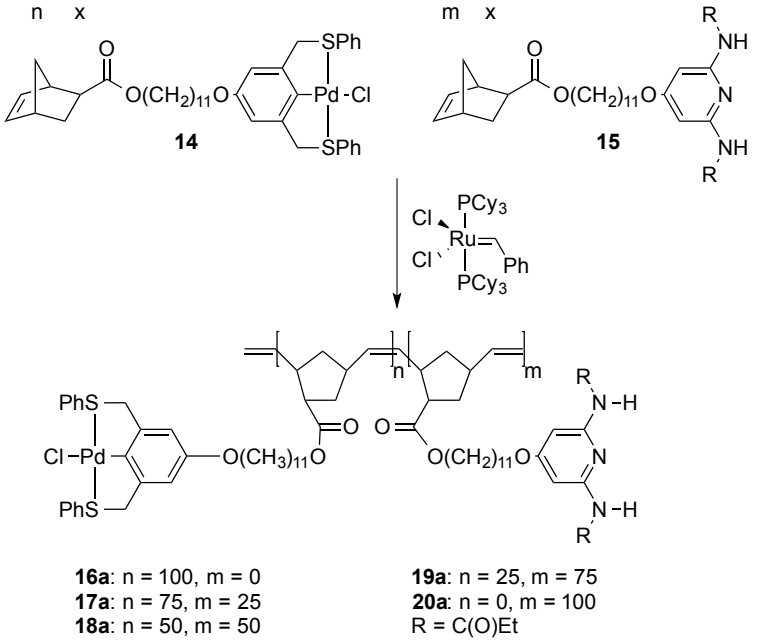

Scheme 1.2 The general polymer backbone synthesis.

have: (1) Norborene polymerizable unit, which could be propagated through ring-opening metethesis polymerization (ROMP);[22] (2) A spacer molecule to enhance the solubility; (3) Pd-pincer complexes allowing for coordination and diaminopyridine functionalities for

three hydrogen bondings. Copolymers **16a**–**20a** were synthesized using Grubbs catalyst via ROMP. Functionalization of copolymers **17a**–**19a** was achieved via three different methodologies in Scheme 1.3: (1) Direct self-assembly of pyridine to the Pd(II) complexes or N-butylthymine to the diaminopyridine units to give **17b**–**19b** and **17c**–**19c**; (2) Stepwise self-assembly either starts from hydrogen bonding (pathway I) or metal-coordination (pathway II); (3) Orthogonal self-assembly by simple addition of both pyridine and *N*-butylthymine (pathway III) to give **17d**–**19d**. Association is always observed preferentially between established host-guest systems even in a mixture of different hosts and guests. Based on those preliminary results, Weck group planned to

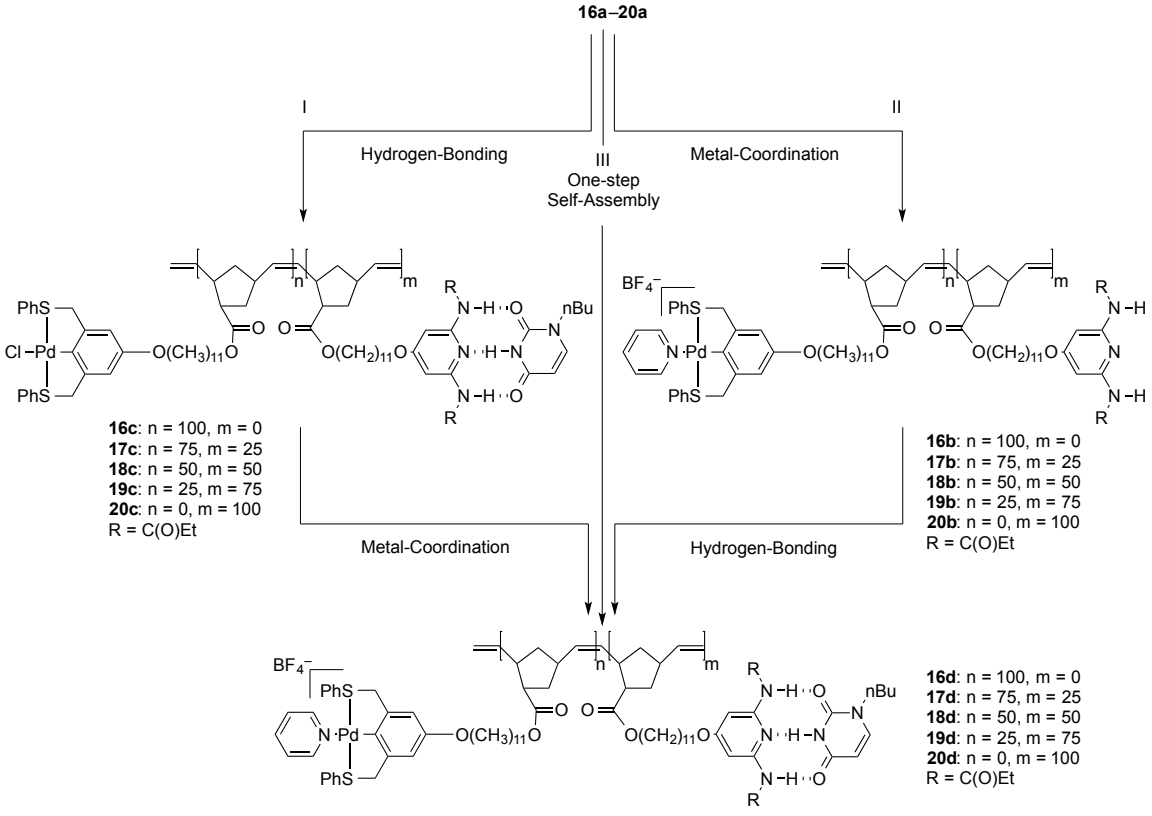

Scheme 1.3 Noncovalent universal polymer backbone functionalization strategies.

design supramolecular smart materials relying on the controlled tuning of molecular-levelled assembly and disassembly. In supramolecular chemistry, the disassembly step has been considered as a significant step in the application of non-covalent interactions. These non-covalent interactions have contributed a lot to the smart material application such as molecular latches[23] and molecular switches.[24] However, all the well-established supramolecular systems are using a single non-covalent interaction for the switch on/off step. The Weck group expanded the scope of tunable assemblies of non-covalent functionalization strategy to copolymers containing three highly selective non-covalent interactions.[20b] In Figure 1.3, the norborene copolymer backbone is functionalized with a palladium coordination complex and two different hydrogen bonding host-guest systems. It is demonstrated that all three non-covalent functionalizations are orthogonal to each other in dichloromethane solvent. While using a 85:15 mixture of chloroform and dioxane, upon the metal coordination of the pincer ligand to the pyridine (on) the cyanuric acid hydrogen bonding to its guest molecule is broken (off). This ON/OFF switching process is independent of the third interaction, i.e. hydrogen bonding between diaminopyridine and thymine.

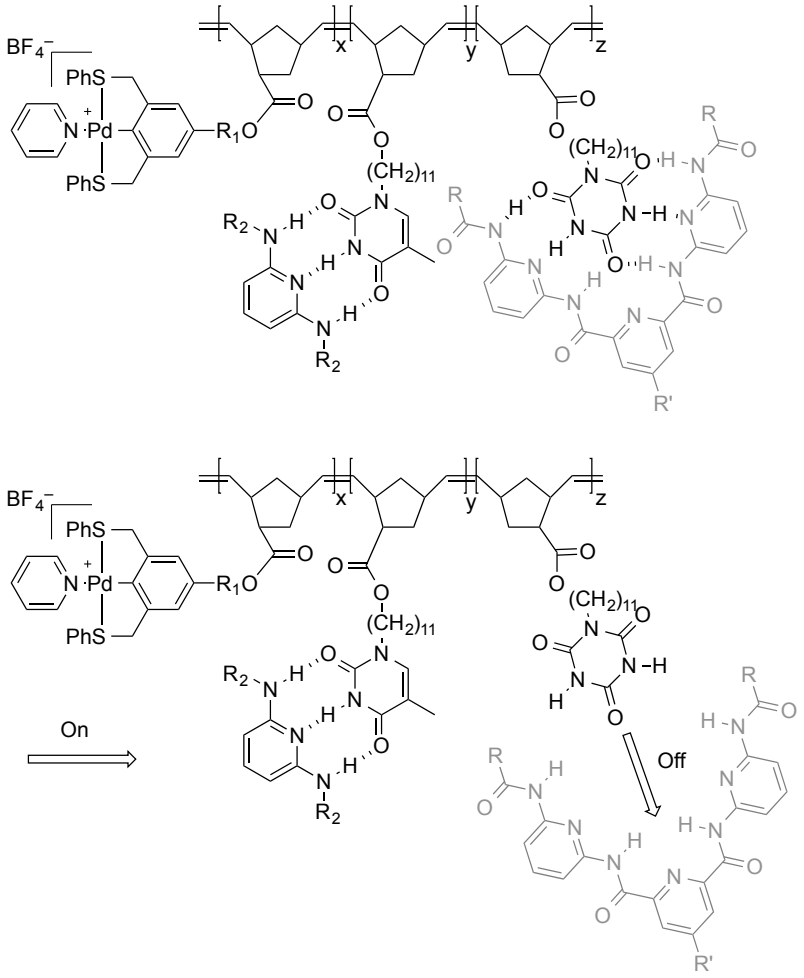

Figure 1.3 Schematic representation of a solvent dependant noncovalently functionalized triblock copolymer (top); selective self-assembly and disassembly in 85:15 mixture of chloroform:dioxane.

1.3 Comparison between Thermodynamic and Kinetic Self-Sorting

1.3.1 Thermodynamic Control of Self-Sorting

Self-sorting can proceed under either thermodynamic or kinetic control.[25] In the thermodynamically controlled self-sorting, the system is sorted at the time it reached the thermodynamic minimum. Thermodynamic self-sorting is dependent on the reversibility of interactions between different building blocks in the DCL until the equilibrium is established. The reversibility is often relying on the use of low-barrier non-covalent interactions or dynamic covalent bonds. In the following paragraph, the research work of Lehn,[26] Sanders,[27] and Nitschke[28] group will be illustrated to give a further review of the progress of thermodynamic self-sorting.

1.3.1.1 Self-Assembly of Metal-Oligopyridine Helicates

Lehn suggested that it is of special importance to investigate the physicochemical features of helicate formation in the study of self-assembly process and the relationship to biological self-assembly systems.[26] In this study, they proposed a selective formation of helicates in the mixture of [oligo(2,2'-bipyridine)] strands **21**–**25** and specific metal ions (Scheme 1.4). The self-assembly of **21** and Cu(I) was first examined that the spontaneous formation of a double helicate $\mathbf{21^2H}$ was the only helicate, no other species being observed. A new question was proposed by Lehn group after this observation: what will happen if a mixture of oligobipyridine strands of different lengths is treated with Cu(I);

will only helicates containing identical strands be formed or will ill-defined mixtures be formed? By mixing the ditopic **21** and tritopic **22** oligobipyridine species, it was found that a mixture of either only the discrete helicates $\mathbf{21^2H}$ and $\mathbf{22^2H}$ or other mixed species

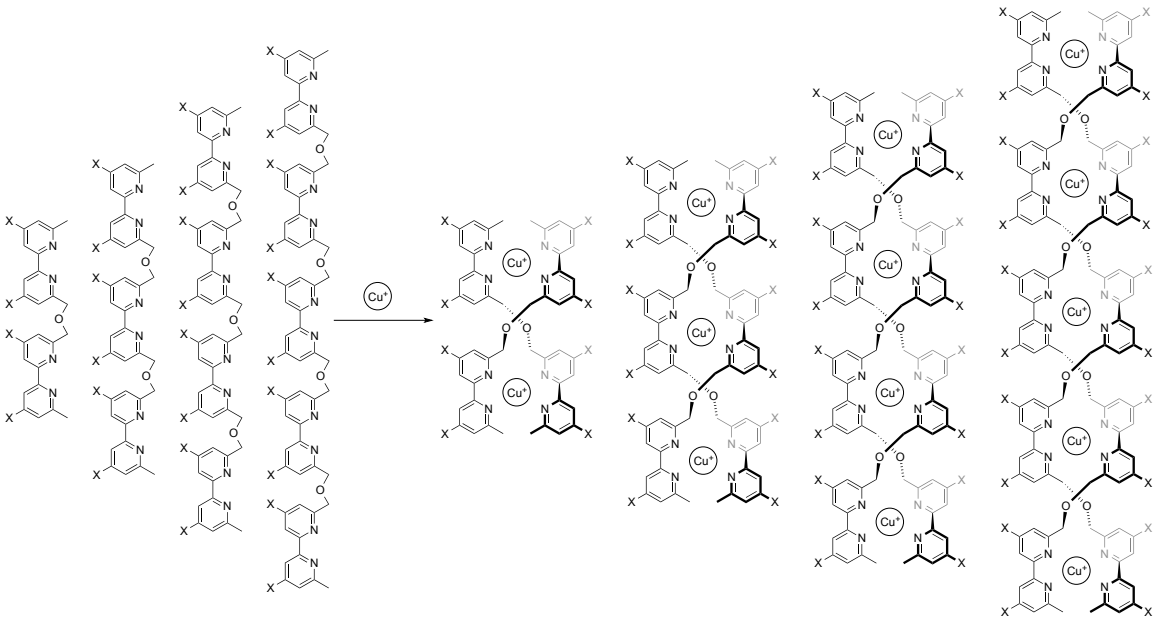

Scheme 1.4 Self-recognition in the self-assembly of the double helicates $\mathbf{21^2H}$ –$\mathbf{24^2H}$ from a mixture of the oligobipyridine strands $\mathbf{21^2H}$ –$\mathbf{24^2H}$ and CuI ions (BF_4^- or PF_6^- anions omitted).

such as a double-helical complex $[(\mathbf{21})_3(\mathbf{22})_2Cu_6]^{6+}$ was formed. It was found that when 3 equivalents of **21a** and 2 equivalents of **22a** were treated with excess $[Cu(CH_3CN)_4]PF_6$ in DCM, only helicates $\mathbf{21a^2H}$ and $\mathbf{22a^2H}$ were identified by ^{1}H NMR spectroscopy without other species observed. In a similar fashion, the mixture of **21b** and **22b** yielded

only **21b^{2}H** and **22b^{2}H** as indicated by ^{1}H NMR and Fast Atom Bombardment (FAB) mass spectroscopy. The mixture of **21b** and **23b** in 2:1 ratio only afforded 2:1 of **21b^{2}H** and **23b^{2}H** with no other mixed-ligand complex observed. Finally, the mixture of different oligobipyridine strands **21b** (1 mg), **22b** (1.5 mg), **23b** (2 mg), and **24b** (2.5 mg) was treated with excess amount of $[Cu(CH_3CN)_4]BF_4$. The ^{1}H NMR at the very first time showed a very complicated pattern indicating a very complex mixture. Lehn group claimed that this was duo to the very slow formation of substituted pentahelicate **24b^{2}H** over several days. The wrapping and unwrapping of the pentahelicates together with the steric hindrance from the $CONEt_2$ slowed down the rate of pentahelicate formation. Because unsubstituted and substituted ligands gave the corresponding double helicates, it was concluded by Lehn group that the oligobipyridine strands proceeded self-recognition or self/nonself-discrimination with Cu(I). The substituents effect here reflected that the unsubstituted ligands had the highest self-recognition capability. This self-sorting phenomenon was further demonstrated in a mixed double/triple helicates formation experiment (Scheme 1.5). Having learned from a previous example that the mixture of 5,5'-disubstituted bipyridine oligomer and Ni(II) would give self-assembly of trinuclear triple helicate **25^{3}H**, Lehn group proposed to mix the two different type of self-assembly to examine their interaction. A mixture of 2 equivalents of **22a**, 3 equivalents of **25**, 3 equivalents of Cu(I), and 3 equivalents of Ni(II), the precipitation of the resulting complexes gave quantitative yield of **22a^{2}H** and **25^{3}H**. These two experiments above sufficiently demonstrated the self-sorting of tetrahedral coordination between Cu(I) and

6,6'-linked tritopic bipyridine ligand **22a** and of the octahedral coordination between Ni(II) and 5,5'-linked tri(bipyridine) strand **25**.

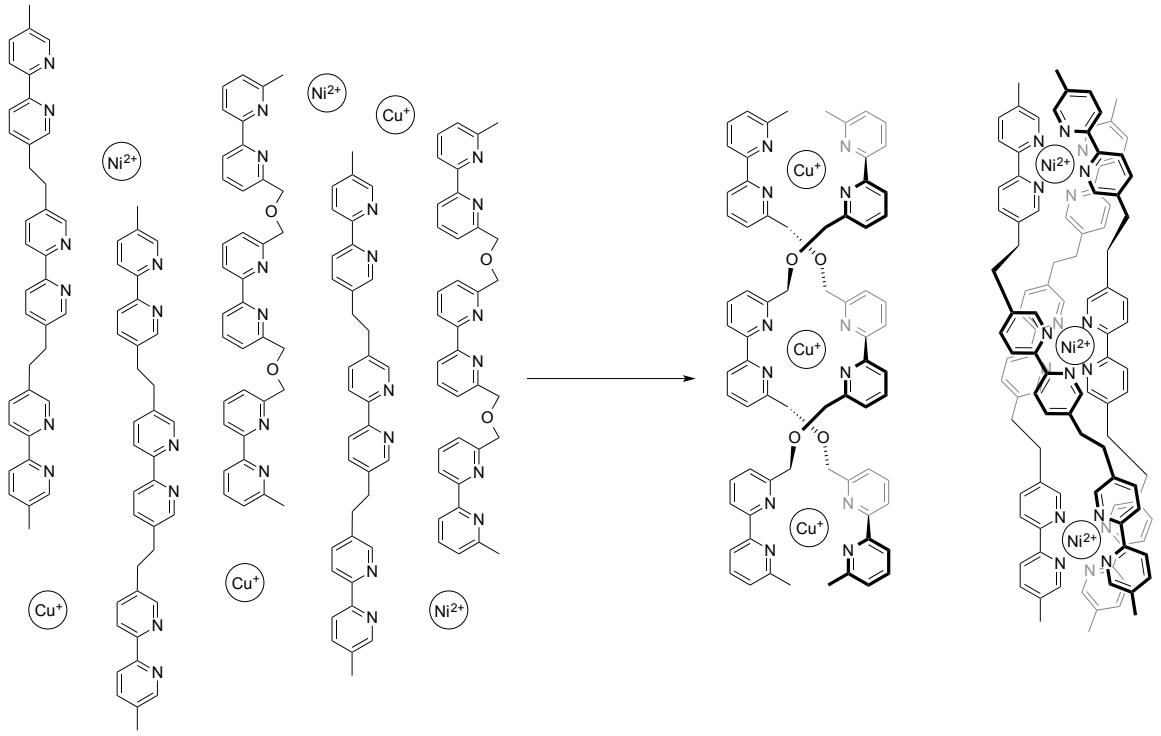

Scheme 1.5 Self-recognition in the self-assembly of the double helicate **22a^{2}H** and the triple helicate **25^{3}H** from a mixture of the oligobipyridine strands **25** and **22a** and of Cu(II) and Ni(II) ions (ClO_4^- anions omitted).

1.3.1.2 Macrocyclization of Esters

In 1996, Sanders group reported an example of self-sorting of macrocyclic trimer from new supramolecular building blocks from the cinchona alkaloids quinine (**26a**) and

cinchonidine (**26b**).[27a] Traditionally, covalently bonded organic structures were synthesized via kinetically controlled irreversible reactions, which lack the ability to proofread and repair the incorrectly formed bonds.[27b] Cinchona alkaloids were selected as the building block because it has been received much attention in the field of asymmetric synthesis, *i.e.* Sharpless dihydroxylation.[29] Quinine has a relatively concave shape, and the functionalities present at position 9 and 10 make it attractive for macrocycle synthesis (Scheme 1.6). Since this cyclization was an transesterification, the hydroxy group at the 9

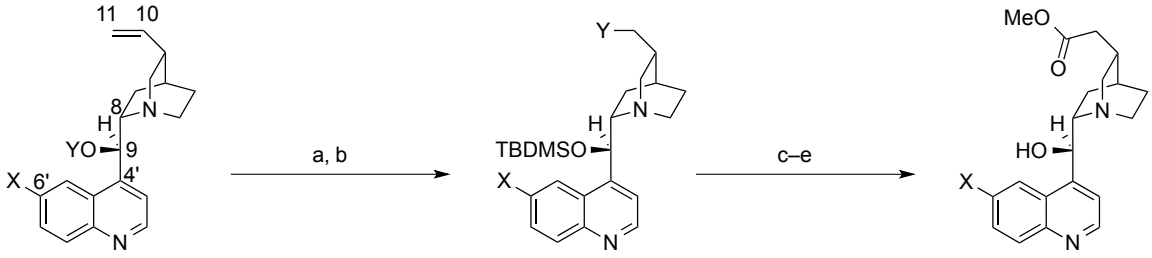

26, Y = H
28, Y = TBDMS
a, X = OMe
b, X = H

29, Y = CH_2OH
30, Y = CO_2H
31, Y = CO_2Me

27

Scheme 1.6 a). TBDMSCl, Et_3N, DMAP, DMF, room temperature; b). 1.5 equiv BH_3•THF, diglyme, 0 °C, Me_3NO, 100 °C; c). Jones reagent, acetone, room temperature; d). MeOH, $HCl_{conc.}$, room temperature; e). TBAF, THF, room temperature.

position was used as the alcohol end and the vinyl group at 10 position was modified as the ester end. The thermodynamic cyclization was carried out using catalyst (5% KOMe/[18]crown-6) in a 5 mM solution of toluene under reflux with azeotropic removal of the methanol product (Scheme 1.7). The cyclization gave a single product cyclic trimer **32a** in high yield (90% by NMR and 84% isolated). The reaction was complete after 20 min and no significant change of products distribution was found in the following 160

min. Cyclization of **27b** also resulted in the corresponding trimer **32b** in an excellent yield. In order to demonstrate that the trimer is the single product other than mixtures of cyclic oligomers, the linear dimer, trimer, and tetramer were synthesized independently

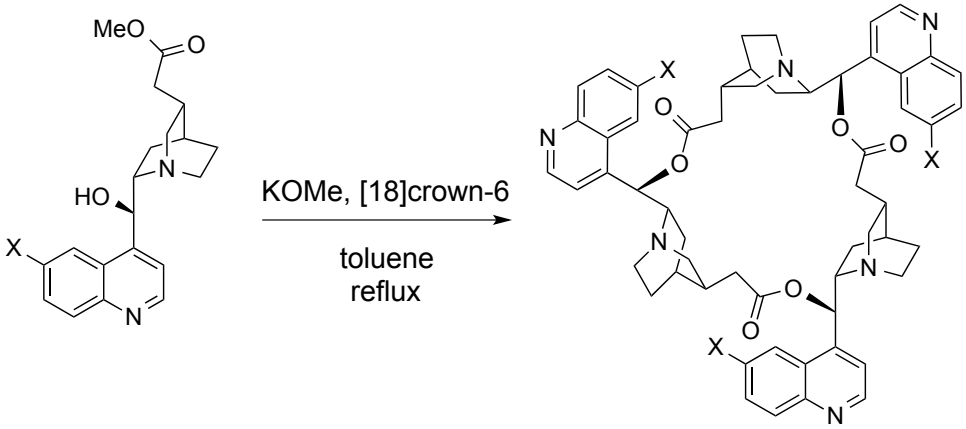

27a, X = OMe
27b, X = H

32a, X = OMe
32b, X = H

Scheme 1.7 Reaction condition: KOMe, [18]crown-6, toluene, reflux.

and were subjected to cyclization under Yamaguchi type kinetic conditions. The linear dimer and tetramer both gave the cyclic tetramer whose NMR spectra were indeed different from the cyclic trimer. The space-filling model suggested that the cyclic dimer was not kinetically accessible. Cyclization of **27a** and **27b** were also carried out under kinetic conditions, which yielded a mixture of cyclic trimer (37%), tetramer (23%), and other higher oligomers (40%) identified by NMR.[27g] These results indicated that although cyclic dimer could not be kinetically obtained, other higher cyclic oligomers could be formed and the narrow distribution of products under thermodynamic condition was not because of the unavailability of other cyclic oligomers. With those results, Sanders group proceeded to determine the reversibility of this cyclization. A mixture of trimer **32a** and

32b was subjected to the same reaction condition in Scheme 1.7 and was examined by Electrospray Mass Spectrometry (ESMS) after work up; it was found that all four possible trimers were present. This work has shown that the thermodynamic transesterification reaction and the new alkaloid derived building block are suitable for macrocyclization self-sorting systems.

In the same year, Sanders group reported another self-sorting of macrocyclization using cholate as the building block (Figure 1.4).[27b] Transesterification again has been

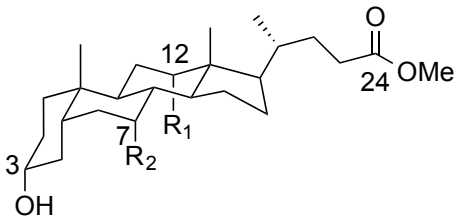

Cholic acid methyl ester $R_1 = R_2 = OH$
33a $R_1 = OCH_2C_6H_4Ph$
33b $R_1 = OCH_2Ph$, $R_2 = OCH_2OCH_2CH_2OMe$
33c $R_1 = R_2 = OCH_2C_6H_4OMe$

Figure 1.4 Functionalization of cholic acid methyl ester **33** with different substitutions before macrocyclization.

chosen as the thermodynamically-driven reaction for macrocyclization since its significance in the field of natural product synthesis[30] and supramolecular chemistry.[31] The design of the building block was analogous to the previous example: it was equiped with a methyl ester group at one end and a hydroxy group at the other end of the structure. There were another characteristic chromophores attached to the position 7 and/or position 12 in order to facilitate the spectroscopic analysis. The monomer deoxycholate **33a** and cholates **33b** and **33c** were synthesized by conventional methods. Cyclic oligomers **34**–

37a–c were also prepared under kinetic conditions and separated by preparative column chromatography. Catalyst screening experiment showed 5 mol% of the complex of potassium methoxide and dicyclohexyl-18-crown-6 is the best catalytic system.[32] The cyclization experiments were carried out at 5 mM concentration of cholate monomer in toluene under reflux (Scheme 1.8). Since each monomer carried the same chromophore,

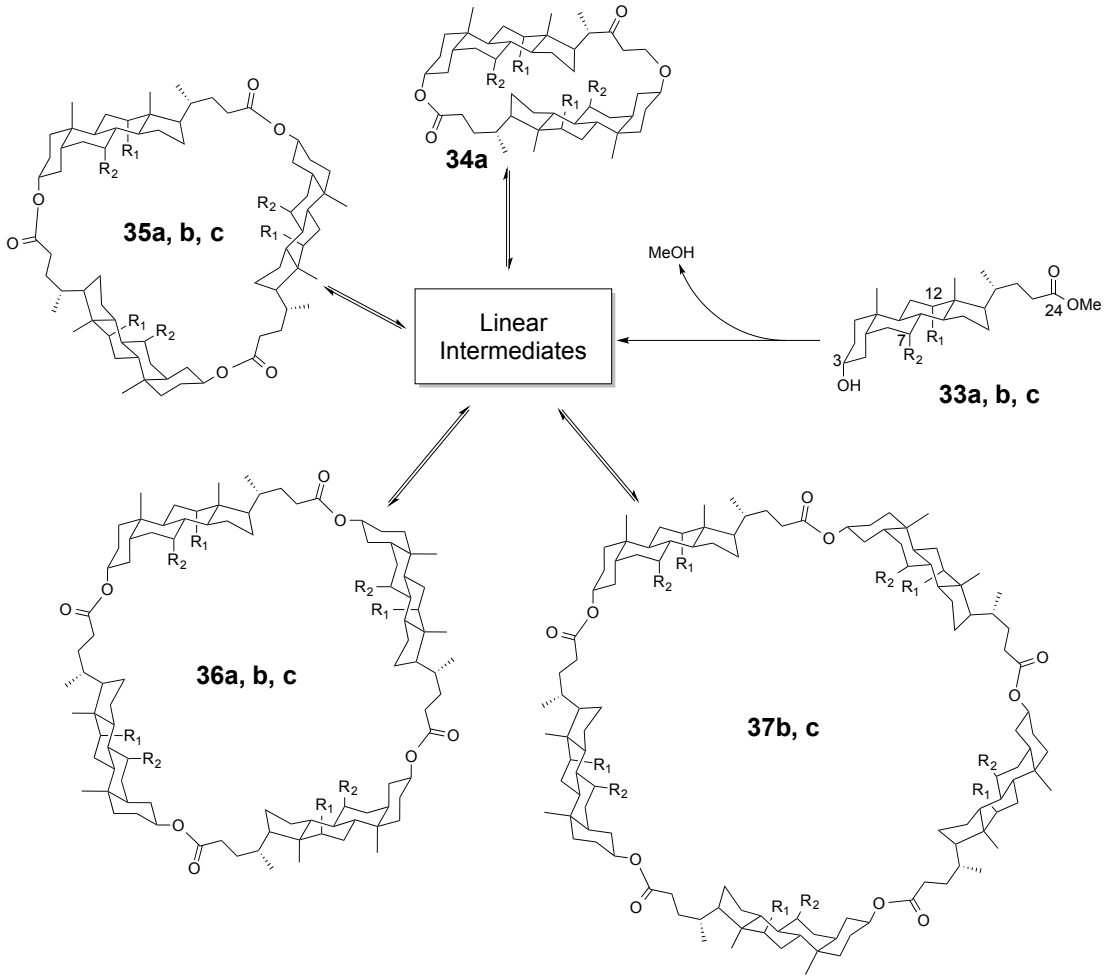

Scheme 1.8 Macrocyclization of cholic acid methyl ester under thermodynamic control. Cyclization condition: KOMe, Dicyclohexyl-18-crown-6, toluene.

it would be convenient to calculate the product distribution simply by UV analysis of HPLC. The result showed that the trimer was the most self-sorted product rather than other cyclic oligomers. Cyclic dimer was only obtained when there was substitution at position 7. The inclination toward trimer of **33c** is less stronger than **33b** was caused by the larger substitution pointing into the cavity from the former. Sanders group continued their work on the demonstration of the thermodynamic and reversible nature of this cyclization. All pure cyclic oligomers were then subjected to the reaction conditions; interestingly, the same products ratio were obtained no matter which cyclic oligomeric starting material was utilized. The theory of thermodynamic cyclizations have been established for two extreme cases: (1) The equation first derived by Jacobson and Stockmeyer and later furthered developed by Mandolini *et al.*[33] assumed that if material is completely strain free with unrestricted rotations, the concentration of larger-size rings is exponentially decaying; (2) If the building block is rigid with fixed internal angles such as Stang's squares[34] or Ogura's hosts,[35] cyclization would give essentially one structure-directed product with negligible amounts of any other products. In Sanders transesterification-type cyclization, the phenomenon arose from cyclocholates was an intermediate case.

The two examples discussed above showed us two important building blocks quinine derivatives and cholate derivatives were applied in supramolecular chemistry for macrocyclizations under thermodynamic control. Only one macrocycle was preferred in both cases, which indicated that self-sorting process happened before the DCL reached its equilibrium. The less stable cyclic oligomers continuously interacted with each other and

sacrificed themselves to generate more of the most stable cyclic oligomer until the whole system reached the thermodynamic minimum. The next section will highlight Nitschke's self-sorting examples of copper-diimine complexes using coordination chemistry method.

1.3.1.3 Self-Sorting of Copper-Imine Complexes

In 2008, Nitschke group reported copper-imine complex self-sorting systems using tetrakis(acetonitrile)copper(I) tetrafluoroborate, 8-quinolinamine (**38)**, 4-methylaniline (**39)**, 2-pyridinecarboxaldehyde (**40)**, 1,10-phenanthroline-2,9-dicarbaldehyde (**41)**, and 2,6-pyridinedicarboxaldehyde (**42)** as building blocks.[28a] The initial inspiration for this research was derived from mimicking living organisms, whose biomolecular machinery is able to create a highly complex set of functional structures form a relatively limited set of basic building blocks. A high degree of compartmentalization happens in the living systems in the process of assembly: although the subcomponents generated from the DCL participate in a wide range of structures formation and interactions that connected them reversibly, biological system has evolved not to interfere with each others' assembly. This compartmentalization often time is physical, *i.e.* two systems are spatially separated by a membrane. However, in prokaryotic systems, this physical compartmentalization is not available so that the system must be dependent on self-sorting to arrange each chemicals' accommodation to avoid the malfunction of the single cell.[14e] Nitschke group's copper-imine complex

system was targeted to describe a self-sorting system in which basic rules that governed the product compartmentalization were discussed. As shown in Scheme 1.9, the reaction

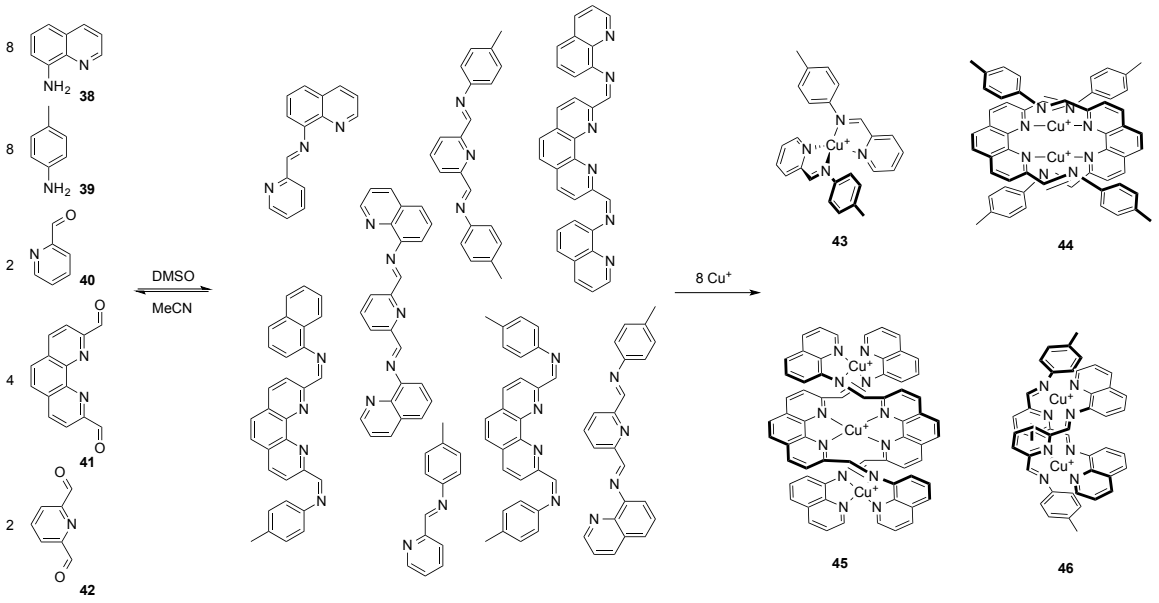

Scheme 1.9 The Cu(I)-templated formation of structures **43**–**46** from amines **38** and **39** together with aldehydes **40**, **41**, and **42**.

of amines **38** and **39** with aldehydes **40**, **41**, and **42** produced a DCL of imines in equilibrium with starting materials and half-formed imines in MeCN/DMSO. After the addition of $CuBF_4$, the system resulted in the clean formation of a mixture of structures **43,**[36] **44,**[37] **45,**[38] **and 46**[39] that were identified by NMR spectroscopy and ESI-MS. Complexes **43**–**46** could also be prepared independently from the constituent subcomponents and Cu(I). It is easy to imagine that there might be more product possibilities from the different subcomponents combinations with Cu(I), but many of them were eliminated during the equilibrium[40] as a consequence of copper's templating effect.[41] This selectivity phenomenon was explained by the Nitschke group as a rule of

valence satisfaction:[39] *the smallest possible structures will be formed in which all Cu(I) ions are tetracoordinate and all nitrogen atoms are bound to a Cu(I) ion.* Di- or trinuclear helicate products would be formed from dialdehydes **40** and **41** since imine ligands derived from these components are poorly configured to chelate a single Cu(I) ion pseudotetrahedrally.[39] Although existing in a very small amout (calculated 1%), complex formed from mixed ligand was occuring, *i.e.*, the product incorporating one ligand from each of **44** and **45**. This product was not detectable by NMR spectroscopy, but was identifiable from ESI-MS. It was also alleged that this rule could be used to predict the outcome of self-sorting reactions from subcomponent systems in Scheme 1.10. Nitschke group also tried to applied the derived rule to a simpler DCL in Scheme 1.10. In

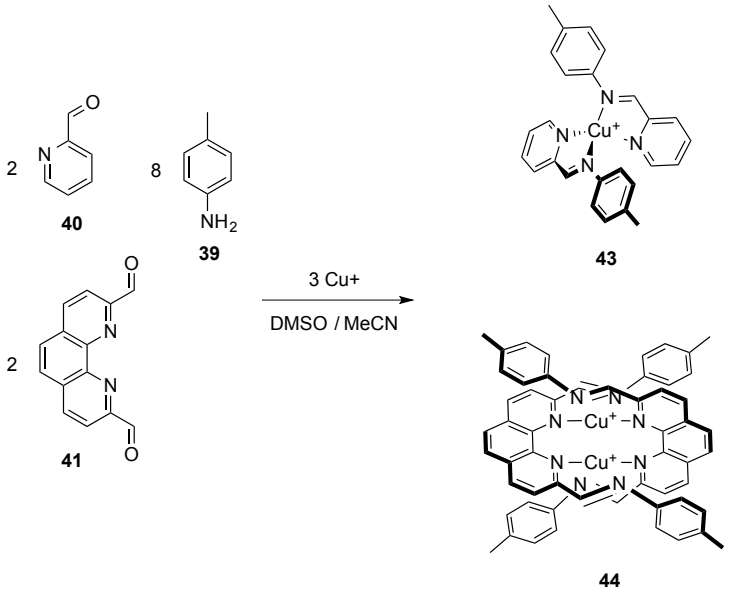

Scheme 1.10 Compounds **39**, **40**, and **41** might only be used to construct the precursors of **43** and **44**.

the presence of one amine **39** and two aldehydes **40** and **41**, the system only allowed two imines to be formed which only led to the formation of complexes **43** and **44**. A more complex system was generated from two amines **38** and **39** and two aldehydes **40** and **41** in Scheme 1.11. When the stoichiometry of **38**, **39**, **40**, **41** equals to 2:4:2:2, the system

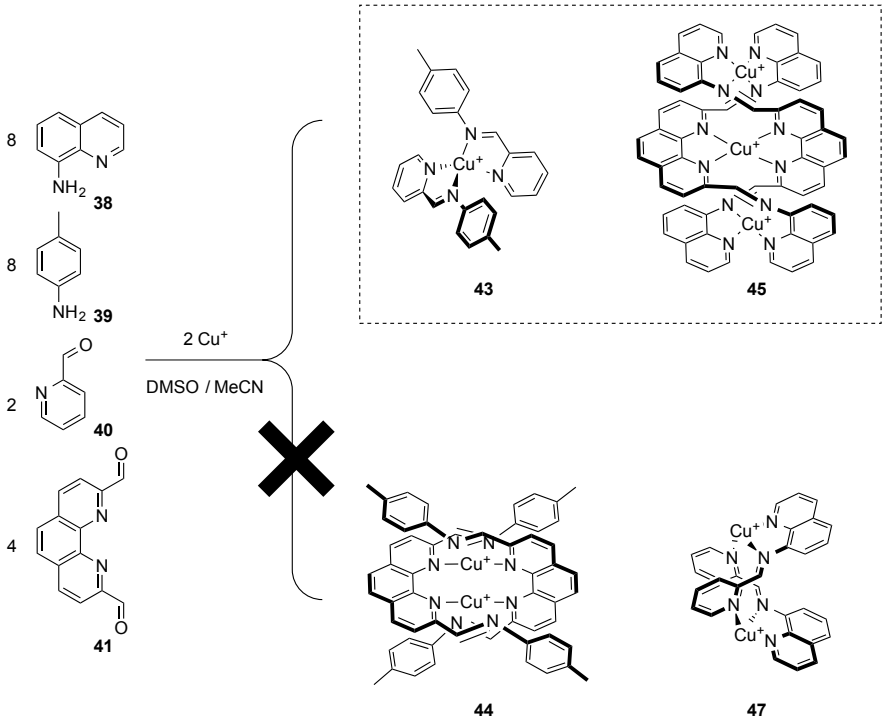

Scheme 1.11 Compounds **43**, **44**, and **45** are all individually allowed, but only **43** and **45** are observed in this system for the given stoichiometry.

only allowed the formation of complex **43** and **45**, which excluded the formation of **44**. Since both dialdehyde **41** and aniline **39** were present in the system, it apparently permitted the evolution of complex **44**. The removal of **41** and **39** from the system would leave **40** and **38** to form complex **47**, which was disobeying the rule that led to the suppression of complex **44**. So, only complex **43** and **45** could only be observed. Based

upon these two examples, it was concluded that the prediction of outcomes are not only dependent on the stability of individual products; the valence satisfaction rule should be applied to the system as a whole, *i.e.* all product structures must collectively obey the rule.

1.3.2 Kinetic Control of Self-Sorting

1.3.2.1 Dynamic Chiral Resolution of Esters

Compared to thermodynamic self-sorting, self-sorting under kinetic control has received less attention so far since it required the system to add a "kinetic stop" to regulate its equilibration, to which more accurate controls needs to be applied.[25b] The concept of combining DCC with kinetically controlled reactivity has plenty of advantages: (1) irreversible reactions allows the generation of stable and isolable products; (2) allows the isolation of thermodynamically not the most stable product from DCLs; (3) chemical systems under both thermodynamic and kinetic control may give better illustration to living systems. In this section, examples representing the application of both thermodynamic and kinetic control will be reviewed.

In 2007, Ramström group reported their kinetically controlled self-sorting experiment using nitroaldol (Henry) reaction and lipase-mediated acylation.[42] Nitroaldol reaction was the first time been applied to generate a DCL.[42a] It was alleged by Ramström group that new reaction types were needed for the rapid generation and screening of sufficiently stable DCLs. With the exception of the robust alkene metathesis

reaction, C−C bond formation has only been explored in a few cases.[43] Because of the significance of C−C bond formation in synthetic organic chemistry, the use of reversible C−C bond formation reaction for DCL generation and the later kinetic trapping may help to develop new dynamic combinatorial systems and achieve discovery of new compounds.

Ramström group first optimized the nitroaldol reaction in order to fit its use in the dynamic combinatorial resolution (DCR) process. Screening of bases was initially carried out to find suitable conditions for DCL generation. Firstly, the reactions were carried out in the presence of 1 equivalent each of the nitroalkane, the aldehyde, and the base; reactions were monitored by ^{1}H NMR spectroscopy by comparing the signals of the aldehydes with those of the nitroaldol adducts. Triethylamine was found to be the optimal base to the system to achieve the stable equilibration and the compatibility to the following enzymatic catalysis step. Secondly, the DCL was established in Scheme 1.12;

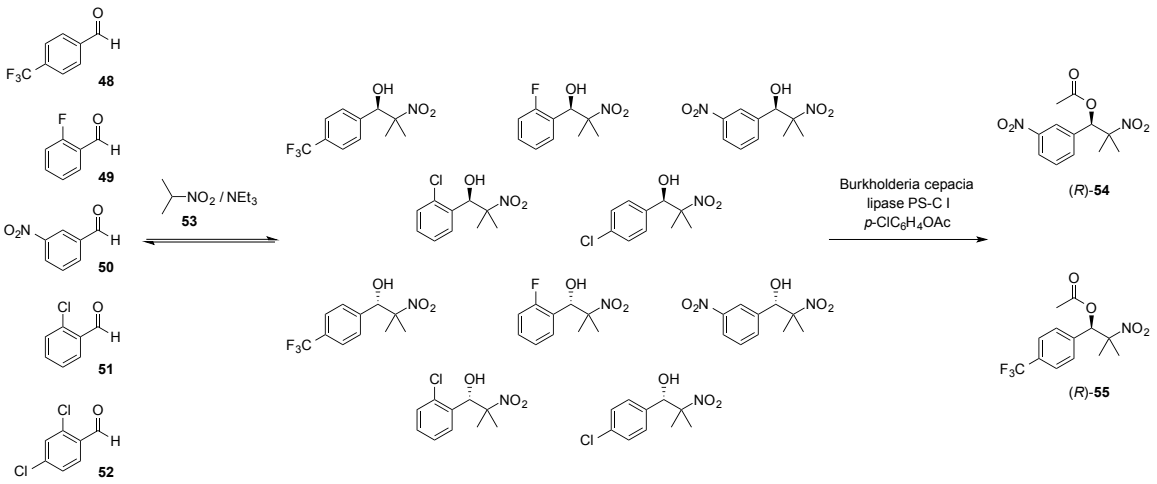

Scheme 1.12 Generation of a dynamic nitroaldol library and lipase-mediated asymmetric resolution.

equimolar amounts of **48–52** were treated with 1 equivalent of **53** to generated a DCL containing ten nitroaldol adducts. Because of the slightly different molar ratio of the aldehydes to the nitroalkane (5:1) in this Henry reaction, the quantity of base used was increased to 10 equivalent to have a reasonable equilibration. Within hours, the system reached to the equilibrium to attain 10 nitroaldol adducts, which were characterized by ^{1}H NMR spectroscopy. In order to solve the enantiomeric purity issue of the whole system, Ramström group tried to use lipase[44] to conduct this DCR. It was also claimed by them that the lipase-catalyzed transesterification of *β*-nitroalcohol substrates has not been reported. After the initial lipase and acyl donor screening, the lipase PS-C I from *Pseudomonas cepacia* and *p*-chlorophenyl acetate were selected to be the optimal catalyst and acyl donor in this DCR system. The lipase PS-C I and *p*-chlorophenyl acetate (5 equivalent) were added together to the nitroaldol library at 40 °C without stirring. The transesterification process was characterized by ^{1}H NMR spectroscopy, which only gave two resolved products. It was found out that the major product was from the aldehyde **50** and 2-nitropropane **53** adduct, which was among the lowest concentration in the DCL before this transformation. Except for the (*R*)-**54** adduct formation; a minor amount of ester (*R*)-**55** was also formed in the reaction. Those two products were obtained in a combined overall yield of 24% after 24 hours. A better yield 80% could be acquired ((*R*)-**54** adduct: 52%, (*R*)-**55** adduct: 33%) after 14 days; the reaction proceeded to completion (95% yield) after 20 days. It was concluded that nitroaldol (Henry) reaction was identified as a new and efficient reaction for DCL generation. Furthermore, it was demonstrated that the DCL under thermodynamic control could be coupled to an

enzymatic DCR process, which would resolve an enantiomerically complex DCL to only two products. The lipase PS-C I from *Pseudomonas cepacia* was also found to be a suitable transesterification catalyst to the 2-nitroalcohol and *p*-chlorophenyl acetate system.

1.3.2.2 Oxidative Self-Sorting of Imines

Miljanić group also developed self-sorting systems under kinetic control. In 2011, we presented a kinetic self-sorting of an imine DCL that occurred during a slow irreversible oxidation.[45] This work was carried out based on the theoretical derivation from the well-known Curtin–Hammett principle.[46] They first conducted simple experiment to prove the hypothesis, namely that *a quickly equilibrating mixture will spontaneously simplify (self-sort) if its components react at very different rates in a slow irreversible reaction.* The oxidative cyclization of aldimines derived from *o*-hydroxy- and *o*-aminoaniline to benzoxazoles and benzimidazoles were chosen as the tool in their research (Scheme 1.13).[47] This oxidative cyclization was selected for the following reasons: (1) the aldimines are generated reversibly as an intermediate; (2) the oxidation step is irreversible; (3) the rate of oxidation step could be modified by substitution of substrates. For example, the reaction between diaminobenzene (**56**) and benzaldehyde (**58**) gave imine (**59**) as an intermediate, which was oxidized *in situ* upon the addition of I_2 to give benzimidazole **61** in 90% yield. It occurred analogously to 2-aminophenol (**57**) to give benzoxazole **62** in 86% yield without the need to isolate imine **60** (Scheme 1.13,

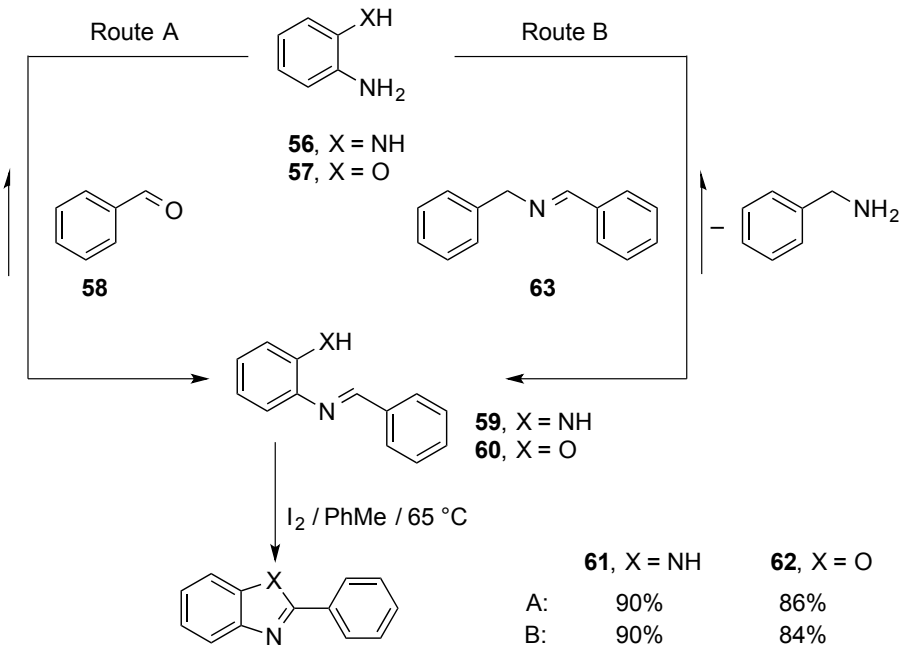

Scheme 1.13 Synthesis of benzazoles by oxidative cyclization of directly (Route A) and indirectly (Route B) prepared imines.

Route A). With the determination of successful oxidative cyclization without isolation of the imine intermediates, Miljanić group moved onto a basic self-sorting system (Scheme 1.13, Route B). Aniline **56** and **57** were treated with imine **63** to generate a DCL containing **56**, **59**, **63**, and benzylamine, which were determined by ^{1}H NMR spectroscopy. Later, I_2 was added to initiate the oxidative cyclization. While **59** was dissipated, **56** and **63** would react further to compensate its loss until all **56** was used up. Eventually, the obtained products included benzylamine and **61** (90% yield). In conclusion, both amines **56** and **57** can produce oxidizable imines (Route A) and extract benzaldehyde out of its nonoxidizable imine **63** (Route B). Both route A and route B gave high yield of benzazoles **61** and **62** independent of direct or indirect oxidation.

After these successful prototype reaction, they continued to construct a [2×2] system using amines **56** and **57** and aldehydes **64** and **65** as the starting materials (Scheme 1.14). As expected, all four imines were formed and could be identified by ^{1}H NMR spectroscopy. The oxidation was initiated by the slow addition of I_2, which oxidized the most electron rich imine **67** the first, to give benzimidazole **70**. This

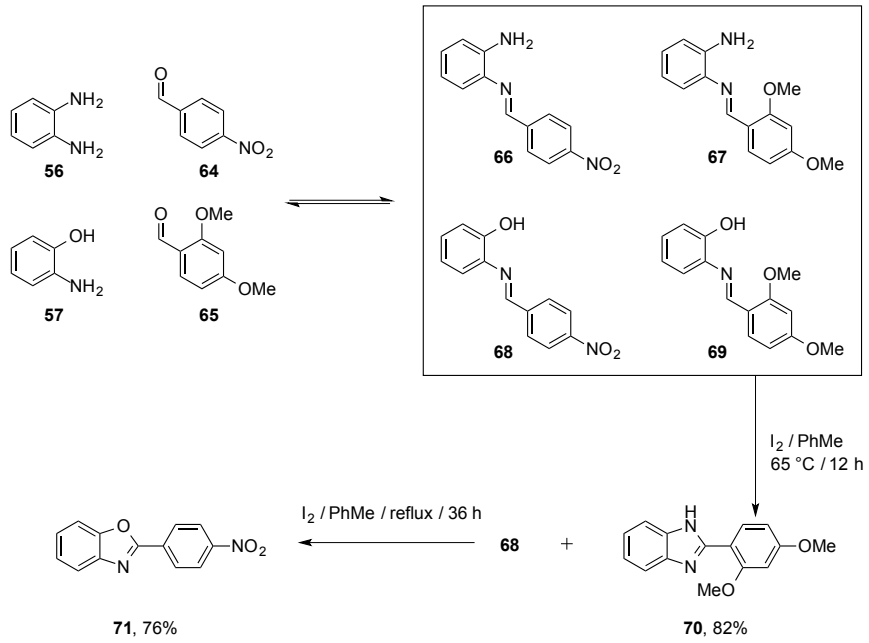

Scheme 1.14 Oxidative self-sorting of a [2×2] mixture of imines.

irreversible oxidation temporarily broke the equilibrium of the system, so that the remaining three imines **66**, **68**, and **69** reequilibrated to produce more of **67**. Ultimately, the [2×2] system resulted in a mixture of **70** (82%) and the most electron poor imine **68**, which could be oxidized under reflux after long and exposure to I_2 to give 76% of benzoxazole **71**. This [2×2] experiment indeed showed a self-sorting scenario during the oxidation process; the only two products are derived from the most electron-rich and the

most electron-poor imines. The success of the [2×2] system encouraged an approach to a more complex [3×3] self-sorting system (Scheme 1.15). Three amines **56**, **57**, **72**, and

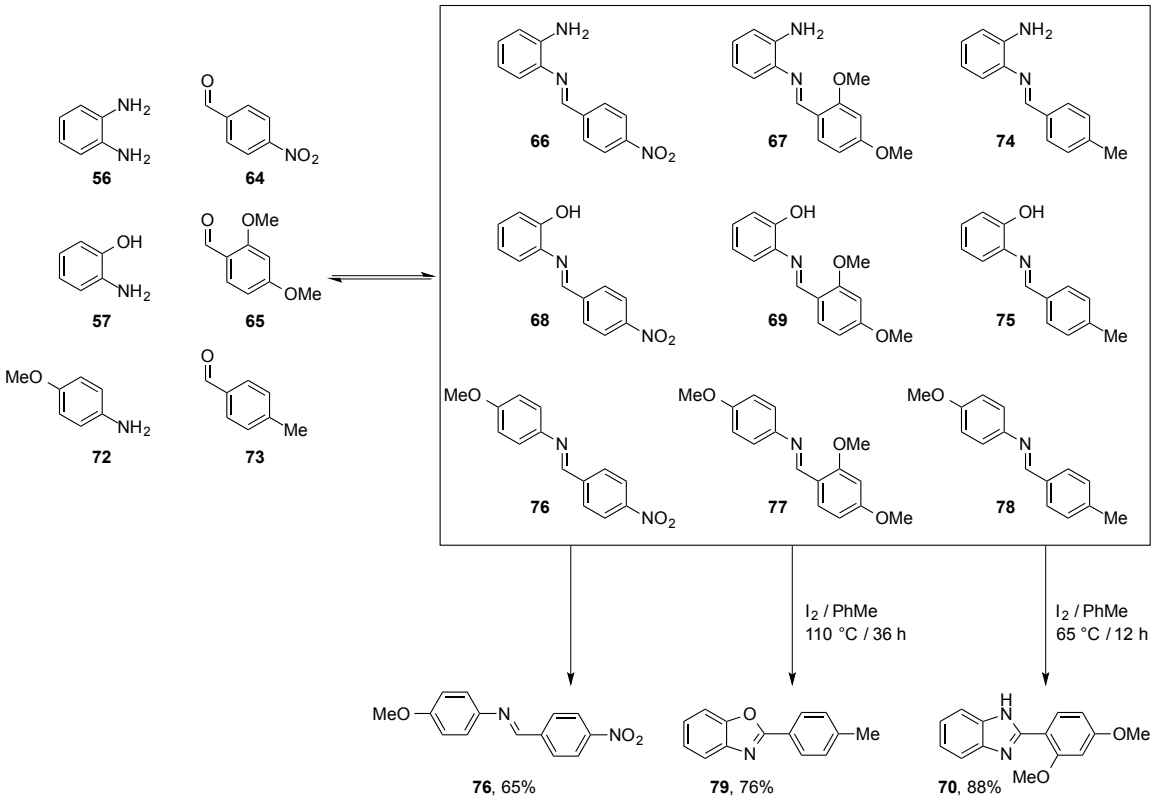

Scheme 1.15 Oxidative self-sorting of a [3×3] mixture of imines.

three aldehydes **64**, **65**, **73** were combined together to give a DCL containing all nine possible imines from which six of them generated from **56** and **57** are oxidizable by I_2. Understandably, the first equivalent of I_2 addition oxidized the most electron rich imine **67** to benzimidazole **70**. The second stage oxidation required higher temperature and prolonged time to afford benzoxazole **79**. Finally, the most electron deficient and non-oxidizable imine **76** was left in the system as the residue. Three major products gave yields 88%, 76%, and 65% respectively after the workup. In conclusion, Miljanić group

has demonstrated a very unique example of self-sorting during the oxidative cyclization. This self-sorting process was kinetically driven while it was thermodynamically enabled since the sorted product was not dependent on the stability of individuals from the DCL but solely relied on their reactivity toward oxidation process. In the next section, more examples using imines to generate DCLs but under different type of kinetic control will be discussed.

1.3.2.3 Distillative Self-Sorting of Imines

Reactive distillation (RD) is a protocol ubiquitous in chemical industry, wherein a chemical reactor is combined with a distillation still. The commercial success of RD was expanded because of the enormous demand for methyl *tert*-butyl ether and high purity methyl acetate. Eastman Kodak is one of the pioneers in improving the process of compacting the chemical plant into a single RD for high purity methyl acetate production. This process demonstrated its ability to render cost-effectiveness and compactness to the chemical plant, and has been explored to expand to several other chemical reactions such as hydration, alkylation, acetalization, and hydrogenation.

Imines are formed reversibly with an aldehyde and an amine. Multiple imines can readily exchange their aldehyde and amine constituents in a solution. In this equilibrating mixture, each imine has their own individual boiling point and one of them has the lowest boiling point. If that imine could be removed from the mixture by distillation, the

equilibrium would be disabled and the system has to reequilibrate to make more of the lightest imine until its complete elimination. This is claimed originally by the Le Châtelier principle. In this scenario, the distilled imines could be produced in excellent yield and the complexity of the DCL could be reduced at the same time. Provided that this process is repeated, multiple chemicals could be produced using a single distillation setup.

In the first experiment, Miljanić group set up a [2×2] system in Scheme 1.16.[48] Two aldehydes **58** and **80** and two amines **81** and **72** were subjected under dehydrative condition to give four imines **82**, **83**, **84**, and **85**. The most volatile imine among the four

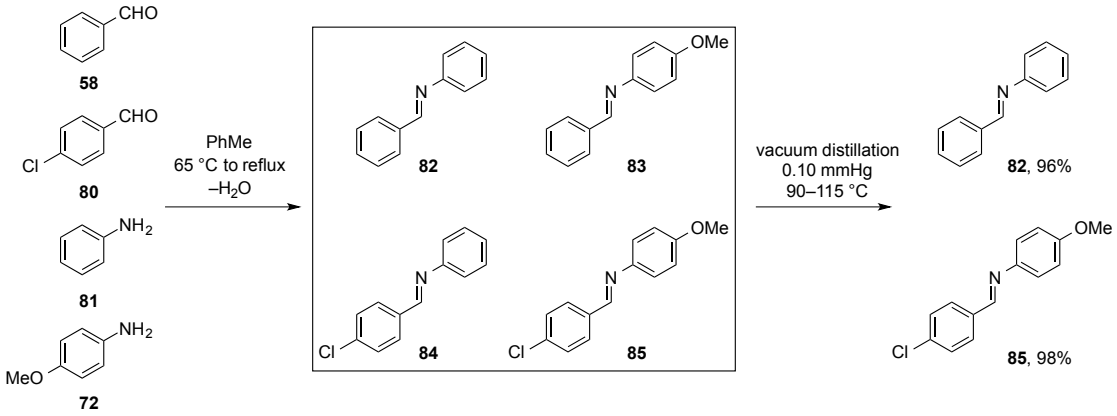

Scheme 1.16 Simplification of a [2×2] mixture of imines during the course of a vacuum distillation.

was **82** and the least volatile imine was **85**. The mixture was then subjected under vacuum distillation (90–115 °C, 0.10 mmHg) to remove imine **82** selectively. During the vacuum distillation, **83** and **84** started to equilibrate to make more of **82** and **85** as a response to the loss of **82** from the system. Eventually, imines **82** and **85** were isolated as the distillate and residue, respectively, in very high yield and purity (98 and 99%). The

success of [2×2] experiment promoted them to a more complex [3×3] system (Scheme 1.17). A DCL containing nine imines was established from aldehydes **58**, **80**, and **86** and amines **81**, **72**, and **87**, among which imine **82** had the lowest boiling point. The preliminary vacuum distillation (100–120 °C, 0.10 mmHg) started to remove **82** from the system and triggered equilibration to generate additional amount of imines **82**, **85**, **89**, **91**, and **92** from imines **83**, **88**, **84**, and **90**. Once **82** has been distilled as the first distillate

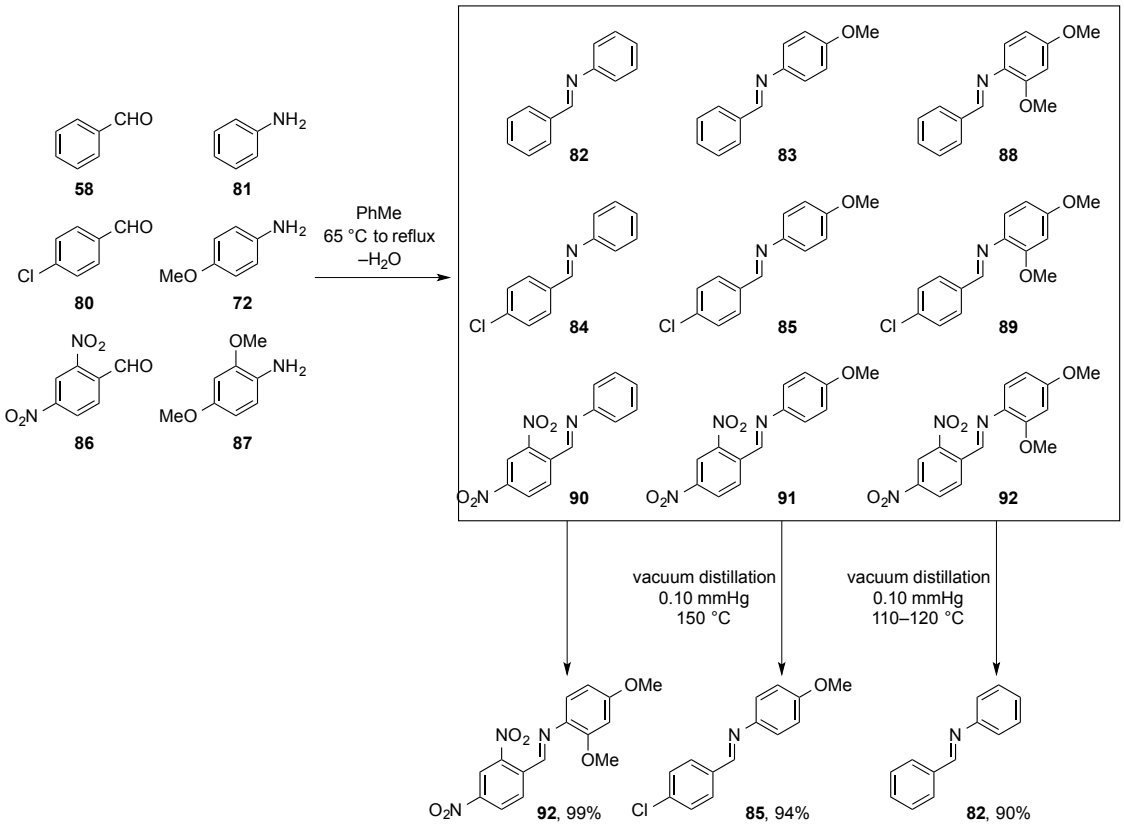

Scheme 1.17 Simplification of a [3×3] mixture of imines during the course of a vacuum distillation.

(yield 90%), the [3×3] system was reduced to a simpler [2×2] system involving **85**, **89**, **91**, and **92**. The next step vacuum distillation (150 °C, 0.10 mmHg) continued to bring

down the complexity of the system to give **85** (94% yield) as the second distillate and **92** (99% yield) as the residue. In the following experiment, Miljanić group also effectively accomplished reactive distillation of [4×4] and [5×5] system. It was concluded that this distillative protocol might have their industrial relevance in reactive distillation of other chemical systems.

1.4 Conclusion

This chapter briefly introduced the phenomenon of self-sorting from early examples of Isaacs and Weck's group and compared thermodynamically controlled with kinetically controlled self-sortings from Lehn, Sanders, Nitschike, Ramström, and Miljanić group's work. DCC has manifested itself as a promising and powerful tool for generating and exploring novel chemical systems. DCLs, as complex molecule mixtures, have provided chances for us to learn emergent properties of existing and new chemistry systems and would be used as a platform to solve potential industrial problems in terms of capital saving, purification integration, and new compound discovery. Chapter 2 discusses self-sorting based on ester reactive distillation and its potential future application in chemical industry. Chapter 3 shows how to use ester scent chemicals and distillation technique to teach students about transesterification in a unique way. Chapter 4 details the discovery of two macrocycle molecules, which we name *cyclotribenzoin* and *cyclotetrabenzoin* using benzoin condensation.

1.5 References

[1] Reek, J. N. H.; Otto S. *Dynamic Combinatorial Chemistry;* Wiley-VCH: Weinheim, Germany, **2010**.

[2] (a) Darmstaedter, L. *J. Chem. Educ.* **1928**, *5*, 36–42. (b) Hudson, C. S. *J. Chem. Educ.* **1941**, *18*, 353–357. (c) Bowman-James, K. *Acc. Chem. Res.* **2005**, *38*, 671–678 and references therein.

[3] Watson, J. D.; Crick, F. H. C. *Nature,* **1953,** *171,* 737–738.

[4] Siedel, F. *Chem. Ber.* **1926,** *59B,* 1894–1908.

[5] Melson, G. A.; Busch, D. H. *J. Am. Chem. Soc.* **1965,** *87,* 1706–1710.

[6] (a) Linstead, R. P. *J. Chem. Soc.* **1934,** 1016–1017. (b) Byrne, G. T.; Linstead, R. P.; Lowe, A. R. *J. Chem. Soc.* **1934,** 1017–1022.

[7] Thompson, M. C.; Busch, D. H. *J. Am. Chem. Soc.* **1964,** *86,* 213–217.

[8] Thompson, M. C.; Busch, D. H. *J. Am. Chem. Soc.* **1962,** *84,* 1762–1763.

[9] Goodman, M. S.; Jubian, V.; Linton, B.; Hamilton, A. D. *J. Am. Chem. Soc.* **1995,** *117,* 11610–11611.

[10] Bilyk, A.; Harding, M. M. *J. Chem. Soc., Chem. Commun.* **1995,** 1697–1698.

[11] Brady, P. A.; Bonar-Law, R. P.; Rowan, S. J.; Suckling, C. J.; Sanders, J. K. M. *Chem. Commun.* **1996,** 319–320.

[12] Hasenknopf, B.; Lehn, J.-M.; Boumediene, N.; Dupont-Gervais, A.; VanDorsselaer, A.; Kneisel, B.; Fenske, D. *J. Am. Chem. Soc.* **1997,** *119,* 10956–10962.

[13] (a) Black, S. P.; Sanders, J. K. M.; Stefankiewicz, A. R. *Chem. Soc. Rev.* **2014**, *43*, 1861–1872. (b) Jin, Y.; Wang. Q.; Taynton, P.; Zhang, W. *Acc. Chem. Res.* **2014**, *47*, 1575–1586. (c) Belowich, M. E.; Stoddard, J. F. *Chem. Soc. Rev.* **2012**, *41*, 2003–2024. (d) Rowan, S. J.; Cantrill, S. J.; Cousins, G. R. L.; Sanders, J. K. M.; Stoddard, J. F. *Angew. Chem. Int. Ed.* **2002**, *41*, 899–952.

[14] (a) Liu, S. M.; Ruspic, C.; Mukhopadhyay, P.; Chakrabarti, S.; Zavalij, P. Y.; Isaacs, L. *J. Am. Chem. Soc.* **2005,** *127,* 15959–15967. (b) Mukhopadhyay, P.; Wu, A. X.; Isaacs, L. *J. Org. Chem.* **2004,** *69,* 6157–6164. (c) Mukhopadhyay, P.; Zavalij, P. Y.; Isaacs, L. *J. Am. Chem. Soc.* **2006,** *128,* 14093–14102. (d) Wu, A. X.; Chakraborty, A.; Fettinger, J. C.; Flowers, R. A.; Isaacs, L. *Angew. Chem. Int. Ed.* **2002,** *41,* 4028–4031. (e) Wu, A. X.; Isaacs, L. *J. Am. Chem. Soc.* **2003,** *125,* 4831–4835.

[15] For a review on H-bond geometry, see: Taylor, R; Kennard, O. *Acc. Chem. Res.* **1984**, *17*, 320–326. For **1a•1a**, the two external amide protons are strongly H-

bonded to the internal amide C=O groups with typical separations (N···O 2.937 Å, H···O 2.088 Å) and angles (N–H···O 162.0°), whereas the structural data indicates that the internal amide N–H groups may benefit from weaker interactions with the ureidyl C=O moiety (N···O 2.909 Å, H···O 2.240 Å; N–H···O 132.6°). For (+)-**2b**•(−)-**2b**, the two external amide protons H-bonded to the internal amide C=O groups have typical geometries (N···O 2.860 Å, H···O 2.014 Å; N–H···O 160.8°), whereas the internal amide protons clearly do not benefit from additional interactions (N···O 3.296 Å, H···O 2.683 Å).

[16] (a) Rowen, A. E.; Elemans, J. A. A. W.; Nolte, R. J. M. *Acc. Chem. Res.* **1999**, *32*, 995–1006. (b) Jansen, R. J.; de Gelder, R.; Rowan, A. E.; Scheeren, H. W.; Nolte, R. J. M. *J. Org. Chem.* **2001**, *66*, 2643–2653. (c) Chen, C.-W.; Whitlock, H. W. *J. Am. Chem. Soc.* **1978**, *100*, 4921–4922; (d) Zimmerman, S. C.; VanZyl, C. M. *J. Am. Chem. Soc.* **1987**, *109*, 7894–7896; (e) Zimmerman, S. C. *Top. Curr. Chem.* **1993**, *165*, 71–102; (f) Harmata, M.; Barnes, C. L.; Karra, S. R.; Elahmad, S. *J. Am. Chem. Soc.* **1994**, *116*, 8392–8393; (g) Klärner, F.-G.; Burkert, U.; Kamieth, M.; Boese, R.; Benet-Buchholz, J. *Chem. Eur. J.* **1999**, *5*, 1700–1707; (h) Brown, S. P.; Schaller, T.; Seelbach, U. P.; Koziol, F.; Ochsenfeld, C.; Klärner, F.-G.; Spiess, H. W. *Angew. Chem. Int. Ed.* **2001**, *40*, 717–720.

[17] Wu, A. X.; Isaacs, L. *J. Am. Chem. Soc.* **2003**, *125*, 4831–4835.

[18] (a) Cai, M.; Shi, X.; Sidorov, V.; Fabris, D.; Lam, Y.-F.; Davis, J. T. *Tetrahedron* **2002**, *58*, 661–671. (b) Castellano, R. K.; Nuckolls, C.; Rebek, J., Jr. *J. Am. Chem. Soc.* **1999**, *121*, 11156–11163. (c) Jolliffe, K. A.; Timmerman, P.; Reinhoudt, D. N. *Angew. Chem., Int. Ed. Engl.* **1999**, *38*, 933–937. (d) Beijer, F. H.; Sijbesma, R. P.; Kooijman, H.; Spek, A. L.; Meijer, E. W. *J. Am. Chem. Soc.* **1998**, *120*, 6791–6769. (e) Wyler, R.; de Mendoza, J.; Rebek, J., Jr. *Angew. Chem., Int. Ed. Engl.* **1993**, *32*, 1699–1701. (f) Hof, F.; Palmer, L. C.; Rebek, J., Jr. *J. Chem. Ed.* **2001**, *78*, 1519–1521.

[19] (a) Gerhardt, W.; Črne, M.; Weck, M. *Chem. –Eur. J.* **2004**, *10*, 6212–6221. (b) Pollino, J. M.; Weck, M. *Chem. Soc. Rev.* **2005**, *34*, 193–207. (c) Burd, C.; Weck, M. *Macromolecules*, **2005**, *38*, 7225–7230. (d) South, C. R.; Burd, C.; Weck, M. *Acc. Chem. Res.* **2007**, *40*, 63–74. (e) Weck, M. *Polym. Int.* **2007**, *56*, 453–460.

[20] (a) Pollino, J. M.; Stubbs, L. P.; Weck, M. *J. Am. Chem. Soc.* **2004**, *126*, 563–567. (b) Burd, C.; Weck, M. *J. Polym. Sci. A Polym. Chem.* **2008**, *46*, 1936–1944.

[21] (a) Stubbs, L. P.; Weck, M. *Chem. Eur. J.* **2003**, *9*, 992–999. (b) Pollino, J. M.; Stubbs, L. P.; Weck, M. *Macromolecules* **2003**, *36*, 2230–2234. (c) Pollino, J. M.; Weck, M. *Synthesis* **2002**, 1277–1285.

[22] (a) Fürstner, A. *Angew. Chem. Int. Ed.* **2000**, *39*, 3012–3043. (b) Trnka, T. M.; Grubbs, R. H. *Acc. Chem. Res.* **2001**, *34*, 18–29.

[23] (a) Wan, Y.; Mitkin, O.; Barnhurst, L.; Kurchan, A.; Kutateladze, A. *Org. Lett.* **2000**, *2*, 113–131. (b) Kim, K. *Chem Soc. Rev.* **2002**, *31*, 96–107. (c) Balzani, V.; Credi, A.; Venturi, M. *Proc. Natl. Acad. Sci. USA* **2002**, *99*, 4814–4817. (d) Brinke, G. T.; Ikkala, O. *Chem. Rev.* **2004**, *4*, 219–230. (e) Cooke, G.; Garety, J. F.; Hewage, S. G.; Jordan, B. J.; Rabani, G.; Rotello, V. M.; Woisel, P. *Org. Lett.* **2007**, *9*, 481–484.

[24] (a) Coskun, A.; Spruell, J. M.; Barin, G.; Dichtel, W. R.; Flood, A. H.; Botros, Y. Y.; Stoddard, J. F. *Chem. Soc. Rev.* **2012**, *41*, 4827–4859. (b) Grunder, S.; McGrier, P. L.; Whalley, A. C.; Boyle, M. M.; Stern, C.; Stoddart, J. F. *J. Am. Chem. Soc.* **2013**, *135*, 17691–17694.

[25] (a) Osowska, K.; Miljanić, O. Š. *Synlett* **2011**, *12*, 1643–1648. (b) Ji, Q.; Lirag, R. C.; Miljanić, O. Š. *Chem. Soc. Rev.* **2014**, *43*, 1873–1884.

[26] Krämer, R.; Lehn, J.-M.; Marquis-Rigault A. *Proc. Natl. Acad. Sci.* **1993**, *90*, 5394–5398.

[27] (a) Rowan, S. J.; Brady, P. A.; Sanders, J. K. M *Angew. Chem. Int. Ed. Engl.* **1996**, *35*, 2143–2145. (b) Brady, P. A.; Bonar-Law, R. P.; Rowan, S. J.; Suckling, C. J.; Sanders, J. K. M. *Chem. Commun.* **1996**, 319–320. (c) Rowan, S. J.; Hamilton, D. G.; Brady, P. A.; Sanders, J. K. M. *J. Am. Chem. Soc.* **1997**, *119*, 2578–2579. (d) Brady, P. A.; Sanders, J. K. M. *J. Chem. Soc., Perkin Trans.* **1997**, *1*, 3237–3253.

(e) Rowan, S. J.; Reynolds, D. J.; Sanders, J. K. M. *J. Org. Chem.* **1999**, *64*, 5804–5814. (f) Kaiser, G.; Sanders, J. K. M. *Chem. Commun.* **2000**, 1763–1764. (g) Rowan, S. J.; Brady, P. A. Sanders, J. K. M. *Tetrahedron Lett.* **1996**, *37*, 6013–6016.

[28] (a) Sarma, R.; Nitschke, J. R. *Angew. Chem. Int. Ed.* **2008**, *47*, 377–380. (b) Hutin, M.; Cramer, C. J.; Gagliardi, L.; Shahi, A. R. M.; Bernardinelli, G.; Cerny, R.; Nitschke, J. R. *J. Am. Chem. Soc.* **2007**, *129*, 8774–8780. (c) Campbell, V. E.; de Hatten, X.; Delsuc, N.; Kauffmann, B.; Huc, I.; Nitschke, J. R. *Nat. Chem.* **2010**, *2*, 684–687.

[29] Wynberg H. *Topics in Stereochemisrry;* Interscience, New York, **1986**.

[30] Paterson, I.; Yeung, K. S.; Ward, R. A.; Smith, J. D.; Cumming J. G.; Lamboley, S. *Tetrahedron* **1995**, *51*, 9467–9486.

[31] (a) Baker, W.; Gilbert B.; Ollis, W. D. *J. Chem. Soc.* **1952**, 1443–1446; (b) Almog, J.; Baldwin, J. E.; Dyer R. L.; Peters, M. *J. Am. Chem. Soc.* **1975**, *97*, 226–227; (c) Bonar-Law R. P.; Sanders, J. K. M. *J. Am. Chem. Soc.* **1995**, *117*, 259–271.

[32] Pedersen, C. J. *J. Am. Chem. Soc.* **1967**, *89*, 7017–7036.

[33] (a) Jacobson H.; Stockmayer, W. *J. Chem. Phys.* **1950**, *18*, 1600–1606; (b) Ercolani, G.; Mandolini, L.; Mencarelli P.; Roelens, S. *J. Am. Chem. Soc.* **1993**, *115*, 3901–3908.

[34] Stang, P. J.; Chen K.; Arif, A. M. *J. Am. Chem. Soc.* **1995**, *117*, 8793–8797.

[35] Fujita, M.; Nagao S.; Ogura, K. *J. Am. Chem. Soc.* **1995**, *117*, 1649–1650.

[36] Schultz, D. Nitschke, J. R. *J. Am. Chem. Soc.* **2006**, *128*, 9887–9892.

[37] Nitschke, J. R.; Schultz, D.; Bernardinelli, G.; Gérard, D. *J. Am. Chem. Soc.* **2004**, *126*, 16538–16543.

[38] Hutin, M.; Franz, R.; Nitschke, J. R. *Chem. Eur. J.* **2006**, *12*, 4077–4082.

[39] Hutin, M.; Bernardenelli, G.; Nitschke, J. R. *Proc. Natl. Acad. Sci. USA* **2006**, *103*, 17655–17660.

[40] Voshell, S. M.; Lee, S. J.; Gagne, M. R. *J. Am. Chem. Soc.* **2006**, *128*, 12422–12423.

[41] (a) Busch, D. H. *Science* **1971**, *171*, 241–248. (b) Brooker, S.; Lan, Y.; Price, J. R. *Dalton Trans.* **2007**, 1807–1820.

[42] (a) Vongvilai, P.; Angelin, M.; Larsson, R.; Ramström, O. *Angew. Chem. Int. Ed.* **2007**, *46*, 948–950. (b) Vongvilai, P.; Larsson, R.; Ramström, O. *Adv. Synth. Catal.*

2008, *350*, 448–452. (c) Vongvilai, P.; Ramström, O. *J. Am. Chem. Soc.* **2009**, *131*, 14419–14425. (d) Sakulsombat, M.; Vongvilai, P.; Ramström, O. *Org. Biomol. Chem.* **2012**, *9*, 1112–1117. (e) Sakulsombat, M.; Zhang, Y.; Ramström, O. *Chem. Eur. J.* **2012**, *18*, 6129–6132. (f) Zhang, Y.; Hu, L.; Ramström, O. *Chem. Commun.* **2013**, *49*, 1805–1807.

[43] (a) Boul, P. J.; Reutenauer, P.; Lehn, J.-M. *Org. Lett.* **2005**, *7*, 15–18. (b) Lins, R. J.; Flitsch, S. L. Turner, N. J.; Irving, E.; Brown, S. A. *Tetrahedron* **2004**, *60*, 771–780. (c) Lins, R. J.; Flitsch, S. L. Turner, N. J.; Irving, E.; Brown, S. A. *Angew. Chem. Int. Ed.* **2002**, *41*, 3405–3407. (d) Henry, L.; *C. R. Hebd. Seances Acad. Sci.* **1895**, *120*, 1265.

[44] (a) Gotor-Fernandez, V.; Brieva, R.; Gotor, V. *J. Mol. Catal. B* **2006**, *40*, 111–120. (b) Breuer, M.; Ditrich, K.; Habicher, T.; Hauer, B.; Kesseler, M.; Sturmer, R.; Zelinski T. *Angew. Chem. Int. Ed.* **2004**, *43*, 788–824. (c) Schmid, A.; Dordick, J. S.; Hauer, B.; Kiener, A.; Wubbolts, M.; Witholt, B. *Nature* **2001**, *409*, 258–268.

[45] Osowska, K.; Miljanić, O. Š. *J. Am. Chem. Soc.* **2011**, *133*, 724–727.

[46] (a) Curtin, D. Y. *Rec. Chem. Prog.* **1954**, *15*, 111–128. (b) Seeman, J. I. *Chem. Rev.* **1983**, *83*, 83–134. (c) Seeman, J. I. *J. Chem. Educ.* **1986**, *63*, 42–48.

[47] (a) Li, Y.; Wang, Y.-L.; Wang, J.-Y. *Chem. Lett.* **2006**, *35*, 460–461. (b) Ponnala, S.; Sahu, D. P. *Synth. Commun.* **2006**, *36*, 2189–2194.

[48] Osowska, K.; Miljanić, O. Š. *Angew. Chem. Int. Ed.* **2011**, *50*, 8345–8349.

Chapter Two Iterative Ester Reactive Distillation: Experimental Design and Characterization[1]

2.1 Introduction

Living organisms have achieved an exquisite level of spatiotemporal control of synthetic chemistry. Within the highly complex chemical mixtures present in a typical cell, hundreds of simultaneous reactions occur without interference, creating dozens of products with absolute chemo-, regio-, and stereoselectivity. Replicating this synthetic prowess in unnatural systems would yield insights of relevance to prebiotic chemistry,[2] allow expedient discovery of new reactions, and possibly dramatically reduce construction and energy costs in the chemical industry, since multiple value-added chemicals could be concurrently produced in a single reactor.

In an effort to achieve analogous selective synthesis starting from "messy" precursor mixtures, our group has been studying how dynamic combinatorial libraries (DCLs),[3] complex equilibrating mixtures of structurally related compounds, simplify in response to external stimuli. We developed kinetic self-sorting[4] protocols in which selective and irreversible distillation,[5] oxidation,[6] or precipitation[7] of imine-based DCLs reduces these mixtures in complexity from n^2 components into n products that can be isolated in high yields and purities. In this chapter, we derive general rules that guide these and other self-sorting processes in mixtures with an arbitrary number of

components, present in any arbitrary stoichiometry. We then proceed to apply these rules to distillative self-sorting of dynamic ester libraries[8] and demonstrate that as many as four pure and industrially relevant esters can be produced in a single reaction setup.

Esters were chosen as substrates because of their numerous uses as solvents, lubricants, fuels, fragrances, and food additives. Smaller esters are industrially produced through transesterification reactions, which are usually characterized by equilibrium constants close to unity. This fundamental obstacle in their preparation is overcome by the use of reactive distillation (RD) processes, in which the chemical reactor doubles as a distillation setup.[9] In these methods, the volatile component, either an ester or water, is continually removed from the reactor via controlled distillation until the equilibrium completely shifts in the direction of the product and the starting materials are fully consumed.[10] In eliminating the separate distillation step, RD yielded some of the chemical industry's most significant savings in energy, construction, and material costs during the past three decades. Several esters are industrially produced through RD-based transesterifications,[11] and RD is attracting attention in the production of biodiesel through transesterification of fatty acids.[12] Despite this significant progress and huge practical relevance, virtually all RD-based transesterifications generate just a single value-added ester as the product.[13]

We hypothesized that in the presence of a suitable acyl exchange catalyst, a multicomponent ester DCL could be used as a platform for an RD process that could generate multiple esters as pure products. Let us consider a general case of an ester

library formally constructed by random esterification of *n* carboxylic acids (labeled as **A**, **B**, **C**, **D**, .., in order of decreasing volatility) with *m* alcohols (labeled as **1**, **2**, **3**, **4**, ..., in order of decreasing volatility). The amounts of individual acids and alcohols may vary (and thus the resulting esters may be present in any ratio), but we set a limiting condition that the total number of moles of acids and alcohols is identical, so that the final mixture includes only esters and none of the unreacted carboxylic acids or alcohols.

Distillation of this mixture will isolate the most volatile ester **A1**, formed from the most volatile acid and the most volatile alcohol,[14] as the first fraction. As **A1** is being removed from the library, equilibrium will shift so as to replenish it, until the mixture runs out of either **A** or **1** (or both). In the next step, two scenarios are possible. If **A** and **1** were exhausted simultaneously, then the next compound to distill out will be **B2**, consuming in the process all other esters that contain either carboxylic acid **B** or alcohol **2**. However, if there was some of, for example, **A** left over in the mixture, then it will combine with the next most volatile alcohol **2**, to yield **A2** as the second fraction, and this process will continue until the mixture runs out of either **A** or **2**. Within the [$n \times m$] matrix of compounds, distillation expresses the most volatile ester until one (or both) of its constituents are depleted, then moves to the next most volatile compound until its components are depleted and so on. Thus, a series of limiting reagent calculations allows the prediction of the distillation products and their amounts based on the composition of the starting library. We have developed a Microsoft Excel algorithm that automates these predictions for libraries with up to [11×11] members.[15] Table 2.1 illustrates three typical examples. In the first case (top), a hypothetical [4×4] mixture is constructed by

combining equimolar amounts of four acids and four alcohols. Here, 4 equivalent each of **A1**, **B2**, **C3**, and **D4** are expected as products, because the balanced stoichiometry leaves no volatile alcohol or acid at the end of each step. Only the four diagonal members of the

Table 2.1 Calculated compositions of three ester libraries before and after iterative reactive distillation: an equimolar [4×4] library (top), an equimolar [3×5] library (middle), and a non-equimolar [4×4] library (bottom and numbers in the table indicate the stoichiometry of esters).

	1	2	3	4
A	1.0	1.0	1.0	1.0
B	1.0	1.0	1.0	1.0
C	1.0	1.0	1.0	1.0
D	1.0	1.0	1.0	1.0

→

	1	2	3	4
A	4.0	0.0	0.0	0.0
B	0.0	4.0	0.0	0.0
C	0.0	0.0	4.0	0.0
D	0.0	0.0	0.0	4.0

	1	2	3
A	1.0	1.0	1.0
B	1.0	1.0	1.0
C	1.0	1.0	1.0
D	1.0	1.0	1.0
E	1.0	1.0	1.0

→

	1	2	3
A	3.0	0.0	0.0
B	2.0	1.0	0.0
C	0.0	3.0	0.0
D	0.0	1.0	2.0
E	0.0	0.0	3.0

	1	2	3	4
A	1.0	1.0	1.0	1.0
B	1.0	1.0	1.0	1.0
C	1.0	1.0	1.0	1.0
D	9.0	1.0	1.0	1.0

→

	1	2	3	4
A	4.0	0.0	0.0	0.0
B	4.0	0.0	0.0	0.0
C	4.0	0.0	0.0	0.0
D	0.0	4.0	4.0	4.0

[4×4] matrix are expressed. In the second case (middle), five carboxylic acids are combined with three alcohols to produce equimolar amounts of 15 esters. In this [3×5] matrix, the distillation "zig-zags", producing first 3 equivalent of **A1** (before it runs out

of **A**), then 2 equivalent of **B1** (before it runs out of **1**), then 1 equivalent of **B2** (when it runs out of **B**), and so on. While the simplification in this case is not great, since a 15-member library reduces into seven final compounds, the isolated "pseudodiagonal" members are still symmetrically positioned within the matrix. The final case (bottom) examines a nonstoichiometric [4×4] library that contains 9 equiv of compound **A4** and **1** equivalent of each of the other compounds. In this case, distillation isolates 4 equivalent each of compounds **A1**−**A3** and **B4**−**D4** (and, interestingly, no **A4**), meaning that excess of one DCL member "pulls" the normal diagonal distribution toward that component.

Guided by this theoretical insight, we proceeded to demonstrate ester self-sorting in practice. We analyzed the behavior of various mixtures of the esters presented in Table 2.2 during reactive distillation.

Table 2.2 Compound codes for esters examined in this study.

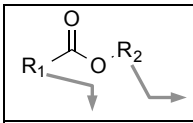	C_2H_5	*n*-C_4H_9	$PhCH_2$	*n*-C_8H_{17}	*n*-$C_{16}H_{33}$
CH_3	**93**	**94**	**95**	**96**	**97**
n-C_3H_7	**98**	**99**	**100**	**101**	**102**
Ph	**103**	**104**	**105**	—	—
n-C_7H_{15}	**106**	**107**	—	**108**	**109**
n-$C_{15}H_{31}$	**110**	**111**	—	**112**	**113**

2.2 Results and Discussion

In our first experiment (Scheme 2.1a), we utilized NaO*t*-Bu as the acyl exchange catalyst, previously reported by Gagné et al.[16] An equimolar mixture[17] of ethyl acetate (**93**, Scheme 2.1a), benzyl acetate (**95**), ethyl benzoate (**103**), and benzyl benzoate (**105**) was exposed to a catalytic amount of 1 M solution of NaO*t*-Bu in THF and then subjected to distillation in vacuo (2.50 mmHg) at 50 °C. After 2 h, the distillate was found to be pure **93**, which was formed in 83% yield as quantified by ^{1}H NMR spectroscopy. Distillation residue contained ester **105** in 95% yield, and small amounts of the crossover esters **95** (5%) and **103** (4%). A similar experiment was successfully performed (Scheme 2.1b) with ethyl butyrate (**98**), butyl butyrate (**99**), **103**, and **105**. Again, the most volatile (**98**, 80%) and the least volatile (**105**, 87%) esters were isolated in high yields with small amounts of the esters of intermediate volatility (see Experimental Section for details).

The NaO*t*-Bu catalyst proved non-optimal in our attempts to perform distillative self-sorting of less volatile esters, for example, in protocols where benzyl or octyl esters were designed to be the more volatile components. Two potential explanations can be offered for this behavior. During the course of ester exchange, *t*-butyl esters are formed as intermediates; these esters are more volatile than, for example, octyl esters of the same acids and can thus be removed through distillation instead of the expected product. The stoichiometry of the alcohol and acid partners would thus be disturbed and lower purity of the resultant products would be expected, although not dramatically, as *t*-butoxide was used in catalytic amounts. The more significant obstacle was logistical: after the *t*-butyl

esters were distilled, the effective role of the catalyst was turned over to a higher alkoxide, and these species were either insoluble or acted as gelling agents. In such a scenario, distillations essentially shut down, and more forcing conditions caused significant decomposition of ester libraries.[18]

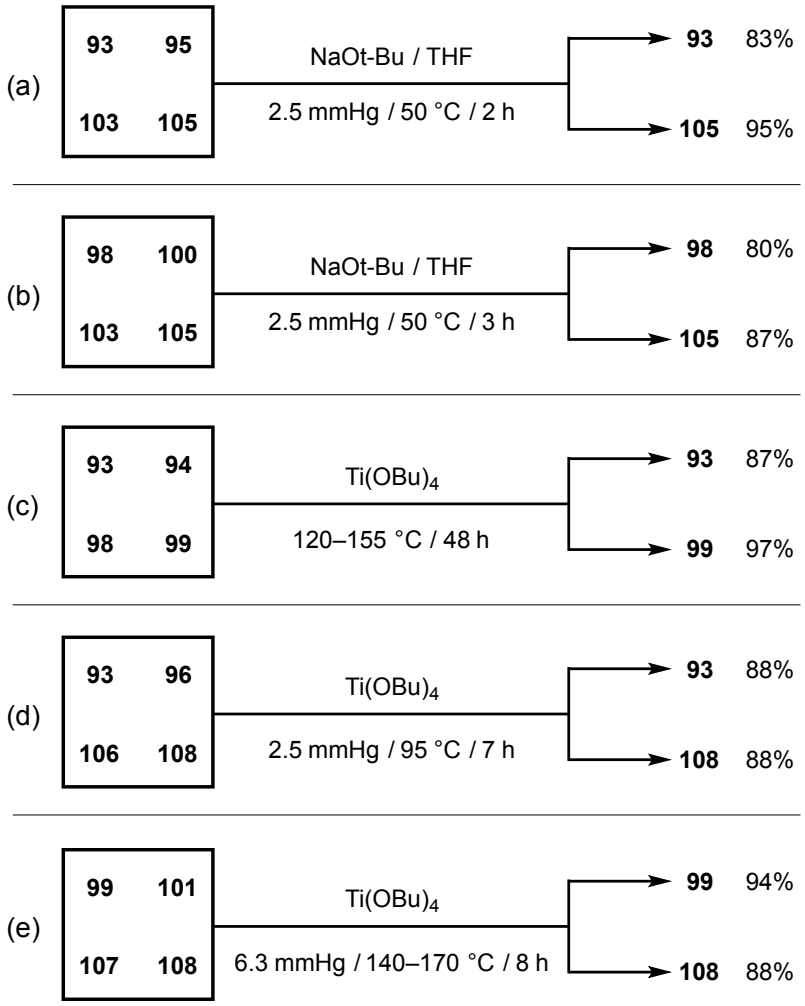

Scheme 2.1 Self-sorting of dynamic [2×2] ester libraries during reactive distillation (all of the starting esters were mixed in equimolar amounts).

Forced to switch the acyl exchange catalyst, we turned to $Ti(OBu)_4$,[19] which was also reported to equilibrate esters in the absence of water or alcohols. With this new catalyst, a four-ester mixture **93**–**99** could be self-sorted (Scheme 2.1c) during a distillation at atmospheric pressure into **93** (87%) and **99** (97%).[20] Two subsequent experiments (Scheme 1d, e) successfully sorted [2×2] ester libraries that contained less volatile ester components, thus critically demonstrating the superiority of $Ti(OBu)_4$ over NaO*t*-Bu, since the latter catalyst proved ineffective in these reactions because of gel formation.

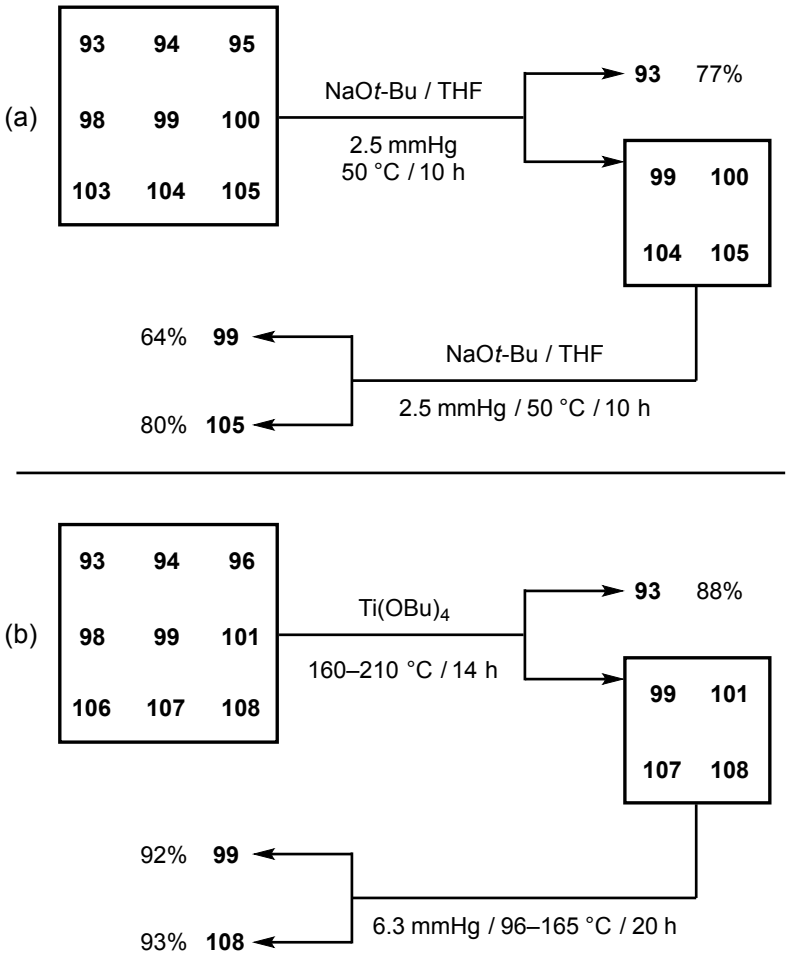

Scheme 2.2 Self-sorting of dynamic [3×3] ester libraries during reactive distillation.

The success of the [2×2] self-sorting experiments suggested that more complex mixtures could be similarly resolved. We next attempted distillative self-sorting of a nine-ester library **93**–**105** (Scheme 2.2a) in the presence of NaO*t*-Bu. Upon vacuum distillation, ethyl acetate (**93**) was isolated as the first fraction in 77% yield; continued distillation resulted in the production of **99** as the second distillate (64%), leaving **105** as the distillation residue (80%). Moderate yields of the three products, as well as the previously noticed gelation problems associated with the use of NaO*t*-Bu with less volatile esters, suggested that an alternative catalyst might perform better. Indeed, the use of $Ti(OBu)_4$ on a [3×3] ester library composed of **93**, **94**, **96**, **98**, **99**, **101**, **106**, **107**, and **108** resulted in a rapidly equilibrating library, which upon two distillation steps yielded first **93** (88%) and then **99** (92%), leaving **108** (93%) as the distillation residue (Scheme 2.2b).

Our most complex experiment targeted a mixture of 16 esters shown in Scheme 2.3, top right. Upon subjection of this library to titanium catalysis and distillation at atmospheric pressure for 72 h, ethyl acetate (**93**) was isolated as the first product in 87% yield. At that point, all other acetates (**94**, **96**, and **97**) and all other ethyl esters (**98**, **106**, and **110**) were also removed from the mixture, because they shared either the acid or the alcohol component with **93**. The second stage of this distillation required the use of a mild vacuum (6.3 mmHg) and an additional portion of the catalyst; after 45 h, this protocol yielded the second pure fraction consisting of **99**, which was isolated in 88% yield. The final [2×2] library composed of **108**–**113** was subjected to distillation in high

vacuum (0.1 mmHg), producing **108** (70%) as the distillate and **113** (85%) as the distillation residue.

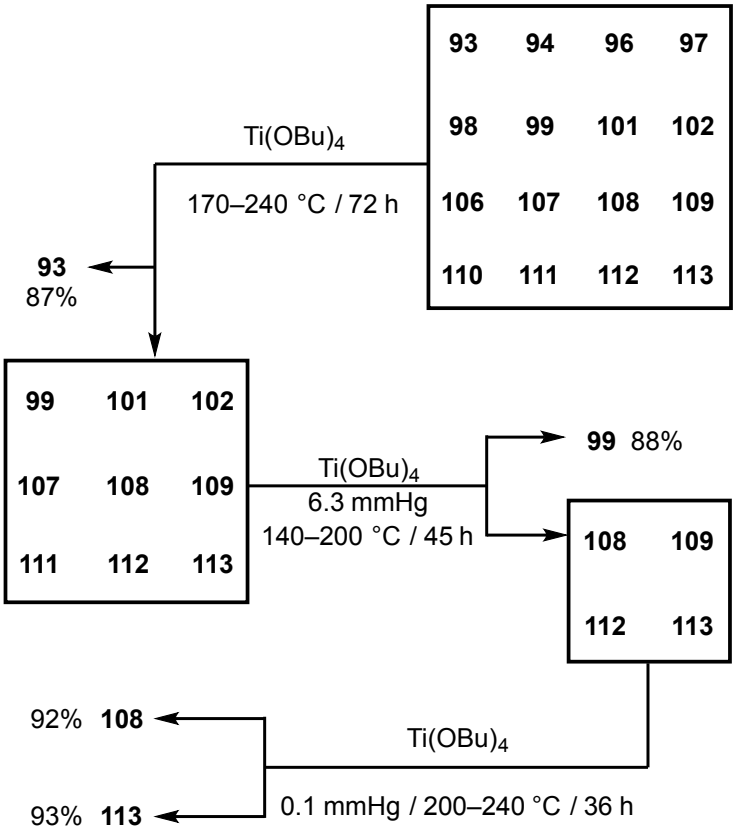

Scheme 2.3 Self-sorting of dynamic [4×4] ester libraries during reactive distillation.

As mentioned previously, the applicability of these iterative self-sorting distillative protocols is not limited to just [n×n] mixtures, nor to strictly equimolar component compositions. To demonstrate this, we constructed a [2×3] mixture shown in Scheme 2.4, in which one component (**103**) was added in 2-fold excess relative to all other ester species, which were otherwise equimolar.[21] Upon distillation of such a library, **93** is formed as the expected first product. Its isolated amount is close to twice the molar

amount of **93** originally added to the mixture; the second equivalent of **93** comes from the extraction of all acetate (1 equivalent from **95**) and the equimolar amount of ethyl esters (1 equivalent from either **98** or **103**). Once the distillation of **93** is complete, the next most volatile fraction is **98**, which extracts the remaining ethyl esters (1 equivalent from **103**) and butanoates (1 equivalent from **100**). Left over is approximately 3 equivalent of **105**, which is commensurate to the original amounts of benzoate (2 equivalent in **103** and 1 equivalent in **105**) and benzyl esters (1 equivalent each in **95**, **100**, and **105**) in the starting library.

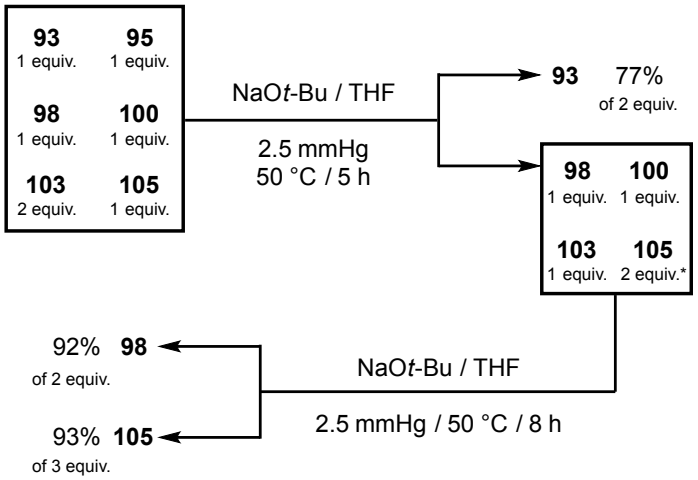

Scheme 2.4 Self-sorting of dynamic [2×3] ester libraries during reactive distillation.

2.3 Conclusions and Outlook

In conclusion, we have prepared nine distillative self-sorting experiments to show ester self-sorting protocol may have potential applications for multiple ester productions

in chemical industrial using reactive distillation. We also first applied $Ti(OBu)_4$ to ester DCLs and demonstrated its capability in ester metathesis. Our ester self-sorting protocol could be employed not only for symmetric [n×n] systems, but also unsymmetric [n×m] systems. By varying the stoichiometry of each component in the library, certain products, not necessarily from the diagonal position, could be expressed. There are also new challenges remain associated with this ester distillative self-sorting such as new catalyst development to catalyze both esterification and ester metathesis at the same time, practical expansion of the substrate dimension, and catalyst tolerance for a broaden substrates such as phenyl and geranyl esters. We also wish to expand this protocol to different chemical reactions, which are currently using reactive distillation for production such as etherification, alkylation, alkene metathesis, and alkyne metathesis. Also of interest would be simplification of complicated—but very abundant—natural mixtures such as hydrolyzed lignin or biodiesel, as such simplification could lead to new and simplified routes to new fuels and value-added chemicals.

2.4 Experimental Section

2.4.1 General Methods

All reactions were performed under nitrogen atmosphere in oven-dried glassware. All reagents and solvents were purchased from commercial suppliers and used without further purification, with the exception of esters **98**–**100**, **104**, and **105**, which were

prepared as described below. NMR spectra were obtained on JEOL ECA-500 spectrometer, with working frequency of 500 MHz for ^{1}H nuclei and 125 MHz for ^{13}C nuclei. ^{1}H NMR chemical shifts are reported in ppm units relative to the residual signal of the solvent ($CDCl_3$: 7.25 ppm). All NMR spectra were recorded at 25°C, and ^{13}C NMR spectra were recorded with simultaneous decoupling of ^{1}H nuclei. Compound 1,3,5-trimethoxybenzene (Alfa Aesar, 99%) was utilized as the internal standard for the calculations of yields of different esters on the basis of integration of ^{1}H NMR spectra of distillates and distillation residues.

Gas chromatography was performed using GC-2010 Shimadzu gas chromatograph. The temperature program that was used for all characterizations started with (1) constant temperature of 50 °C for 1 min, followed by (2) monotonous temperature ramping from 50 °C to 270 °C within 4 min, and finally (3) constant temperature of 270 °C for 10 min. Dodecane (Alfa Aesar, 99%) was utilized as an internal standard for the calculation of yields based on the integration of gas chromatograms.

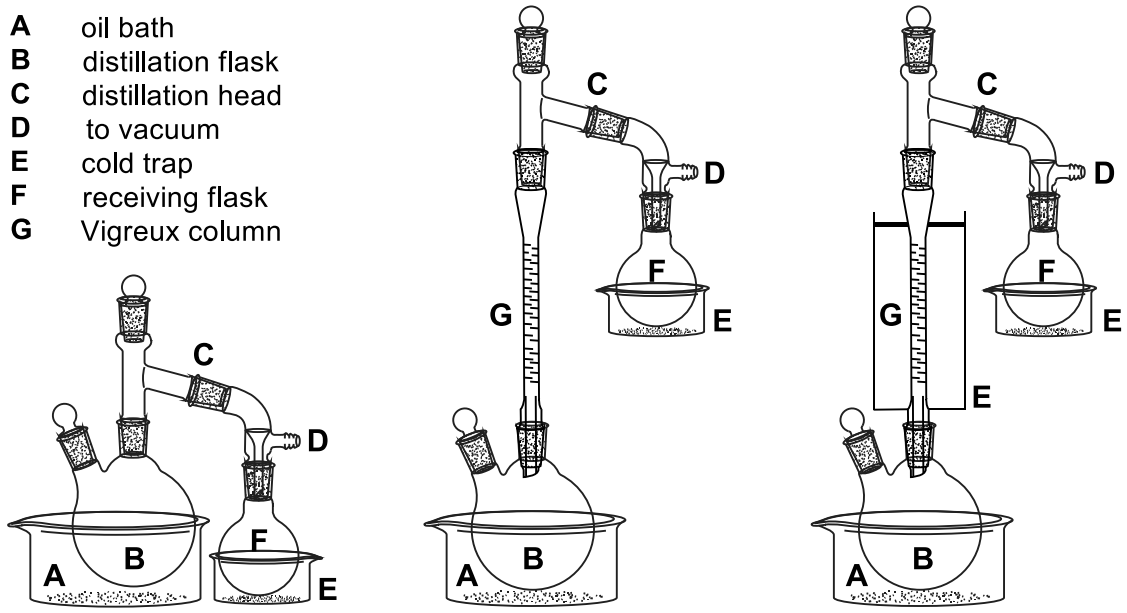

Figure 2.1 General setups used for the ester self-sorting reactions

2.4.2 Synthesis of Ester Starting Materials

Ethyl Butyrate (**98**)

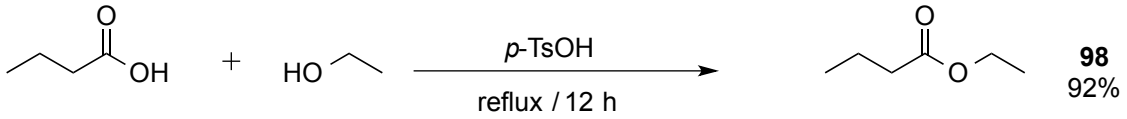

Butyric acid (4.45 g, 4.50 mL, 50.0 mmol), *p*-toluenesulfonic acid (0.50 g, 2.50 mmol), and EtOH (4.65 g, 6.0 mL, 100 mmol) were placed in a round bottom flask (50 mL). The flask was fitted with a reflux condenser and a Dean-Stark trap with filled with activated 4 Å molecular sieves. The mixture was set to reflux under nitrogen atmosphere. After 12 h, the reaction mixture was diluted with pentane and washed with H_2O (3 × 50

mL). Removal of pentane by fractional distillation gave ester **98** (5.37 g, 92%) as a colorless liquid.

98: ^{1}H NMR ($CDCl_3$): 4.13 (q, ^{3}J=6.8 Hz, 2H), 2.27 (t, ^{3}J=7.4 Hz, 2H), 1.65 (sextet, ^{3}J=7.4 Hz, 2H), 1.26 (t, ^{3}J=6.8 Hz, 3H), 0.96 (t, ^{3}J=7.4 Hz, 3H) ppm. ^{13}C NMR ($CDCl_3$): 173.61, 60.13, 36.32, 18.57, 14.32, 13.70 ppm. Spectral data agree with a previous literature report.[22]

Butyl Butyrate (**99**)

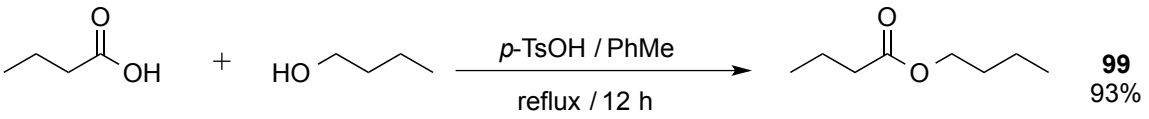

Butyric acid (4.45 g, 4.50 mL, 50.0 mmol) and 1-butanol (3.74 g, 4.60 mL, 50.0 mmol) were mixed with *p*-toluenesulfonic acid (0.50 g, 2.50 mmol) and PhMe (15 mL) in a 50 mL round bottom flask. A reflux condenser and a Dean-Stark trap filled with 4 Å molecular sieves were attached to the reaction flask and the mixture was heated at reflux for 12 h. After that time, the mixture was diluted with Et_2O (50 mL), and washed with saturated aqueous solutions of $NaHCO_3$. The aqueous phase was extracted with an additional amount of Et_2O. After washing with brine three times, the ethereal solution was dried over anhydrous $MgSO_4$. The solvent was removed in vacuo to give **99** (6.71 g, 93%) as a colorless liquid.

99: ^{1}H NMR ($CDCl_3$): 4.07 (t, ^{3}J=6.8 Hz, 2H), 2.27 (t, ^{3}J=7.5 Hz, 2H), 1.69–1.40 (m, 6H) 0.9 (t, ^{3}J=6.4 Hz, 6H) ppm. ^{13}C NMR ($CDCl_3$): 173.77, 64.06, 36.26, 30.74, 19.17, 18.50, 13.70, 13.66 ppm. Spectral data agree with a previous literature report.[23]

Butyl Benzoate (**104**)

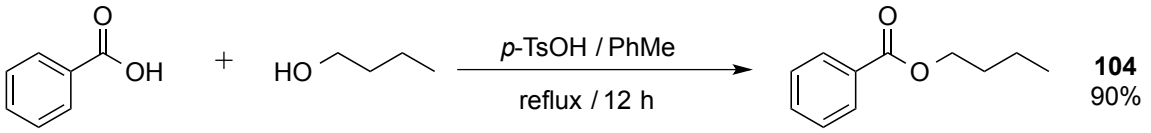

Benzoic acid (6.17 g, 50.0 mmol) and 1-butanol (3.74 g, 4.60 mL, 50.0 mmol) were mixed with *p*-toluenesulfonic acid (0.50 g, 2.50 mmol) and PhMe (15 mL) in a 50 mL round bottom flask. A reflux condenser and a Dean-Stark trap filled with 4 Å molecular sieves were attached to the reaction flask and the mixture was heated at reflux for 12 h. After that time, the mixture was diluted with Et_2O (50 mL), and washed with saturated aqueous solution of $NaHCO_3$. The aqueous phase was extracted with an additional amount of Et_2O. After washing with brine three times, the ethereal solution was dried over anhydrous $MgSO_4$. The solvent was removed in vacuo to give **104** (8.0 g, 90%) as a colorless liquid.

104: ^{1}H NMR ($CDCl_3$): 8.06 (d, ^3J=8.7 Hz, 2H), 7.56 (t, ^3J=7.2 Hz, 1H), 7.41–7.46 (m, 2H), 4.33 (t, ^3J=6.6 Hz, 2H), 1.71–1.81 (m, 2H), 1.43–1.53 (m, 2H), 0.98 (t, ^3J=7.5 Hz, 3H) ppm. ^{13}C NMR ($CDCl_3$): 166.61, 132.79, 130.66, 129.58, 128.34, 64.80, 30.88, 19.34, 13.78 ppm. Spectral data agree with a previous literature report.[24]

Benzyl Butyrate (**100**)

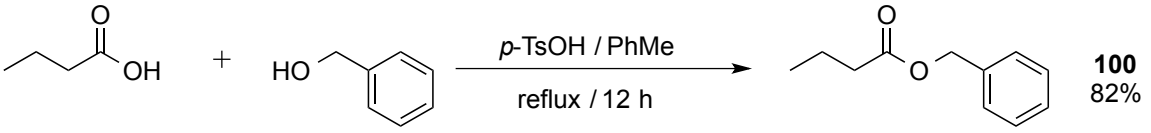

Butyric acid (4.45 g, 4.50 mL, 50.0 mmol), *p*-toluenesulfonic acid (0.50 g, 2.50 mmol), and PhMe (15 mL) were added to a 50 mL two-neck round bottom flask. The

reaction flask was fitted with a reflux condenser and a Dean-Stark trap, and the mixture was set to reflux under nitrogen atmosphere. Benzyl alcohol (5.46 g, 5.20 mL, 50.0 mmol) was added to the reaction flask using a syringe pump, during the course of 6 h. After 12 h, the mixture was diluted with Et_2O (50 mL), and saturated aqueous $NaHCO_3$ solution was added to remove the catalyst. The aqueous layer was extracted with additional Et_2O, and the combined ethereal solution was washed with brine three times, and dried over $MgSO_4$. Solvent was removed in vacuo to give **99** (7.33 g, 82%) as a colorless liquid.

100: ^{1}H NMR ($CDCl_3$): 7.45–7.35 (m, 5H), 5.13 (s, 2H), 2.35 (t, ^3J=7.3 Hz, 2H), 1.68 (sextet, ^3J=7.3 Hz, 2H), 0.96 (t, ^3J=7.3 Hz, 3H) ppm. ^{13}C NMR ($CDCl_3$): 173.50, 136.32, 128.64, 128.27 (2C), 66.11, 36.26, 18.56, 13.78 ppm. Spectral data agree with a previous literature report.[25]

Benzyl Benzoate (**105**)

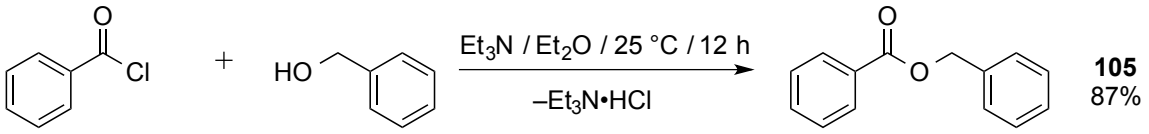

In a 50 mL round bottom flask, benzoyl chloride (7.10 g, 5.90 mL, 50.0 mmol) was dissolved in dry Et_2O (20 mL) under nitrogen atmosphere. A mixture of benzyl alcohol (5.46 g, 5.20 mL, 50.0 mmol) and NEt_3 (6.13 g, 8.20 mL, 60.0 mmol) was slowly added to the Et_2O solution using a syringe pump. After 12 h, the mixture was washed with H_2O (3×50 mL) and dried over $MgSO_4$. After removal of the solvent, **105** was obtained as a colorless liquid (9.22 g, 87%).

105: ^{1}H NMR ($CDCl_3$): 8.10 (d, ^{3}J=7.0 Hz, 2H), 7.59 (t, ^{3}J=7.5 Hz, 1H), 7.37–7.50 (m, 7H), 5.40 (s, 2H) ppm. ^{13}C NMR ($CDCl_3$): 166.54, 136.26, 133.21, 130.32, 129.89, 128.78, 128.57, 128.43, 128.36, 66.84 ppm. Spectral data agree with a previous literature report.[26]

2.4.3 Reactive Distillations of [2×2] Ester Libraries

*2.4.3.1 Ethyl Acetate (**93**) and Benzyl Benzoate (**105**)*

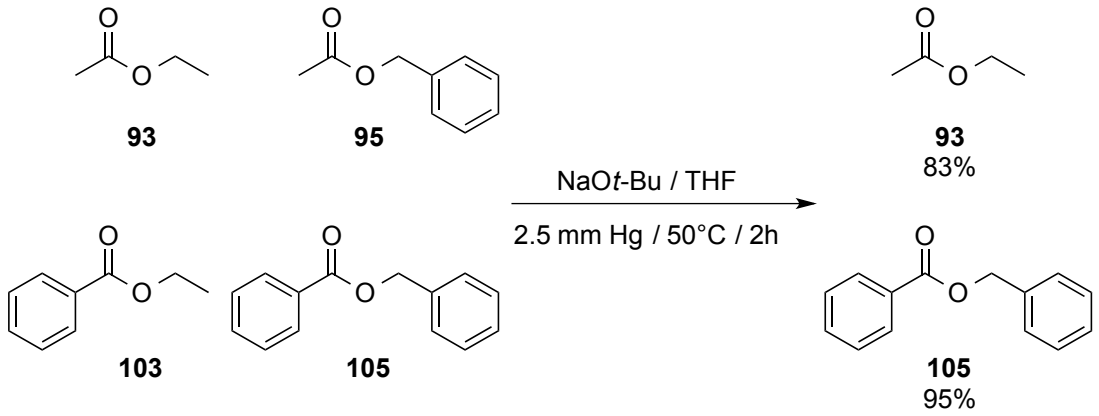

Equimolar amounts of ethyl acetate (**93**, 445 mg, 5.00 mmol), ethyl benzoate (**103**, 758 mg, 5.00 mmol), benzyl acetate (**95**, 758 mg, 5.00 mmol), and benzyl benzoate (**105**, 1.07 g, 5.00 mmol) were added to a 25 mL two-neck round bottom flask. The reaction flask was equipped with a short path distillation head that connected it with a receiving flask placed in an *i*-PrOH/CO_2 ice bath. The mixture was heated up to 50 °C. A 1M solution of NaO*t*-Bu in THF (0.5 mL) was injected into reaction flask in five 0.1 mL portions, with injections separated by 10 min. The distillation setup was placed under

vacuum (2.5 mmHg) when the first loading of catalyst was added. After 2 h, the distillate (1.60 g) was collected as a colorless liquid. ^{1}H NMR spectroscopy confirmed the identity of this liquid as a mixture of **93** (732 mg, 8.31 mmol, 83% yield) and THF (solvent, 720 mg, 9.98 mmol). Esters **95**, **103**, and **105** could not be observed in the distillate. The residue (2.17 g) was identified by ^{1}H NMR spectroscopy as a mixture of **105** (2.02 g, 9.51 mmol, 95% yield), **95** (13.5 mg, 0.09 mmol, 5% yield), and **103** (9.91 mg, 0.07 mmol, 4% yield).

93: ^{1}H NMR ($CDCl_3$): 4.11 (q, ^{3}J=7.1 Hz, 2H), 2.03 (s, 3H), 1.20 (t, ^{3}J=7.1 Hz, 3H) ppm. ^{13}C NMR ($CDCl_3$): 170.8, 60.1, 20.7, 13.9 ppm. Spectral data agree with a previous literature report.[27]

105: ^{1}H NMR ($CDCl_3$): 8.10 (d, ^{3}J=7.0 Hz, 2H), 7.59 (t, ^{3}J=7.5 Hz, 1H), 7.37–7.50 (m, 7H), 5.40 (s, 2H) ppm. ^{13}C NMR ($CDCl_3$): 166.54, 136.26, 133.21, 130.32, 129.89, 128.78, 128.57, 128.43, 128.36, 66.84 ppm. Spectral data agree with a previous literature report.[25]

Calculation of the Yields based on the Integration of ^{1}H NMR Spectra

Internal standard 1,3,5-trimethoxybenzene (123 mg, 0.73 mmol) was added to a 339 mg-aliquot of the distillate. From their relative integrals in the ^{1}H NMR spectrum (Figure 2.2), the number of moles of **93** was calculated as 0.73 mmol × 1.62 ÷ (2/3) = 1.76 mmol. Thus, the total number of moles of **93** in the distillate was 1.76 mmol × 1598

mg ÷ 339 mg = 8.31 mmol, corresponding to the yield of **93** of 8.31 mmol ÷ 10.0 mmol × 100% = 83%.

Analogous yield calculation procedure was applied to the distillation residue: 1,3,5-trimethoxybenzene (138 mg, 0.81 mmol) was added to a 339 mg-aliquot of the distillation residue. The number of moles of **105** in the aliquot was calculated to be 0.81 mmol × 1.22 ÷ (2/3) = 1.48 mmol. The total number of moles of **105** in the whole of distillation residue was 1.48 mmol × 2171 mg ÷ 339 mg = 9.51 mmol, corresponding to the yield of 9.51 mmol ÷ 10.0 mmol × 100% = 95%. Yields of intermediate volatility esters **95** and **103** were similarly estimated at 5% and 4%, respectively.

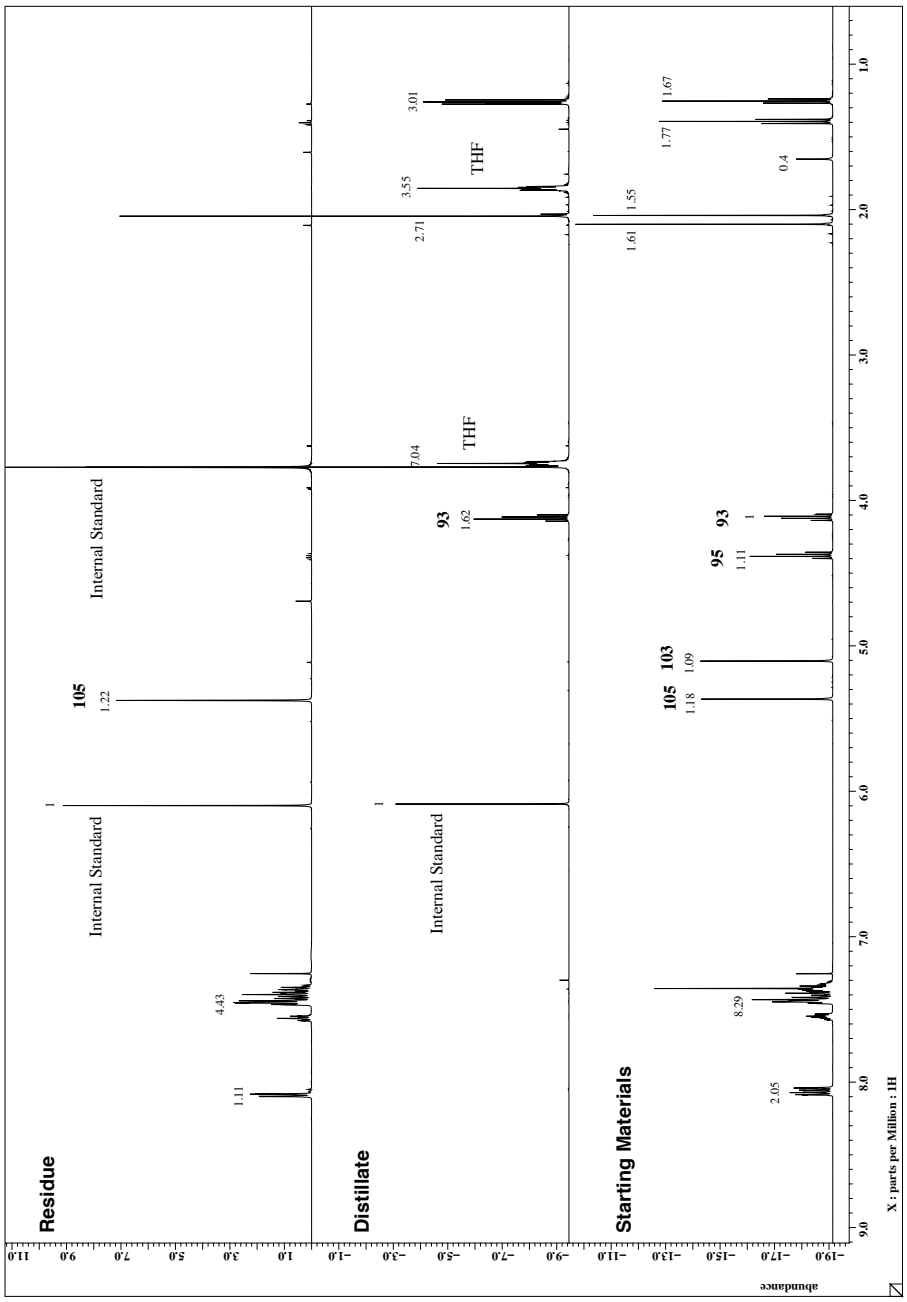

Figure 2.2 ^{1}H NMR spectra of the starting mixture (bottom) of esters **93**, **95**, **103**, and **105**, and the distillate (middle) and distillation residue (top) obtained after the reactive distillation of that mixture.

*2.4.3.2 Ethyl Butyrate (**98**) and Benzyl Benzoate (**105**)*

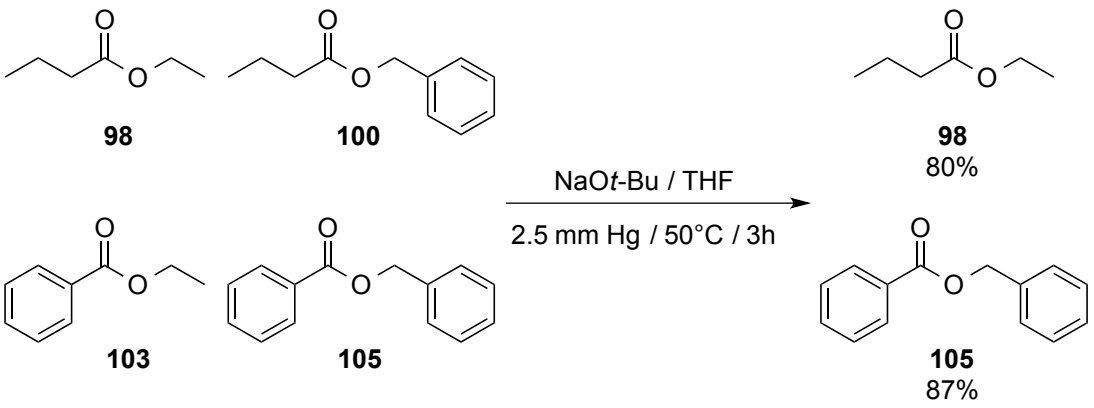

Equimolar amounts of ethyl butyrate (**98**, 587 mg, 5.00 mmol), ethyl benzoate (**103**, 758 mg, 5.00 mmol), benzyl butyrate (**100**, 900 mg, 5.00 mmol), and benzyl benzoate (**105**, 1.07 g, 5.00 mmol) were added to a 25 mL two-neck pear-shaped flask. The reaction flask was equipped with a short path distillation head that connected it with a receiving flask placed in an *i*-PrOH/CO_2 ice bath. The mixture was heated up to 50 °C. A 1 M solution of NaO*t*-Bu in THF (0.5 mL) was injected into reaction flask in five 0.1 mL portions, with injections separated by 10 min. The distillation setup was placed under vacuum (2.5 mmHg) when the first loading of catalyst was added. After 3 h, the distillate (1.98 g) was collected as a colorless liquid. ^{1}H NMR spectroscopy confirmed the identity of this liquid as a mixture of **98** (935 mg, 8.05 mmol, 80% yield) and THF (solvent, 917 mg, 12.7 mmol). Esters **100**, **103**, and **105** were not observed in the distillate. The residue (2.35 g) was identified by ^{1}H NMR spectroscopy as a mixture of **105** (1.84 g, 8.69 mmol, 87% yield), **100** (216 mg, 1.21 mmol, 12% yield), and **103** (118 mg, 0.78 mmol, 8% yield).

98: ^{1}H NMR ($CDCl_3$): 4.13 (q, ^{3}J=6.8 Hz, 2H), 2.27 (t, ^{3}J=7.4 Hz, 2H), 1.65 (sextet, ^{3}J=7.4 Hz, 2H), 1.26 (t, ^{3}J=6.8 Hz, 3H), 0.96 (t, ^{3}J=7.4 Hz, 3H) ppm. ^{13}C NMR ($CDCl_3$): 173.61, 60.13, 36.32, 18.57, 14.32, 13.70 ppm. Spectral data agree with a previous literature report.[21]

105: ^{1}H NMR ($CDCl_3$): 8.10 (d, ^{3}J=7.0 Hz, 2H), 7.59 (t, ^{3}J=7.5 Hz, 1H), 7.37–7.50 (m, 7H), 5.40 (s, 2H) ppm. ^{13}C NMR ($CDCl_3$): 166.54, 136.26, 133.21, 130.32, 129.89, 128.78, 128.57, 128.43, 128.36, 66.84 ppm. Spectral data agree with a previous literature report.[25]

Calculation of the Yields based on the Integration of ^{1}H NMR Spectra

Internal standard 1,3,5-trimethoxybenzene (156 mg, 0.92 mmol) was added to a 250 mg-aliquot of the distillate. From their relative integrals in the ^{1}H NMR spectrum (Figure 2.3), the number of moles of **98** was calculated as 0.92 mmol ÷ 1.36 ÷ (2/3) = 1.01 mmol. Thus, the total number of moles of **98** in the distillate was 1.01 mmol × 1984 mg ÷ 250 mg = 8.05 mmol, corresponding to the yield of **98** of 8.05 mmol ÷ 10.0 mmol × 100% = 80%.

Analogous yield calculation procedure was applied to the distillation residue: 1,3,5-trimethoxybenzene (147 mg, 0.86 mmol) was added to a 276 mg-aliquot of the residue. The number of moles of **105** in the aliquot was calculated to be 0.86 mmol ÷ 1.27 ÷ (2/3) = 1.02 mmol. The total number of moles of **105** in the whole of the distillation residue was 1.02 mmol × 2346 mg ÷ 276 mg = 8.69 mmol, corresponding to the yield of 8.69 mmol ÷ 10.0 mmol × 100% = 87%. Yields of intermediate volatility

esters **100** and **103** were similarly estimated at 12% and 8%, respectively.

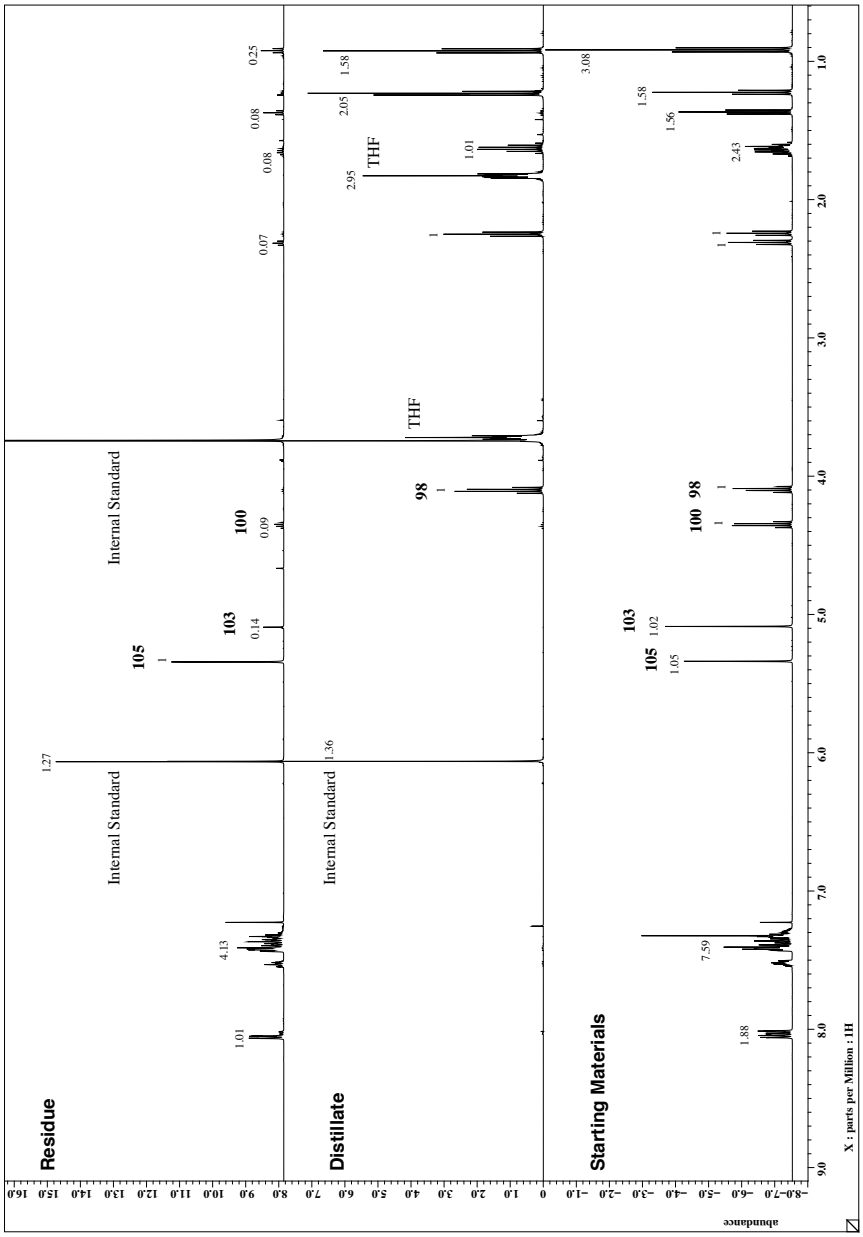

Figure 2.3 ^{1}H NMR spectra of the starting mixture (bottom) of esters **98**, **100**, **103**, and **105**, and the distillate (middle) and distillation residue (top) obtained after the reactive distillation of that mixture.

*2.4.3.3 Ethyl Acetate (**93**) and Butyl Butyrate (**99**)*

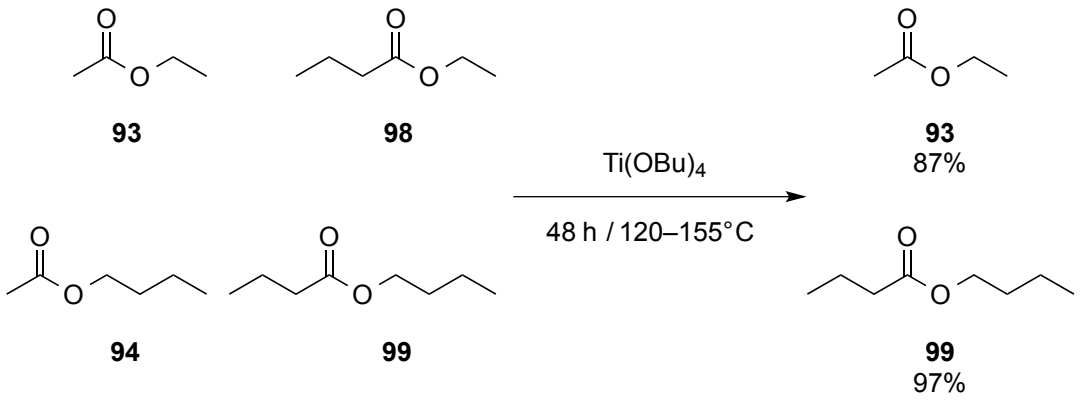

Titanium *n*-butoxide (413 mg, 1.20 mmol) and an equimolar mixture of **93** (2.67 g, 30.0 mmol), **94** (3.52 g, 30.0 mmol), **98** (3.52 g, 30.0 mmol), and **99** (4.37 g, 30.0 mmol) were placed in a 100 mL round bottom flask. The flask was fitted with a short path distillation head which connected it to a receiving flask that was placed in an *i*-PrOH/CO_2 ice bath (−78 °C). This mixture was heated from 120 to 155 °C for 48 h. The distillate (4.86 g) was collected as a colorless liquid. ^{1}H NMR spectroscopy confirmed the identity of this liquid as mostly **93** (4.58 g, 52.1 mmol, 87% yield). The residue (9.40 g) was identified by ^{1}H NMR spectroscopy as pure **99** (8.41 g, 58.3 mmol, 97% yield).

93: ^{1}H NMR ($CDCl_3$): 4.11 (q, ^3J=7.1 Hz, 2 H), 2.03 (s, 3 H), 1.20 (t, ^3J=7.1 Hz, 3 H) ppm. ^{13}C NMR ($CDCl_3$): 170.8, 60.1, 20.7, 13.9 ppm. Spectral data agree with a previous literature report.[26]

99: ^{1}H NMR ($CDCl_3$): 4.07 (t, ^3J=6.8 Hz, 2H), 2.27 (t, ^3J=7.5 Hz, 2H), 1.69–1.40 (m, 6H) 0.9 (t, ^3J=6.4 Hz, 6H) ppm. ^{13}C NMR ($CDCl_3$): 173.77, 64.06, 36.26, 30.74, 19.17, 18.50, 13.70, 13.66 ppm. Spectral data agree with a previous literature report.[22]

Calculation of the Yields based on the Integration of ^{1}H NMR Spectra

Internal standard 1,3,5-trimethoxybenzene (39 mg, 0.23 mmol) was added to a 824 mg-aliquot of the distillate. From their relative integrals in the ^{1}H NMR spectrum (Figure 2.4), the number of moles of **93** was calculated to be at least 0.23 mmol × [41.63 – (2.14 × 1.5)] = 8.84 mmol. Thus, the total number of moles of **93** in the distillate was 8.50 mmol × 4860 mg ÷ 824 mg = 52.1 mmol, corresponding to the yield of **93** of 52.1 mmol ÷ 60.0 mmol × 100% = 87%. Minor fractions were not quantified because of the extensive overlap of their ^{1}H NMR spectral peaks.

Analogous yield calculation procedure was applied to the distillation residue: 1,3,5-trimethoxybenzene (46 mg, 0.27 mmol) was added to a 755 mg-aliquot of the residue. The number of moles of **99** in the aliquot was calculated to be at least 0.27 mmol × [13.01 – (0.97 × 1.5)] ÷ (2/3) = 4.68 mmol. The total number of moles of **99** in the whole of the distillation residue was 4.68 mmol × 9400 mg ÷ 755 mg = 58.3 mmol, corresponding to the yield of 58.3 mmol ÷ 60.0 mmol × 100% = 97%. Minor fractions were not quantified because of the extensive overlap of their ^{1}H NMR spectral peaks.

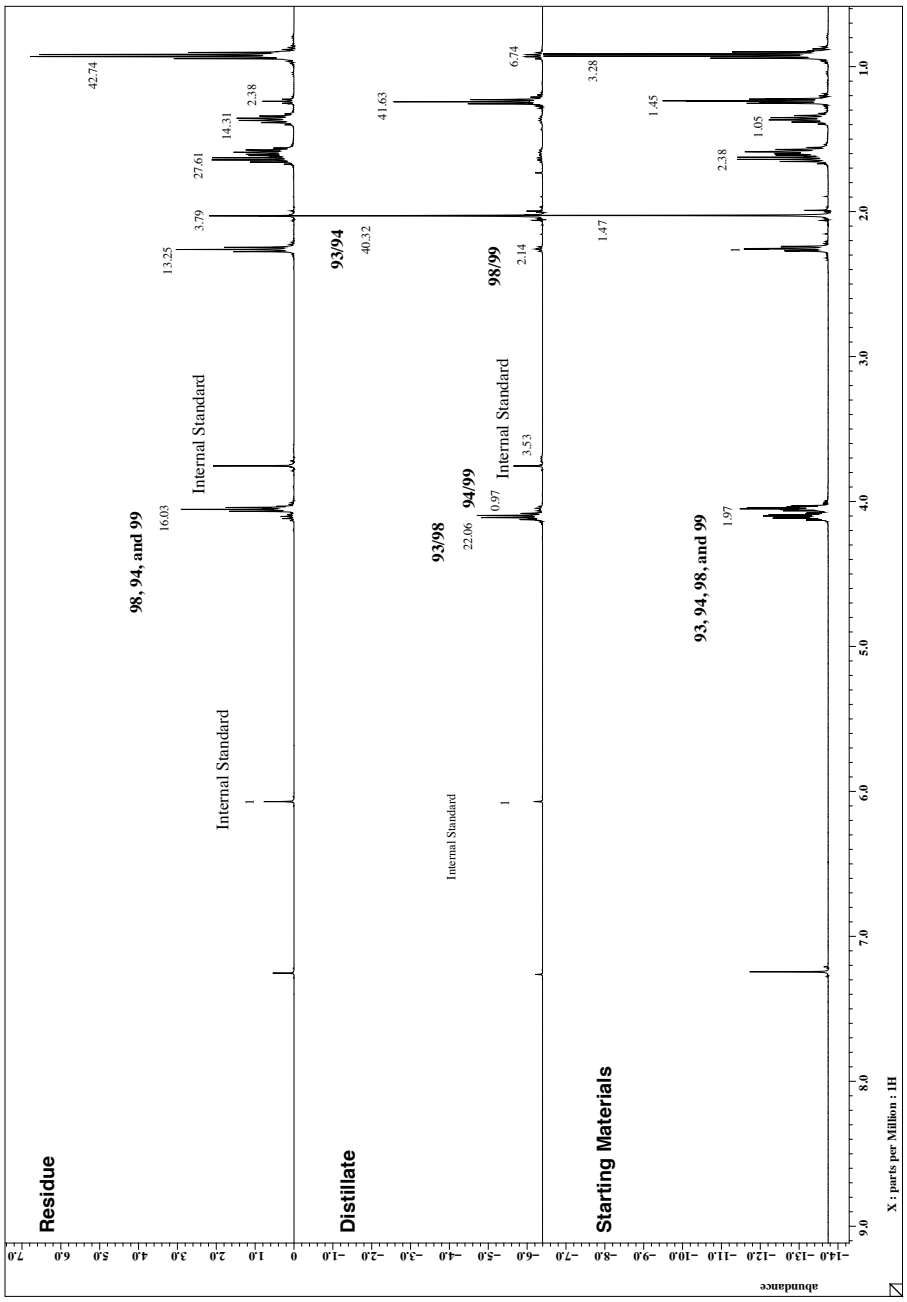

Figure 2.4 ^{1}H NMR spectra of the starting mixture (bottom) of esters **93**, **94**, **98**, and **99**, and the distillate (middle) and distillation residue (top) obtained after the reactive distillation of that mixture.

*2.4.3.4 Ethyl Acetate (**93**) and Octyl Octanoate (**108**)*

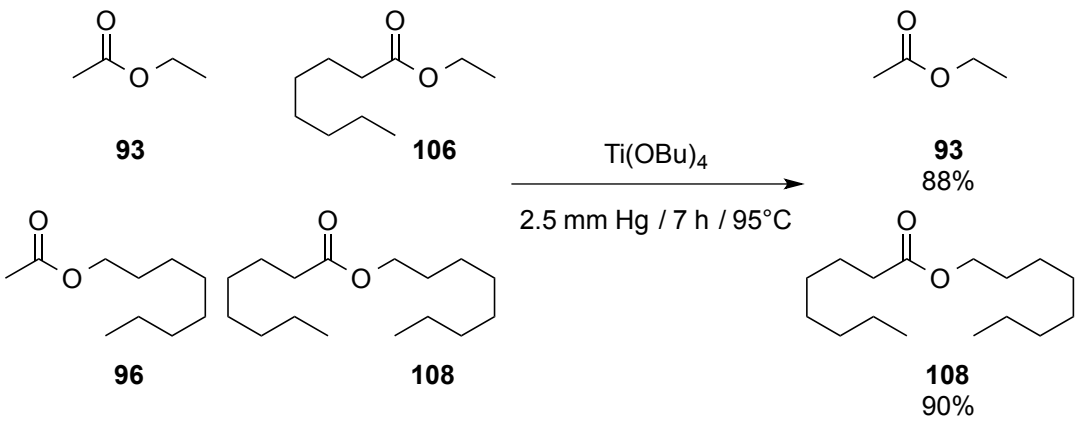

Titanium *n*-butoxide (138 mg, 0.40 mmol) and an equimolar mixture of **93** (0.89 g, 10.0 mmol), **96** (1.74 g, 10.0 mmol), **106** (1.74 g, 10.0 mmol), and **108** (2.59 g, 10.0 mmol) were placed into a 100 mL round bottom flask. The reaction flask was equipped with a 185 mm-long Vigreux column that was cooled by an *i*-PrOH/CO_2 cold trap (–30 °C). Short path distillation head was used to connect the top of the Vigreux column with a receiving flask which was placed into a separate *i*-PrOH/CO_2 ice bath (–78 °C). This reaction mixture was heated at 95 °C for 7 h under vacuum (2.5 mm Hg). The distillate (1.56 g) was collected as a colorless liquid. ^{1}H NMR spectroscopy confirmed the identity of this liquid as **93** (1.55 g, 17.6 mmol, 88% yield). Other three esters—**96**, **106**, and **108**—could not be identified in the distillate. Using a combination of ^{1}H NMR spectroscopy and gas chromatography (see below), the residue (5.24 g) was identified as a mixture dominated by **108** (4.61 g, 18.0 mmol, 90% yield), and with minor contributions from **106** (232 mg, 1.35 mmol, 7% yield) and **96** (140 mg, 0.81 mmol, 4% yield).

93: ^{1}H NMR ($CDCl_3$): 4.11 (q, ^{3}J=7.1 Hz, 2 H), 2.03 (s, 3 H), 1.20 (t, ^{3}J=7.1 Hz, 3 H) ppm. ^{13}C NMR ($CDCl_3$): 170.8, 60.1, 20.7, 13.9 ppm. Spectral data agree with a previous literature report.[26]

108: ^{1}H NMR ($CDCl_3$): 4.04 (t, ^{3}J=6.7 Hz, 2H), 2.28 (t, ^{3}J=7.5 Hz, 1H), 1.60 (m, 4H), 1.29 (m, 18H), 0.86 (t, ^{3}J=6.4 Hz, 6H) ppm. ^{13}C NMR ($CDCl_3$): 174.08, 64.46, 34.47, 31.76 (2C), 29.29, 29.20, 29.03, 28.72 (2C), 25.11 (2C), 22.73, 22.69, 14.15 (2C) ppm. Spectral data agree with a previous literature report.[28]

Calculation of the Yields based on the Integration of ^{1}H NMR Spectra

Internal standard 1,3,5-trimethoxybenzene (38 mg, 0.23 mmol) was added to a 886 mg-aliquot of the distillate. From their relative integrals in the ^{1}H NMR spectrum (Figure 2.5), the number of moles of **93** was calculated to be 0.23 mmol × 29.5 ÷ (2/3) = 10.0 mmol. Thus, the total number of moles of **93** in the distillate was 10.0 mmol × 1555 mg ÷ 886 mg = 17.6 mmol, corresponding to the yield of **93** of 17.6 mmol ÷ 20.0 mmol × 100% = 88%. Minor fractions were not quantified because of the extensive overlap of their ^{1}H NMR spectral peaks.

Analogous yield calculation procedure was applied to the distillation residue: 1,3,5-trimethoxybenzene (36 mg, 0.21 mmol) was added to a 1043 mg-aliquot of the residue. Using this method, yields of intermediate volatility esters **96** and **106** could be estimated at 7% and 4%, respectively. The yield of **108**—the major component in the distillation residue—was obtained using gas chromatography, because of (1) its complex

spectrum which overlaps with some of its side products', and (2) possible overlap with some of the peaks of residual $Ti(OBu)_4$—which affected the ^1H NMR spectroscopic, but not the gas chromatographic measurements.

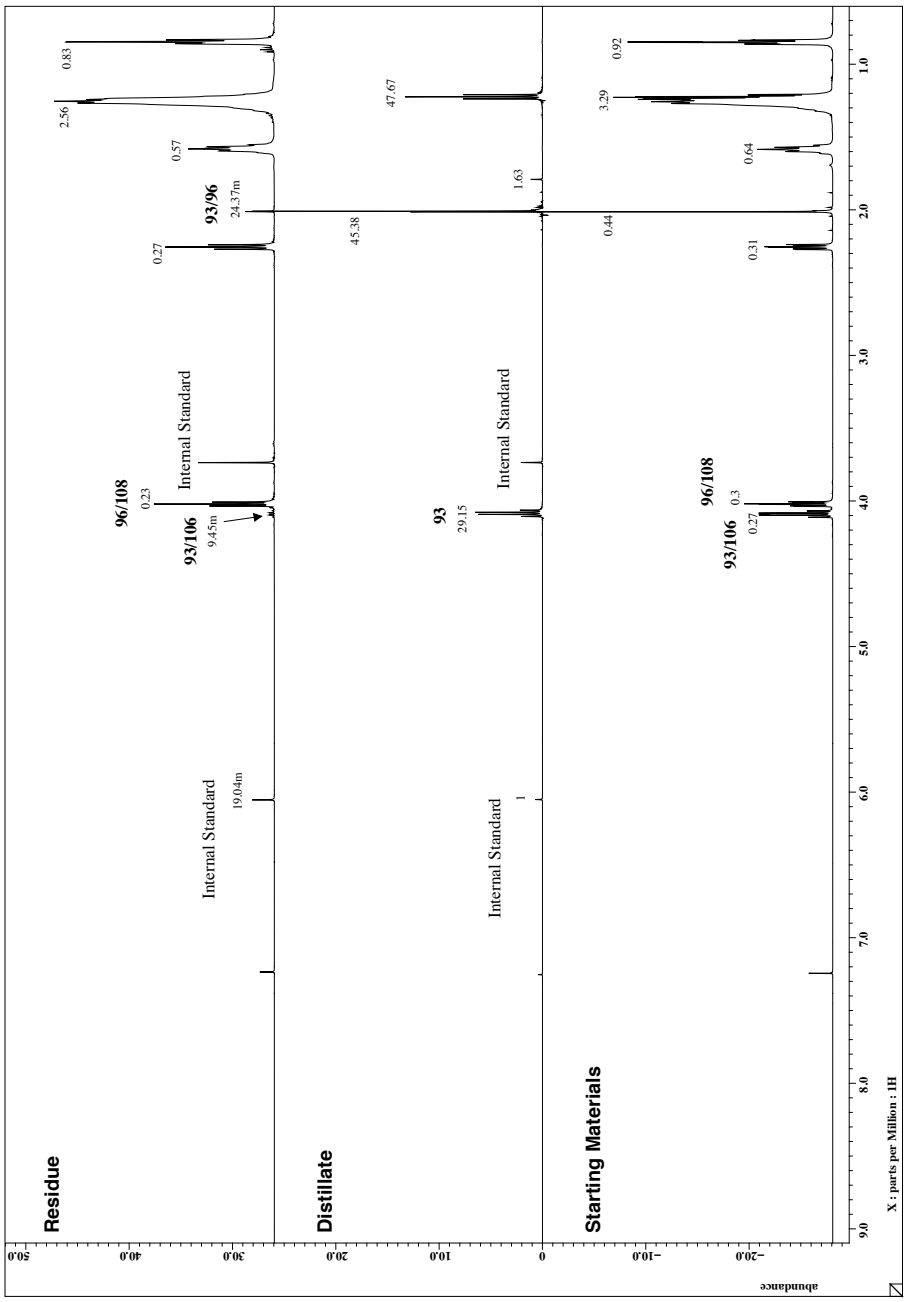

Figure 2.5 ^{1}H NMR spectra of the starting mixture (bottom) of esters **93**, **96**, **106**, and **108**, and the distillate (middle) and distillation residue (top) obtained after the reactive distillation of that mixture.

*Calculation of the Yield of **108** based on the Integration of Gas Chromatogram (GC) Peaks*

For the purpose of quantification of yield of **108**, we determined a response factor (F) for this ester with respect to dodecane, which was used as GC internal standard. The area of ester signal / mass of ester = F × area of standard signal / mass of standard. That is, $a_e / m_e = F \times a_s / m_s$. Therefore, a_e and m_e of a pure sample of **108** and a_s and m_s of GC internal standard (dodecane) were used to calculate F value. Five independent determinations of the F value were performed (0.787, 0.792, 0.760, 0.799, 0.803), yielding an average F = 0.788. This value was then used to calculate the amount of **108** in the distillation residue of this reactive distillation (Figure 2.6). A 43.3 mg-aliquot of the distillation residue was added to a glass vial, followed by addition of dodecane (29.9 mg) and THF (3 mL) as the solvent. The mixture was subjected to gas chromatography using the temperature program described in the General Methods section. From the integration, mass of **108** could be calculated as $m_e = (a_e \times m_s) / (a_s \times F)$ = (16605040 × 29.9 mg) / (16515649 × 0.788) = 38.1 mg. The total mass of **108** in the distillation residue was 38.1 mg × 5.24 g ÷ 43.3 mg = 4.61 g. The yield of **108** is 4.61 g ÷ 256.42 g mol^{-1} ÷ 20.0 mmol × 100% = 90%.

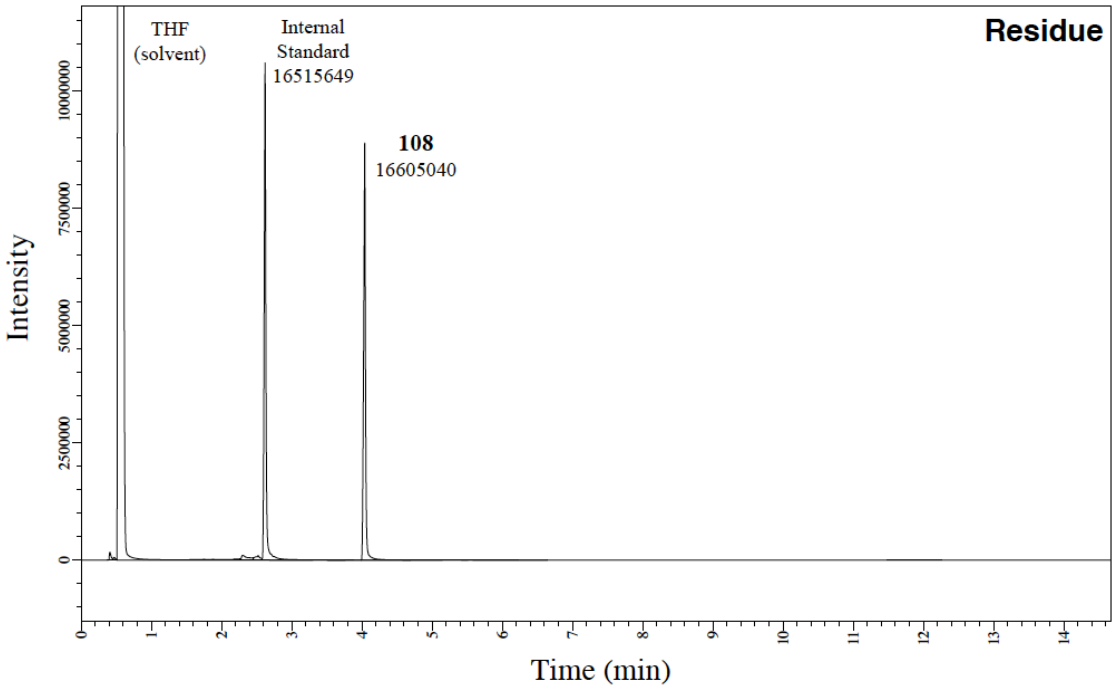

Figure 2.6 Gas chromatogram of the distillation residue from the reactive distillation of an equimolar mixture of **93**, **96**, **106**, and **108**, with internal standard (dodecane) added for calibration. THF was used as the solvent.

*2.4.3.5 Butyl Butyrate (**99**) and Octyl Octanoate (**108**)*

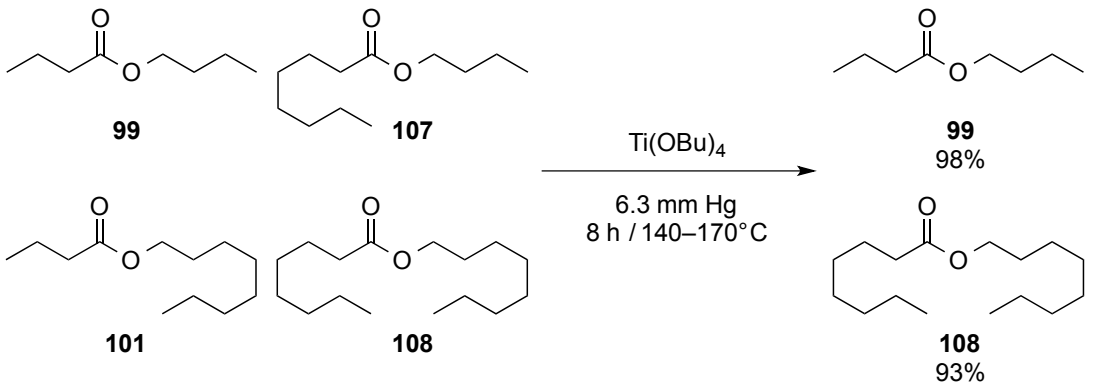

Titanium *n*-butoxide (138 mg, 0.40 mmol) and an equimolar mixture of **99** (1.46 g, 10.0 mmol), **101** (2.02 g, 10.0 mmol), **107** (2.02 g, 10.0 mmol), and **108** (2.59 g, 10.0 mmol) were added to a 100 mL round bottom flask. The reaction flask was equipped with a short path distillation head, which connected it to a receiving flask that was placed in an *i*-PrOH/CO_2 ice bath (–78 °C). This reaction was heated from 140 to 170 °C for 8 h under vacuum (6.3 mm Hg). Using gas chromatography, the distilled liquid (2.85 g) was identified as **99** (2.83 g, 19.6 mmol, 98% yield). The distillation residue (5.32 g) was analogously identified as a mixture dominated by **108** (4.51 g, 17.6 mmol, 93% yield), with minor contributions from **107** and **101**, which could not be quantified individually as the peaks of these two compounds extensively overlap both in in gas chromatograms (Figure 2.7 and Figure 2.8) and ^{1}H NMR spectra (Figure 2.9).

99: ^{1}H NMR ($CDCl_3$): 4.07 (t, ^3J=6.8 Hz, 2H), 2.27 (t, ^3J=7.5 Hz, 2H), 1.69–1.40 (m, 6H) 0.9 (t, ^3J=6.4 Hz, 6H) ppm. ^{13}C NMR ($CDCl_3$): 173.77, 64.06, 36.26, 30.74, 19.17, 18.50, 13.70, 13.66 ppm. Spectral data agree with a previous literature report.[22]

108: ^{1}H NMR ($CDCl_3$): 4.04 (t, ^3J=6.7 Hz, 2H), 2.28 (t, ^3J=7.5 Hz, 1H), 1.60 (m, 4H), 1.29 (m, 18H), 0.86 (t, ^3J=6.4 Hz, 6H) ppm. ^{13}C NMR ($CDCl_3$): 174.08, 64.46, 34.47, 31.76 (2C), 29.29, 29.20, 29.03, 28.72 (2C), 25.11 (2C), 22.73, 22.69, 14.15 (2C) ppm. Spectral data agree with a previous literature report.[27]

*Calculation of the Yields of **99** and **108** based on the Integration of GC Peaks*

For the purpose of quantification of yields of **99** and **108**, we determined response factors (F) for these esters with respect to dodecane as the GC internal standard. The area of ester signal / mass of ester = F × area of standard signal / mass of standard. That is, a_e / $m_e = F \times a_s / m_s$. Therefore, a_e and m_e of a pure samples of **99** and **108** and a_s and m_s of GC internal standard (dodecane) were used to calculate F value. Five independent determinations of the F value were performed for **99** (0.624, 0.658, 0.663, 0.653, 0.658), yielding an average F = 0.651 for **99**. Five independent determinations of the F value were performed for **108** (0.787, 0.792, 0.760, 0.799, 0.803), yielding an average F = 0.788 for **108**. This value was then used to calculate the amounts of **99** and **108** in the distillate and distillation residue of this reactive distillation (Figures 2.7 and 2.8, respectively). A 47.4 mg-aliquot of the distillate was added to a glass vial, followed by addition of dodecane (28.3 mg) and THF (3 mL) as the solvent. The mixture was subjected to gas chromatography using the temperature program described in the General Methods section. From the integration, mass of **99** could be calculated as $m_e = (a_e \times m_s) / (a_s \times F)$ = (17249466 × 28.3 mg) / (15907455 × 0.651) = 47.1 mg. The total mass of **99** in the distillation residue was 47.1 mg × 2.85 g ÷ 47.4 mg = 2.83 g. The yield of **99** is 2.83 g ÷ 144.21 g mol^{-1} ÷ 20.0 mmol × 100% = 98%.

A 41.4 mg-aliquot of the distillation residue was added to a glass vial, followed by addition of dodecane (28.2 mg) and THF (3 mL) as the solvent. The mixture was subjected to gas chromatography using the temperature program described in the General

Methods 2.4.1 section. From the integration, mass of **108** could be calculated as $m_e = (a_e \times m_s) / (a_s \times F)$ = (16604867 × 28.2 mg) / (15989277 × 0.788) = 37.2 mg. The total mass of **108** in the distillation residue was 37.2 mg × 5.32 g ÷ 41.4 mg = 4.78 g. The yield of **108** is 4.78 g ÷ 256.42 g mol^{-1} ÷ 20.0 mmol × 100% = 93%.

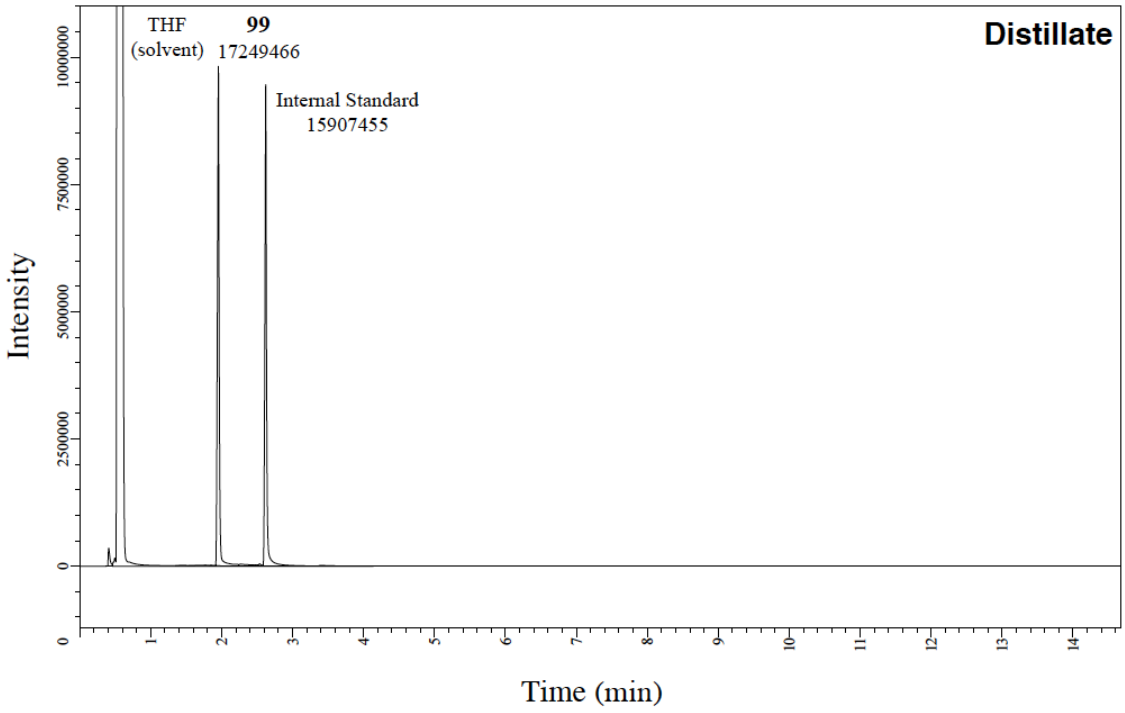

Figure 2.7 Gas chromatogram of the distillate from the reactive distillation of a mixture of **99**, **101**, **107**, and **108**, with internal standard (dodecane) added for calibration. THF was used as the solvent.

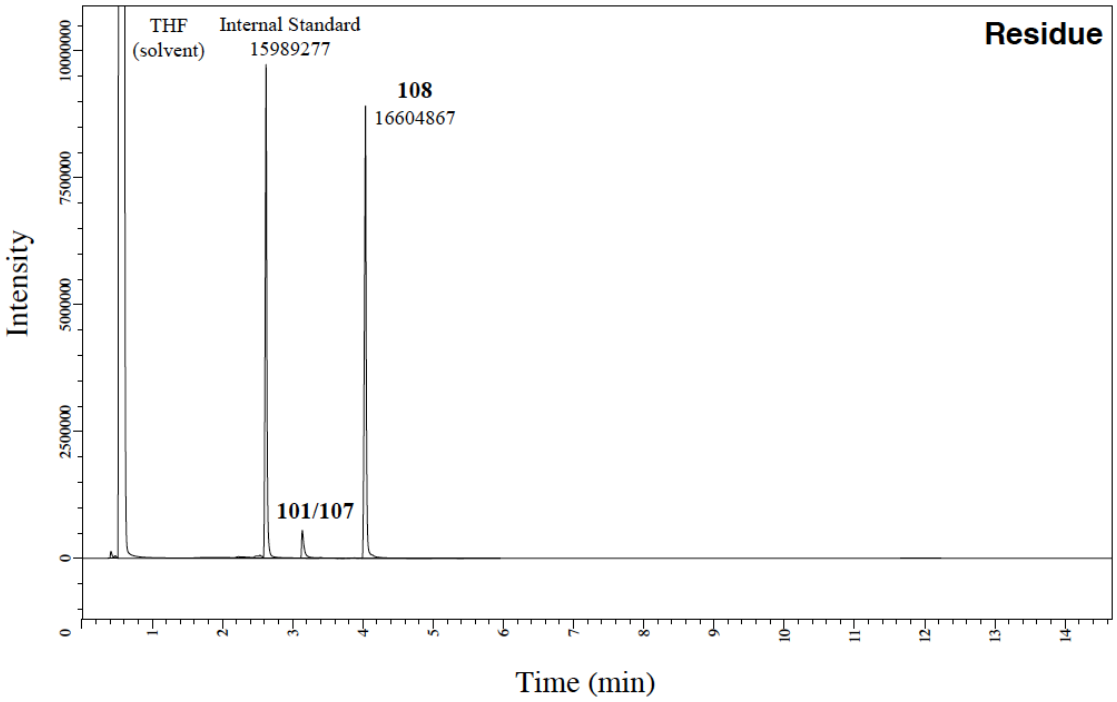

Figure 2.8 Gas chromatogram of the distillation residue from the reactive distillation of a mixture of **99**, **101**, **107**, and **108**, with internal standard (dodecane) added for calibration. THF was used as the solvent.

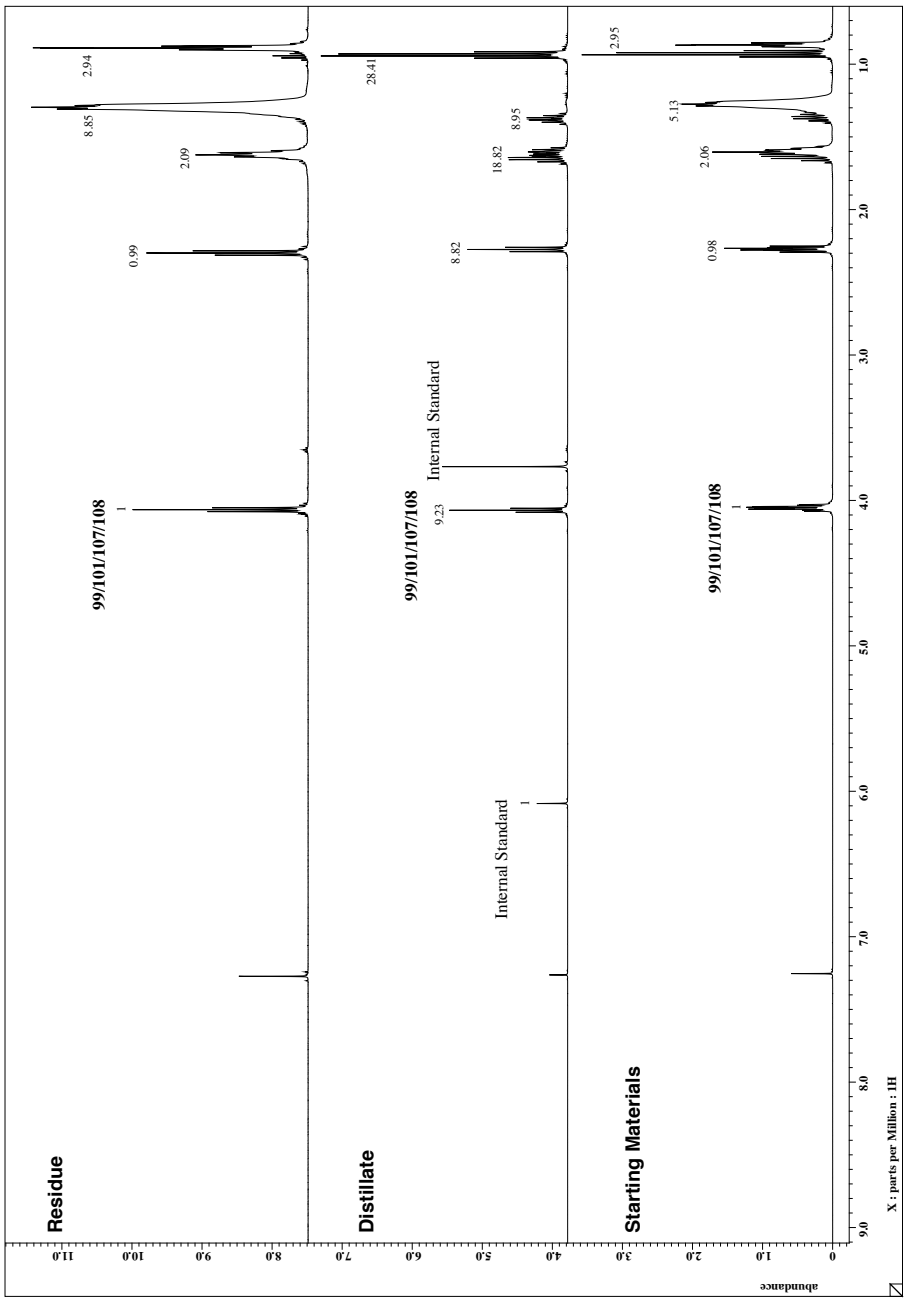

Figure 2.9 ^{1}H NMR spectra of the starting mixture (bottom) of esters **99**, **101**, **107**, and **108**, and the distillate (middle) and distillation residue (top) obtained after the reactive distillation of that mixture.

2.4.4 Reactive Distillations of [3×3] Ester Libraries

*2.4.4.1 Ethyl Acetate (**93**), Butyl Butyrate (**99**), and Benzyl Benzoate (**105**)*

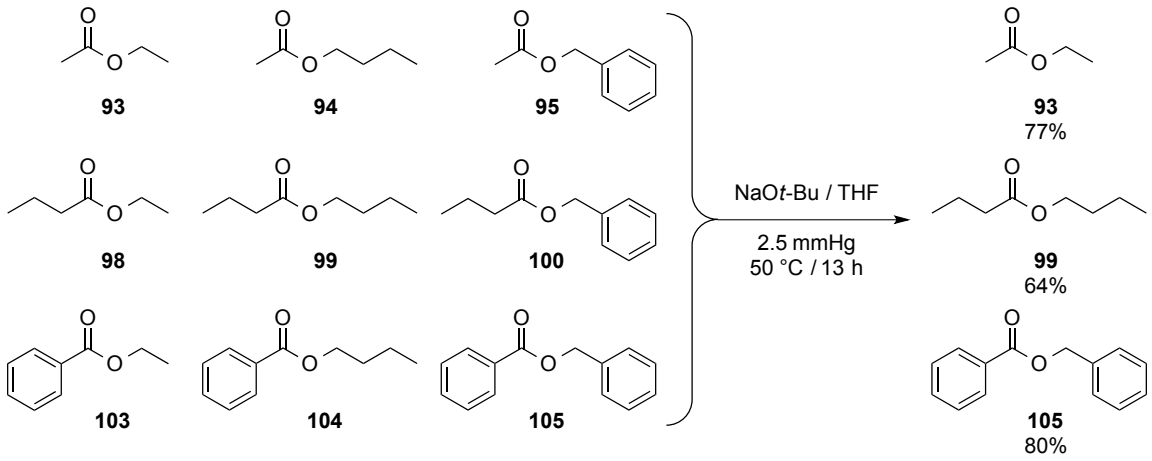

An equimolar mixture of **93** (890 mg, 10.0 mmol), **98** (1.17 g, 10.0 mmol), **103** (1.56 g, 10.0 mmol), **94** (1.17 g, 10.0 mmol), **99** (1.46 mg, 10.0 mmol), **104** (1.80 g, 10.0 mmol), **95** (1.52 g, 10.0 mmol), **100** (1.80 g, 10.0 mmol), and **105** (2.14 g, 10.0 mmol) was added to a 25 mL two-neck round bottom flask. The reaction flask was equipped with a 185 mm-long Vigreux column that was cooled by an *i*-PrOH/CO_2 cold trap (–55 to –50 °C). Short path distillation head was placed on top of the Vigreux column, connecting it to a receiving flask, which was placed into a separate *i*-PrOH/CO_2 ice bath (–78 °C). A 0.05 mL-portion of a 1M solution of NaO*t*-Bu in THF was injected into the reaction flask every 30 min for 10 h. Vacuum (2.5 mmHg) was started at the same time as the first loading of catalyst. The first step of this distillation was carried out at 50 °C over the course of 10 h. The first distillate was collected as a colorless liquid. ^{1}H NMR spectroscopy confirmed the identity of this liquid as a mixture of **93** (2.03 g, 23.1 mmol, 77% yield), **94** (41.4 mg, 0.36 mmol, 1% yield), **98** (91.0 mg, 0.78 mmol, 3% yield), and

THF (solvent, 2.59 g, 35.9 mmol). The second distillate was collected after another 10 h of distillation without the Vigreux column, during which a 0.05 mL-portion of a 1M solution of NaO*t*-Bu in THF was injected into the reaction flask every 30 min. ^{1}H NMR spectroscopy confirmed the identity of this liquid as a mixture of **99** (2.76 g, 19.2 mmol, 64% yield), **94** (205 mg, 1.76 mmol, 6% yield), **98** (37.5 mg, 0.32 mmol, 1% yield), **100** (54.9 mg, 0.31 mmol, 1% yield), **104** (47.9 mg, 0.27 mmol, 1% yield), and THF (solvent, 1.43 g, 19.9 mmol). The residue was identified by ^{1}H NMR spectroscopy as a mixture of **105** (5.11 g, 24.1 mmol, 80% yield), **100** (473 mg, 2.66 mmol, 9% yield), and **104** (452 mg, 2.54 mmol, 8% yield).

93: ^{1}H NMR ($CDCl_3$): 4.11 (q, ^{3}J=7.1 Hz, 2 H), 2.03 (s, 3 H), 1.20 (t, ^{3}J=7.1 Hz, 3 H) ppm. ^{13}C NMR ($CDCl_3$): 170.8, 60.1, 20.7, 13.9 ppm. Spectral data agree with a previous literature report.[26]

99: ^{1}H NMR ($CDCl_3$): 4.07 (t, ^{3}J=6.8 Hz, 2H), 2.27 (t, ^{3}J=7.5 Hz, 2H), 1.69–1.40 (m, 6H) 0.9 (t, ^{3}J=6.4 Hz, 6H) ppm. ^{13}C NMR ($CDCl_3$): 173.77, 64.06, 36.26, 30.74, 19.17, 18.50, 13.70, 13.66 ppm. Spectral data agree with a previous literature report.[22]

105: ^{1}H NMR ($CDCl_3$): 8.10 (d, ^{3}J=7.0 Hz, 2H), 7.59 (t, ^{3}J=7.5 Hz, 1H), 7.37–7.50 (m, 7H), 5.40 (s, 2H) ppm. ^{13}C NMR ($CDCl_3$): 166.54, 136.26, 133.21, 130.32, 129.89, 128.78, 128.57, 128.43, 128.36, 66.84 ppm. Spectral data agree with a previous literature report.[25]

Calculation of the Yields based on the Integration of ^{1}H NMR Spectra

Internal standard 1,3,5-trimethoxybenzene (173 mg, 1.02 mmol) was added to a 512 mg-aliquot of the first distillate. From their relative integrals in the ^{1}H NMR spectrum (Figure 2.10), the number of moles of **93** was calculated to be 1.02 mmol × 1.49 ÷ (2/3) = 2.27 mmol. Thus, the total number of moles of **93** in the first distillate was 2.27 mmol × 5210 mg ÷ 512 mg = 23.1 mmol, corresponding to the yield of **93** of 23.1 mmol ÷ 30.0 mmol × 100% = 77%. Analogous calculation allowed us to estimate the yields of minor fractions **94** and **98** at 1% and 3%, respectively.

Similar yield calculation procedure was applied to the second distillate: 1,3,5-trimethoxybenzene (163 mg, 0.96 mmol) was added to a 569 mg-aliquot of the residue. The number of moles of **99** in the aliquot was calculated to be 0.96 mmol × [1.94 – (0.32 × 2/3)] ÷ (2/3) = 2.49 mmol. The total number of moles of **99** in the whole of the second distillate was 2.49 mmol × 4379 mg ÷ 569 mg = 19.2 mmol, corresponding to the yield of 19.2 mmol ÷ 30.0 mmol × 100% = 64%. Equivalent calculation allowed us to estimate the yields of minor fractions **94**, **98**, **100**, and **103** at 6%, 1%, 1%, and 1%, successively.

Analogous yield calculation procedure was applied to the distillation residue as well: 1,3,5-trimethoxybenzene (181 mg, 1.07 mmol) was added to a 712 mg-aliquot of the residue. The number of moles of **105** in the aliquot was calculated to be 1.07 mmol × 1.64 ÷ (2/3) = 2.62 mmol. The total number of moles of **105** in the whole of the distillation residue was 2.62 mmol × 6539 mg ÷ 712 mg = 24.1 mmol, corresponding to

the yield of 24.1 mmol ÷ 30.0 mmol × 100% = 80%. Analogous calculation allowed us to estimate the yields of minor fractions **100** and **104** at 9% and 8%, respectively.

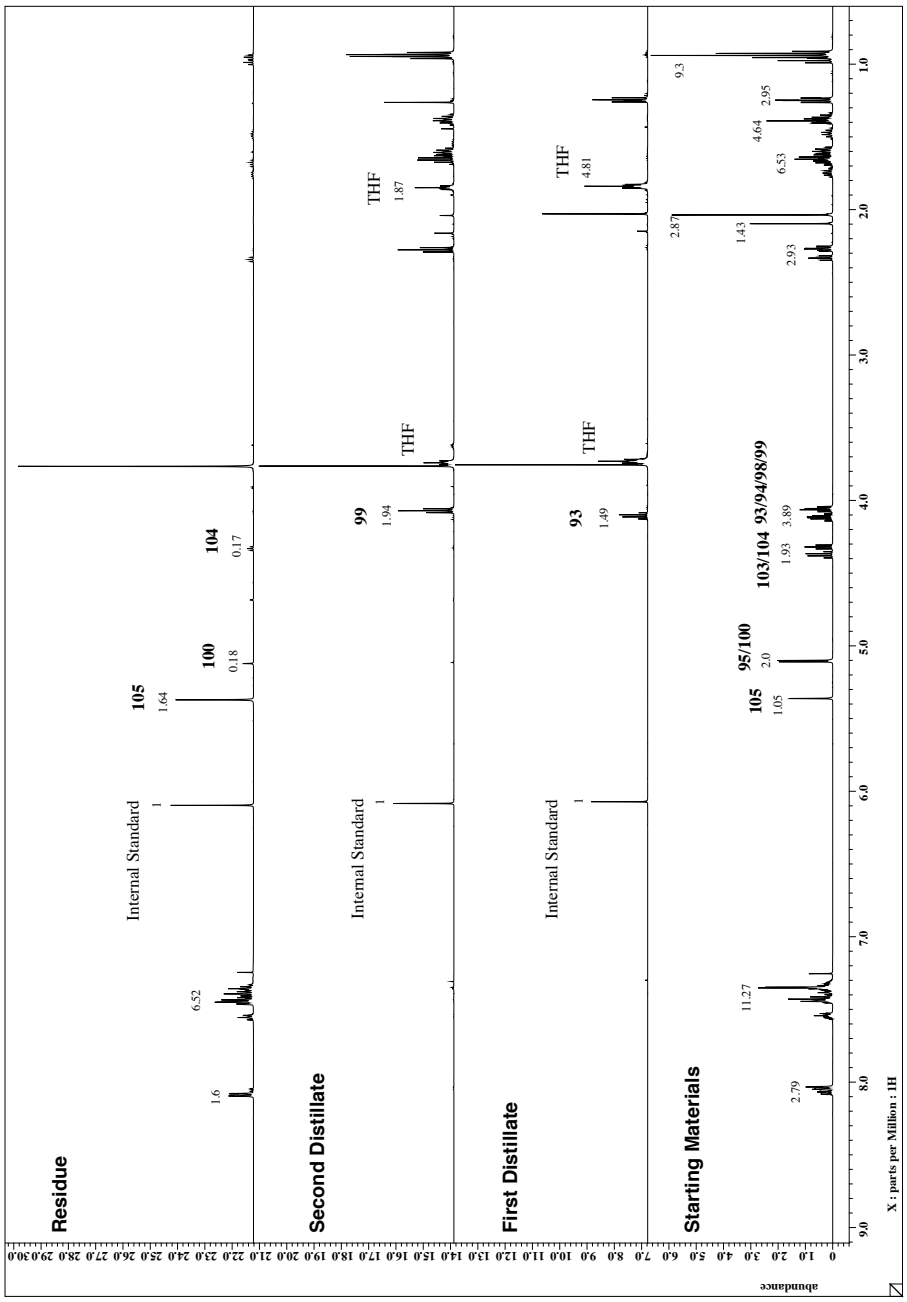

Figure 2.10 ^{1}H NMR spectra of the starting mixture (bottom) of esters **93–105**, and the two distillates (middle) and distillation residue (top) obtained after the reactive distillation of that mixture.

*2.4.4.2 Ethyl Acetate (**93**), Butyl Butyrate (**99**), and Octyl Octanoate (**108**)*

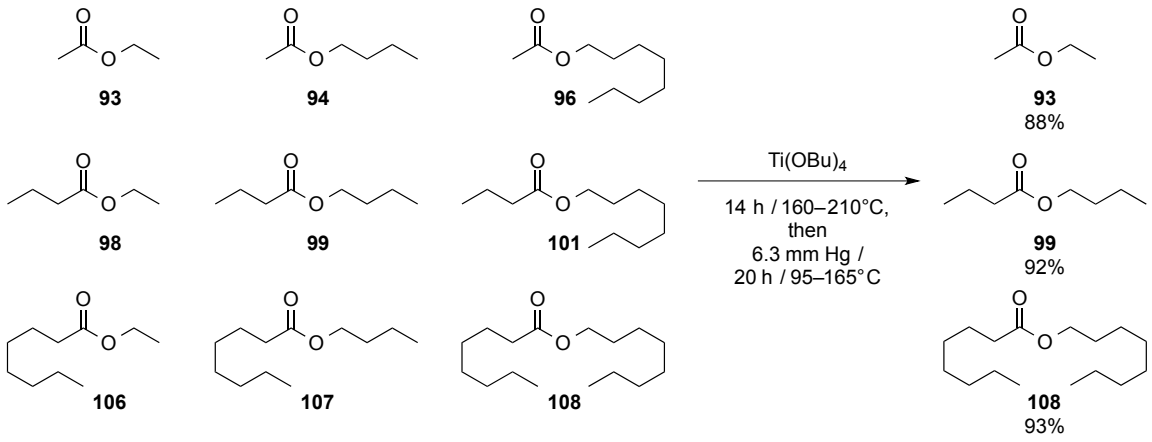

Titanium *n*-butoxide (0.93 g, 2.70 mmol) and an equimolar mixture of **93** (2.67 g, 30.0 mmol), **94** (3.52 g, 30.0 mmol), **96** (5.22 g, 30.0 mmol), **98** (3.52 g, 30.0 mmol), **99** (4.37 g, 30.0 mmol), **101** (6.07 g, 30.0 mmol), **106** (5.22 g, 30.0 mmol), **107** (6.07 g, 30.0 mmol), and **108** (7.77 g, 30.0 mmol) was added to a 100 mL round bottom flask. The flask was fitted with a Vigreux column, and a short path distillation head was used to connect it to a receiving flask, which was placed in an *i*-PrOH/CO_2 ice bath (–78 °C). The first step of the distillation was carried out at atmospheric pressure for 14 h, with temperature slowly being raised from 160 to 210 °C. The first distillate (9.51 g) was collected as a colorless liquid. ^{1}H NMR spectroscopy confirmed the identity of this liquid as a mixture dominated by **93** (7.01 g, 79.6 mmol, 88% yield), and with minor contributions from **94** and **98**. The reaction flask was then equipped with a 185 mm-long Vigreux column and placed under vacuum (6.25 mmHg) for the second step of the distillation. The second distillate (12.0 g) was collected after another 9.5 hours. ^{1}H NMR spectroscopy confirmed the identity of this liquid as a mixture of **99** (11.9 g, 82.8 mmol,

92% yield) and small amounts of **94** and **98**. Finally, the distillation residue (24.0 g) was identified by ^{1}H NMR spectroscopy and gas chromatography as a mixture of **108** (21.5 g, 82.8 mmol, 93% yield) and small amounts of **107** and **101**.

93: ^{1}H NMR ($CDCl_3$): 4.11 (q, ^{3}J=7.1 Hz, 2 H), 2.03 (s, 3 H), 1.20 (t, ^{3}J=7.1 Hz, 3 H) ppm. ^{13}C NMR ($CDCl_3$): 170.8, 60.1, 20.7, 13.9 ppm. Spectral data agree with a previous literature report.[26]

99: ^{1}H NMR ($CDCl_3$): 4.07 (t, ^{3}J=6.8 Hz, 2H), 2.27 (t, ^{3}J=7.5 Hz, 2H), 1.69–1.40 (m, 6H) 0.9 (t, ^{3}J=6.4 Hz, 6H) ppm. ^{13}C NMR ($CDCl_3$): 173.77, 64.06, 36.26, 30.74, 19.17, 18.50, 13.70, 13.66 ppm. Spectral data agree with a previous literature report.[22]

108: ^{1}H NMR ($CDCl_3$): 4.04 (t, ^{3}J=6.7 Hz, 2H), 2.28 (t, ^{3}J=7.5 Hz, 1H), 1.60 (m, 4H), 1.29 (m, 18H), 0.86 (t, ^{3}J=6.4 Hz, 6H) ppm. ^{13}C NMR ($CDCl_3$): 174.08, 64.46, 34.47, 31.76 (2C), 29.29, 29.20, 29.03, 28.72 (2C), 25.11 (2C), 22.73, 22.69, 14.15 (2C) ppm. Spectral data agree with a previous literature report.[27]

Calculation of the Yields based on the Integration of ^{1}H NMR Spectra

Internal standard 1,3,5-trimethoxybenzene (81 mg, 0.48 mmol) was added to a 808 mg-aliquot of the first distillate. From their relative integrals in the ^{1}H NMR spectrum (Figure 2.12), the number of moles of **93** was calculated to be 0.48 mmol × [16.57 – (1.59 × 1.5)] = 6.77 mmol. Thus, the total number of moles of **93** in the first distillate was 6.77 mmol × 9510 mg ÷ 808 mg = 79.6 mmol, corresponding to the yield of **93** of 79.6 mmol ÷ 90.0 mmol × 100% = 88%.

Similar yield calculation procedure was applied to the second distillate: 1,3,5-trimethoxybenzene (97 mg, 0.57 mmol) was added to a 930 mg-aliquot of the residue. The number of moles of **99** in the aliquot was calculated to be 0.57 mmol × [(8.12 – 0.96 × (2/3))] ÷ (2/3) = 6.38 mmol. The total number of moles of **99** in the whole of the second distillate was 6.38 mmol × 12030 mg ÷ 930 mg = 82.6 mmol, corresponding to the yield of 82.6 mmol ÷ 90.0 mmol × 100% = 92%.

Yield of **108** was calculated from gas chromatography data, as described below.

*Calculation of the Yield of **108** based on the Integration of GC Peaks*

For the purpose of quantification of yield of **108**, we determined a response factor (F) for this ester with respect to dodecane, which was used as GC internal standard. The area of ester signal / mass of ester = F × area of standard signal / mass of standard. That is, $a_e / m_e = F \times a_s / m_s$. Therefore, a_e and m_e of a pure sample of **108** and a_s and m_s of GC internal standard (dodecane) were used to calculate F value. Five independent determinations of the F value were performed (0.787, 0.792, 0.760, 0.799, 0.803), yielding an average F = 0.788. This value was then used to calculate the amount of **108** in the distillation residue of this reactive distillation (Figure 2.11). A 48.8 mg-aliquot of the distillation residue was added to a glass vial, followed by addition of dodecane (28.1 mg) and THF (3 mL) as the solvent. The mixture was subjected to gas chromatography using the temperature program described in the General Methods section. From the integration, mass of **108** could be calculated as $m_e = (a_e \times m_s) / (a_s \times F)$ = (19942883 × 28.1 mg) / (16240111 × 0.788) = 43.8 mg. The total mass of **108** in the distillation residue was 43.8

mg × 24.0 g ÷ 48.8 mg = 21.5 g. The yield of **108** is 21.5 g ÷ 256.42 g mol^{-1} ÷ 90.0 mmol × 100% = 93%.

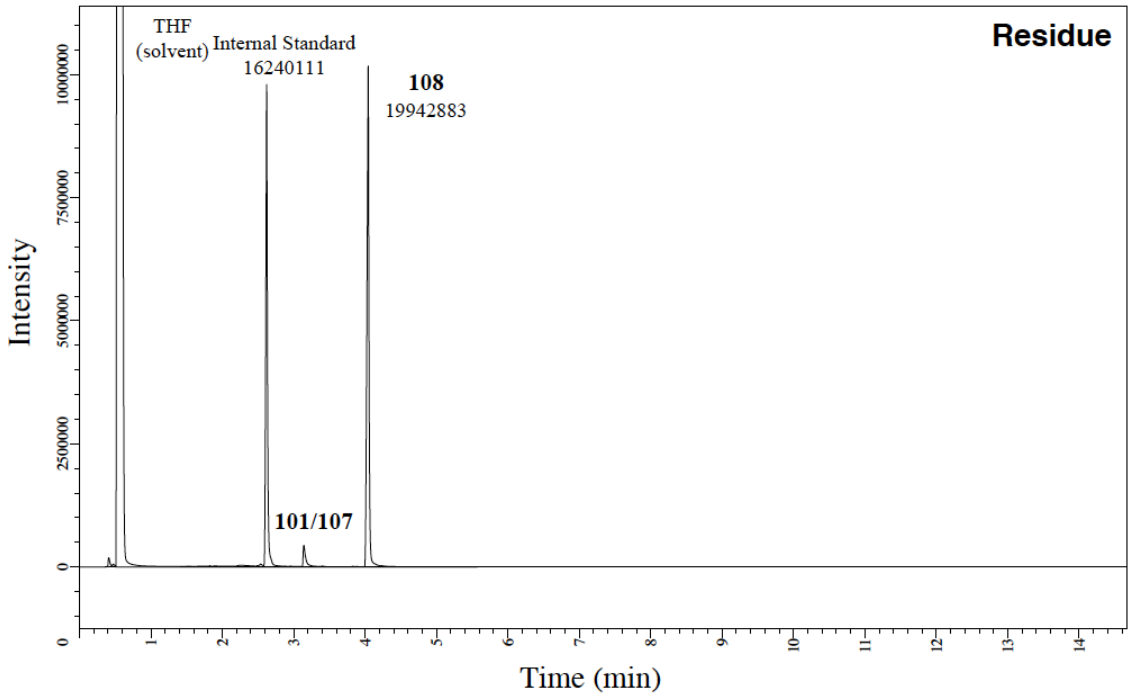

Figure 2.11 Gas chromatogram of the distillation residue from the reactive distillation of an equimolar mixture of **93**, **94**, **96**, **98**, **99**, **101**, **106**, **107**, and **108**, with internal standard (dodecane) added for calibration. THF was used as the solvent.

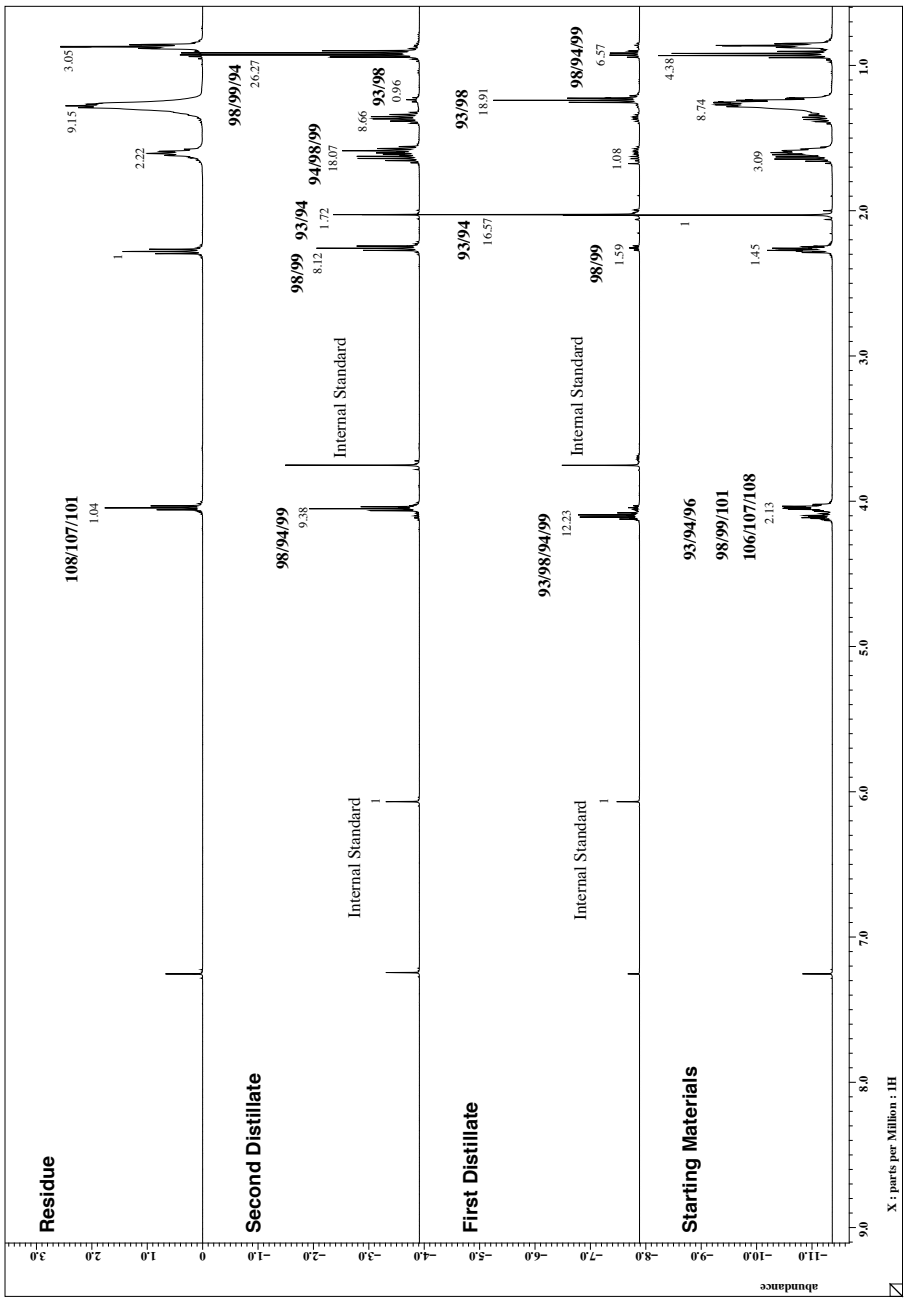

Figure 2.12 ^{1}H NMR spectra of the starting mixture (bottom) of esters **93**, **94**, **96**, **98**, **99**, **101**, **106**, **107**, and **108**, and the two distillates (middle) and distillation residue (top) obtained after the reactive distillation of that mixture.

2.4.5 Reactive Distillations of [4×4] Ester Libraries

*2.4.5.1 Ethyl Acetate (**93**), Butyl Butyrate (**99**), Octyl Octanoate (**108**), and Cetyl Palmitate (**113**)*

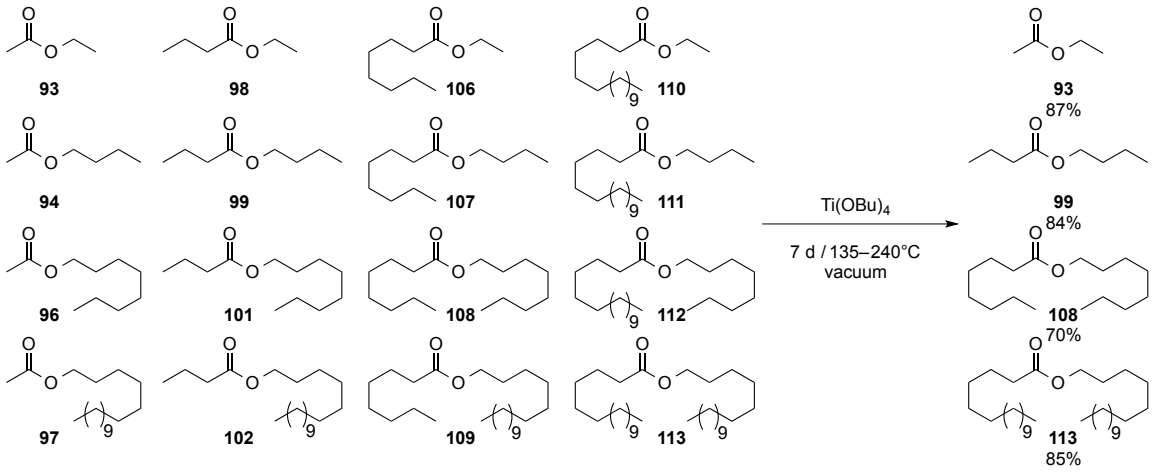

Titanium *n*-butoxide (0.50 mL, 49.8 mg, 1.46 mmol) and an equimolar mixture of **93** (0.89 g, 10.0 mmol), **94** (1.17 g, 10.0 mmol), **96** (1.74 g, 10.0 mmol), **97** (2.90 g, 10.0 mmol), **98** (1.17 g, 10.0 mmol), **99** (1.46 g, 10.0 mmol), **101** (2.02 g, 10.0 mmol), **102** (3.19 g, 10.0 mmol), **106** (1.74 g, 10.0 mmol), **107** (2.02 g, 10.0 mmol), **108** (2.59 g, 10.0 mmol), **109** (3.76 g, 10.0 mmol), **110** (2.90 g, 10.0 mmol), **111** (3.19 g, 10.0 mmol), **112** (3.76 g, 10.0 mmol), and **113** (4.91 g, 10.0 mmol) were placed into a 100 mL round bottom flask. Short path distillation head was used to connect the reaction flask with a receiving flask, which was placed in a liquid N_2 bath (–196 °C). The first step of the distillation was performed at atmospheric pressure over 72 h and the mixture was gradually heated up from 170 to 240 °C. The first distillate (3.50 g) was collected as a colorless liquid, and ^{1}H NMR spectroscopy of this liquid confirmed its identity as a

mixture of **93** (3.07 g, 34.9 mmol, 87% yield) and **94** and **98** as trace components. The reaction flask was then equipped with a 100 mm-long Vigreux column and placed under vacuum (6.3 mmHg) for the second step of the distillation. The second distillate (7.00 g) was collected after the mixture was heated from 135 to 195 °C during the course of additional 45 h. The temperature was slowly increased from 135 to 155 °C in the first 4 h and additional $Ti(OBu)_4$ (0.10 mL, 99.6 mg, 0.29 mmol) was added to the reaction flask. Temperature was then increased from 155 to 165 °C over 6 h and another portion of $Ti(OBu)_4$ (0.10 mL, 99.6 mg, 0.29 mmol) was added to the reaction flask. Finally, temperature was increased from 165 to 190 °C over the course of 19 h and the final portion of $Ti(OBu)_4$ (0.10 mL, 99.6 mg, 0.29 mmol) was added to the reaction flask. Temperature was brought from 190 to 195 °C over the course of last 16 h. Using a combination of ^1H NMR spectroscopy and gas chromatography, the second distillate was identified as a mixture of **99** (4.86 g, 33.7 mmol, 84% yield), and minute amounts of **94** and **98**. The third distillate (9.70 g) was collected after high vacuum (0.10 mm Hg) distillation at temperature from 200 to 240 °C during the course of another 24 h. The temperature was slowly increased from 200 to 240 °C in the first 4 h, followed by the addition of $Ti(OBu)_4$ (0.10 mL, 99.6 mg, 0.29 mmol) to the reaction flask. The Vigreux column was removed and the mixture was heated from 205 to 220 °C for 4 h, followed by another portion of $Ti(OBu)_4$ (0.10 mL, 99.6 mg, 0.29 mmol). Finally, the temperature was increased from 220 to 240 °C over 4 h and the temperature was kept at 240 °C for 12 h. A combination of ^1H NMR spectroscopy and gas chromatogaphy confirmed the identity of the third distillate liquid as a mixture of **108** (7.40 g, 28.9 mmol, 72% yield)

and small amounts of **101** and **107**. The residue (20.3 g) was identified by ^{1}H NMR spectroscopy and gas chromatography as a mixture of **113** (17.2 g, 35.8 mmol, 90% yield) and small amounts of **109** and **112**.

93: ^{1}H NMR ($CDCl_3$): 4.11 (q, ^{3}J=7.1 Hz, 2 H), 2.03 (s, 3 H), 1.20 (t, ^{3}J=7.1 Hz, 3 H) ppm. ^{13}C NMR ($CDCl_3$): 170.8, 60.1, 20.7, 13.9 ppm. Spectral data agree with a previous literature report.[26]

99: ^{1}H NMR ($CDCl_3$): 4.07 (t, ^{3}J=6.8 Hz, 2H), 2.27 (t, ^{3}J=7.5 Hz, 2H), 1.69–1.40 (m, 6H) 0.9 (t, ^{3}J=6.4 Hz, 6H) ppm. ^{13}C NMR ($CDCl_3$): 173.77, 64.06, 36.26, 30.74, 19.17, 18.50, 13.70, 13.66 ppm. Spectral data agree with a previous literature report.[22]

108: ^{1}H NMR ($CDCl_3$): 4.04 (t, ^{3}J=6.7 Hz, 2H), 2.28 (t, ^{3}J=7.5 Hz, 1H), 1.60 (m, 4H), 1.29 (m, 18H), 0.86 (t, ^{3}J=6.4 Hz, 6H) ppm. ^{13}C NMR ($CDCl_3$): 174.08, 64.46, 34.47, 31.76 (2C), 29.29, 29.20, 29.03, 28.72 (2C), 25.11 (2C), 22.73, 22.69, 14.15 (2C) ppm. Spectral data agree with a previous literature report.[27]

113: ^{1}H NMR ($CDCl_3$): 4.04 (t, ^{3}J=6.7 Hz, 2H), 2.28 (t, ^{3}J=7.5 Hz, 2H), 1.57–1.61 (m, 4H), 1.24–1.29 (m, 50H), 0.85–0.88 (m, 6H) ppm. ^{13}C NMR ($CDCl_3$): 174.16, 64.51, 34.64, 32.03, 29.80, 29.58, 29.48, 29.38, 28.74, 26.04, 25.13, 22.80, 14.23 ppm. Spectral data agree with a previous literature report.[29]

Calculation of the Yields based on the Integration of ^{1}H NMR Spectra

Internal standard 1,3,5-trimethoxybenzene (80.5 mg, 0.47 mmol) was added to a 670 mg-aliquot of the distillate. From their relative integrals in the ^{1}H NMR spectrum

(Figure 2.13), the number of moles of **93** was calculated as 0.47 mmol × [14.73 – (0.42 × 1.5)] = 6.68 mmol. Thus, the total number of moles of **93** in the distillate was 6.68 mmol × 3500 mg ÷ 670 mg = 34.9 mmol, corresponding to the yield of **93** of 34.9 mmol ÷ 40.0 mmol × 100% = 87%.

Calculation of the Yields based on the Integration of GC Peaks

For the purpose of quantification of yields of **99**, **108**, and **113** we determined response factors (*F*) for these esters with respect to dodecane as the GC internal standard. The area of ester signal / mass of ester = *F* × area of standard signal / mass of standard. That is, $a_e / m_e = F \times a_s / m_s$. Therefore, a_e and m_e of a pure samples of **99**, **108**, and **113**, and a_s and m_s of GC internal standard (dodecane) were used to calculate *F* values. Five independent determinations of the *F* value were performed for **99** (0.624, 0.658, 0.663, 0.653, 0.658), yielding an average *F* = 0.651 for **99**. Five independent determinations of the *F* value were performed for **108** (0.787, 0.792, 0.760, 0.799, 0.803), yielding an average *F* = 0.788 for **108**. Four independent determinations of the *F* value were performed for **113** (0.863, 0.857, 0.882, 0.828), yielding an average *F* = 0.857 for **113**. These values were then used to calculate the amounts of **99**, **108**, and **113** in the distillates and distillation residue of this reactive distillation (Figures 2.14, 2.15, and 2.16, successively). A 50.5 mg-aliquot of the first distillate was added to a glass vial, followed by addition of dodecane (28.7 mg) and THF (3 mL) as the solvent. The mixture was subjected to gas chromatography using the temperature program described in the General Methods section. From the integration, mass of **99** could be calculated as $m_e = (a_e \times m_s) /$

($a_s \times F$) = (13392345 × 28.7 mg) / (16122856 × 0.651) = 36.6 mg. The total mass of **99** in the distillation residue was 36.6 mg × 7.00 g ÷ 50.5 mg = 5.07 g. The yield of **99** is 5.07 g ÷ 144.21 g mol^{-1} ÷ 40.0 mmol × 100% = 88%.

A 43.5 mg-aliquot of the second distillate was added to a glass vial, followed by addition of dodecane (30.3 mg) and THF (3 mL) as the solvent. The mixture was subjected to gas chromatography using the temperature program described in the General Methods section. From the integration, mass of **108** could be calculated as $m_e = (a_e \times m_s) / (a_s \times F)$ = (14360829 × 30.3 mg) / (17269926 × 0.788) = 32.0 mg. The total mass of **108** in the distillation residue was 32.0 mg × 9.70 g ÷ 43.5 mg = 7.14 g. The yield of **108** is 7.14 g ÷ 256.42 g mol^{-1} ÷ 40.0 mmol × 100% = 70%.

A 41.9 mg-aliquot of the distillation residue was added to a glass vial, followed by addition of dodecane (33.2 mg) and THF (3 mL) as the solvent. The mixture was subjected to gas chromatography using the temperature program described in the General Methods section. From the integration, mass of **108** could be calculated as $m_e = (a_e \times m_s) / (a_s \times F)$ = (15973173 × 33.2 mg) / (18431583 × 0.857) = 33.6 mg. The total mass of **108** in the distillation residue was 33.6 mg × 20.3 g ÷ 41.9 mg = 16.3 g. The yield of **108** is 16.3 g ÷ 480.85 g mol^{-1} ÷ 40.0 mmol × 100% = 85%.

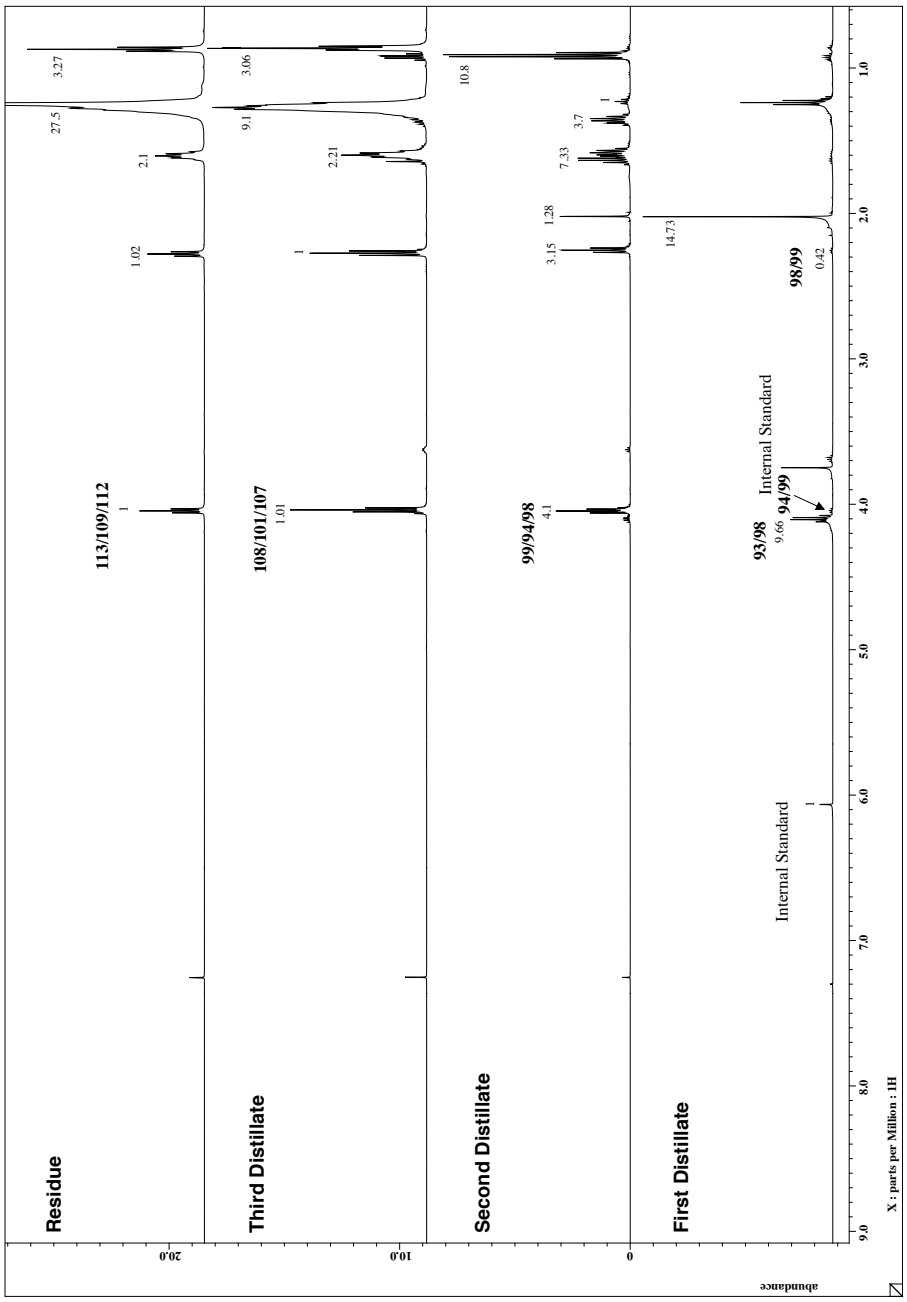

Figure 2.13 ^{1}H NMR spectra of the three distillates and the distillation residue resulting from the reactive distillation of an equimolar mixture of esters **93**, **94**, **96**, **97**, **98**, **99**, **101**, **102**, **106**, **107**, **108**, **109**, **110**, **111**, **112**, and **113**.

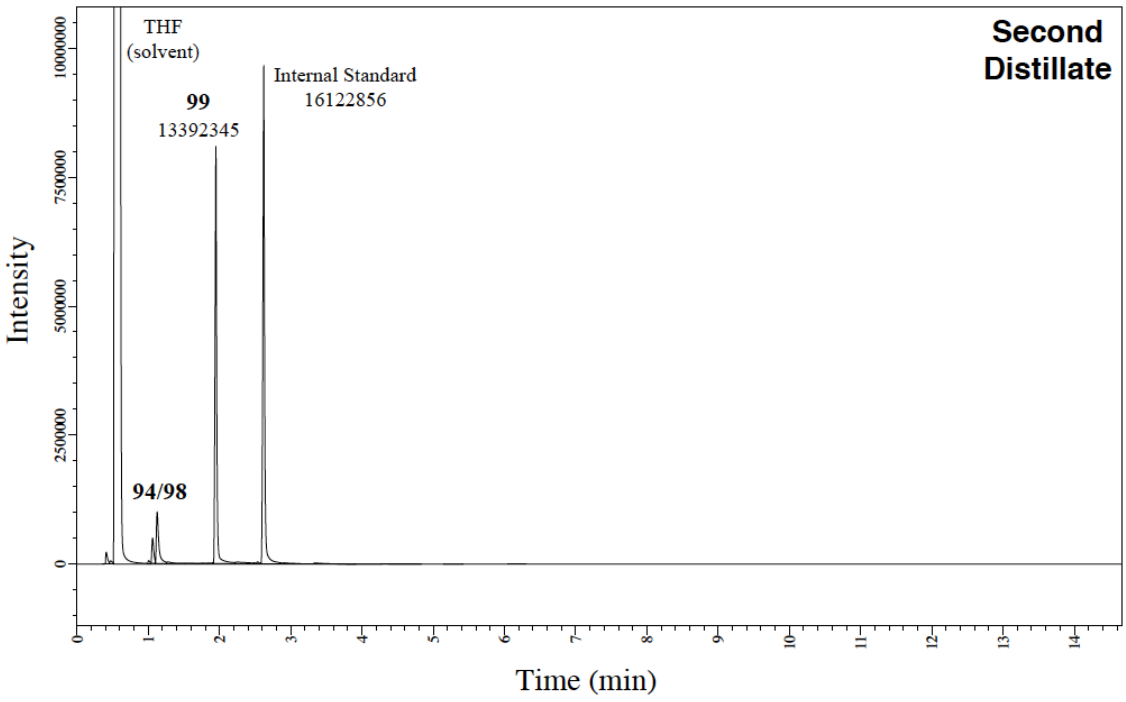

Figure 2.14 Gas chromatogram of the second distillate from the reactive distillation of an equimolar mixture of **93**, **94**, **96**, **97**, **98**, **99**, **101**, **102**, **106**, **107**, **108**, **109**, **110**, **111**, **112**, and **113**, with internal standard (dodecane) added for calibration. THF was used as the solvent.

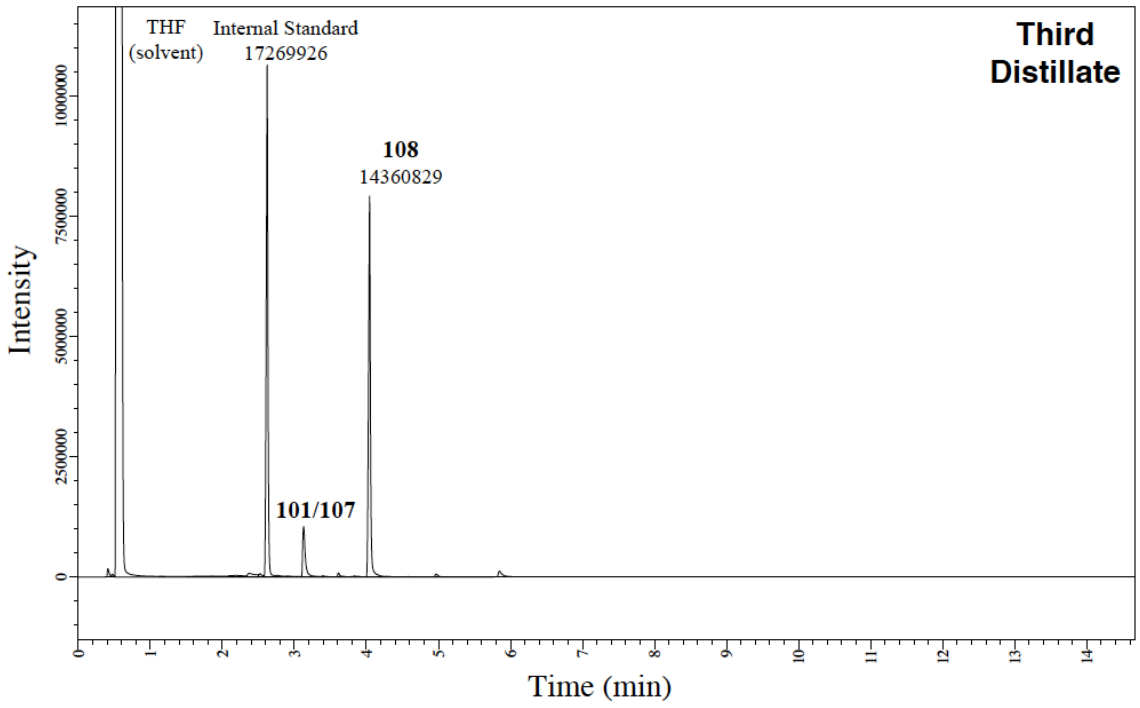

Figure 2.15 Gas chromatogram of the third distillate from the reactive distillation of an equimolar mixture of **93**, **94**, **96**, **97**, **98**, **99**, **101**, **102**, **106**, **107**, **108**, **109**, **110**, **111**, **112**, and **113**, with internal standard (dodecane) added for calibration. THF was used as the solvent.

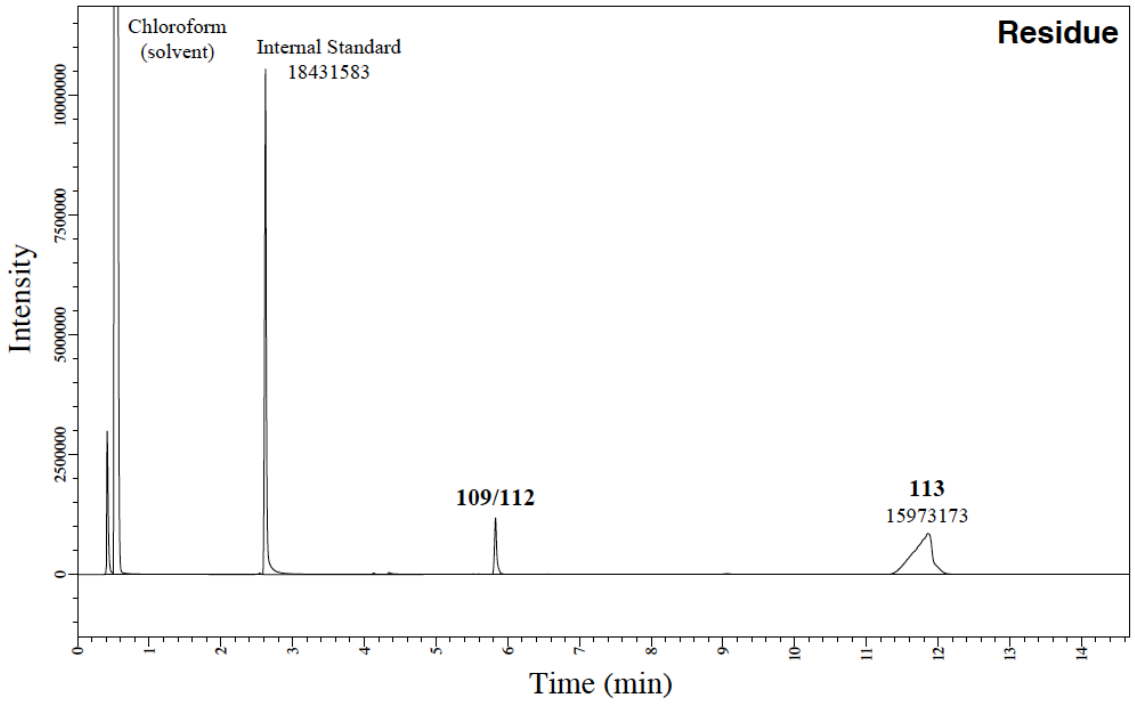

Figure 2.16 Gas chromatogram of the distillation residue from the reactive distillation of an equimolar mixture of **93**, **94**, **96**, **97**, **98**, **99**, **101**, **102**, **106**, **107**, **108**, **109**, **110**, **111**, **112**, and **113**, with internal standard (dodecane) added for calibration. THF was used as the solvent.

2.4.6 Reactive Distillations of [2×3] Ester Libraries

*2.4.6.1 Ethyl Acetate (**93**), Ethyl Butyrate (**98**), and Benzyl Benzoate (**105**)*

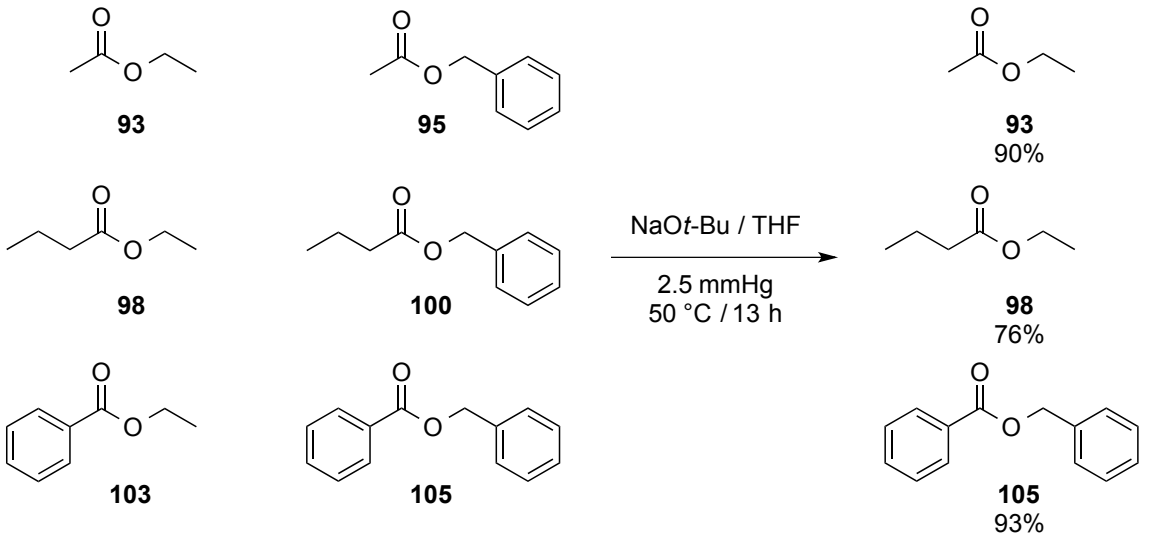

A mixture of **93** (890 mg, 10.0 mmol), **98** (1.17 g, 10.0 mmol), **103** (3.03 g, 20.0 mmol), **95** (1.52 g, 10.0 mmol), **100** (1.80 g, 10.0 mmol), and **105** (2.14 g, 10.0 mmol) was added to a 25 mL two-neck round bottom flask. The reaction flask was equipped with a 185 mm-long Vigreux column cooled by a *i*-PrOH/CO_2 cold trap (–55 to –50 °C). Short path distillation head was placed on top of the Vigreux column, connecting it to the receiving flask, which was placed in a separate *i*-PrOH/CO_2 ice bath (–78 °C). A 0.05 mL-aliquot of a 1M sodium *tert*-butoxide in THF solution was injected into the reaction flask every 30 min for 5 h. Vacuum (2.5 mm Hg) was started at the same time as the first loading of catalyst was added. The first step of the distillation was performed at 50 °C for 5 h, resulting in the first distillate, which was collected as a colorless liquid. ^{1}H NMR spectroscopy confirmed the identity of this liquid as a mixture of **93** (1.58 g, 17.9 mmol,

90% yield), **98** (106 mg, 0.91 mmol, 5% yield), and THF (solvent, 888 mg, 12.4 mmol). The second distillate was collected after another 8 h of distillation without the Vigreux column. A 0.05 mL-aliquot of a 1M sodium *tert*-butoxide in THF solution was injected into the reaction flask every 30 min for 8 h. ^{1}H NMR spectroscopy confirmed the identity of this liquid as a mixture of **93** (35.9 mg, 0.41 mmol, 2% yield), **98** (1.75 g, 15.1 mmol, 76% yield) and THF (solvent, 1.62 g, 22.5 mmol). Esters **95**, **103**, **100**, and **105** were not observed in either of the distillates. The remainder in the distillation flask was identified by ^{1}H NMR spectroscopy as a mixture of **105** (5.90 g, 27.8 mmol, 93% yield), **100** (209 mg, 1.18 mmol, 6% yield), and **103** (199 mg, 1.33 mmol, 7% yield).

93: ^{1}H NMR ($CDCl_3$): 4.11 (q, ^{3}J=7.1 Hz, 2 H), 2.03 (s, 3 H), 1.20 (t, ^{3}J=7.1 Hz, 3 H) ppm. ^{13}C NMR ($CDCl_3$): 170.8, 60.1, 20.7, and 13.9 ppm. Spectral data agree with a previous literature report.[26]

98: ^{1}H NMR ($CDCl_3$): 4.13 (q, ^{3}J=6.8 Hz, 2H), 2.27 (t, ^{3}J=7.4 Hz, 2H), 1.65 (sextet, ^{3}J=7.4 Hz, 2H), 1.26 (t, ^{3}J=6.8 Hz, 3H), 0.96 (t, ^{3}J=7.4 Hz, 3H) ppm. ^{13}C NMR ($CDCl_3$): 173.61, 60.13, 36.32, 18.57, 14.32, and 13.70 ppm. Spectral data agree with a previous literature report.[21]

105: ^{1}H NMR ($CDCl_3$): 8.10 (d, ^{3}J=7.0 Hz, 2H), 7.59 (t, ^{3}J=7.5 Hz, 1H), 7.37–7.50 (m, 7H), 5.40 (s, 2H) ppm. ^{13}C NMR ($CDCl_3$): 166.54, 136.26, 133.21, 130.32, 129.89, 128.78, 128.57, 128.43, 128.36, and 66.84 ppm. Spectral data agree with a previous literature report.[25]

Calculation of the Yields based on the Integration of ^{1}H NMR Spectra

Internal standard 1,3,5-trimethoxybenzene (673 mg, 3.96 mmol) was added to a 740 mg-aliquot of the first distillate. From their relative integrals in the ^{1}H NMR spectrum (Figure 2.17), the number of moles of **93** was calculated to be 3.96 mmol × 1 ÷ (2/3) ÷ 1.34 = 4.43 mmol. Thus, the total number of moles of **93** in the first distillate was 4.43 mmol × 2989 mg ÷ 740 mg = 17.9 mmol, corresponding to the yield of **93** of 17.9 mmol ÷ 20.0 mmol × 100% = 90%. Analogous calculation allowed us to estimate the yields of **98** at 5%.

Similar yield calculation procedure was applied to the second distillate: 1,3,5-trimethoxybenzene (340 mg, 2.00 mmol) was added to a 571 mg-aliquot of the residue. The number of moles of **99** in the aliquot was calculated to be 2.00 mmol × 1.1 ÷ (2/3) ÷ 1.49 = 2.22 mmol. The total number of moles of **99** in the whole of the second distillate was 2.22 mmol × 3892 mg ÷ 571 mg = 15.1 mmol, corresponding to the yield of 15.1 mmol ÷ 20.0 mmol × 100% = 76%. Equivalent calculation allowed us to estimate the yields of **93** at 2%.

Analogous yield calculation procedure was applied to the distillation residue as well: 1,3,5-trimethoxybenzene (342 mg, 2.01 mmol) was added to a 969 mg-aliquot of the residue. The number of moles of **105** in the aliquot was calculated to be 2.01 mmol × 1.30 ÷ (2/3) = 3.93 mmol. The total number of moles of **105** in the whole of the distillation residue was 3.93 mmol × 6862 mg ÷ 969 mg = 27.8 mmol, corresponding to

the yield of 27.8 mmol ÷ 30.0 mmol × 100% = 93%. Analogous calculation allowed us to estimate the yields of minor fractions **100** and **103** at 6% and 7%, respectively.

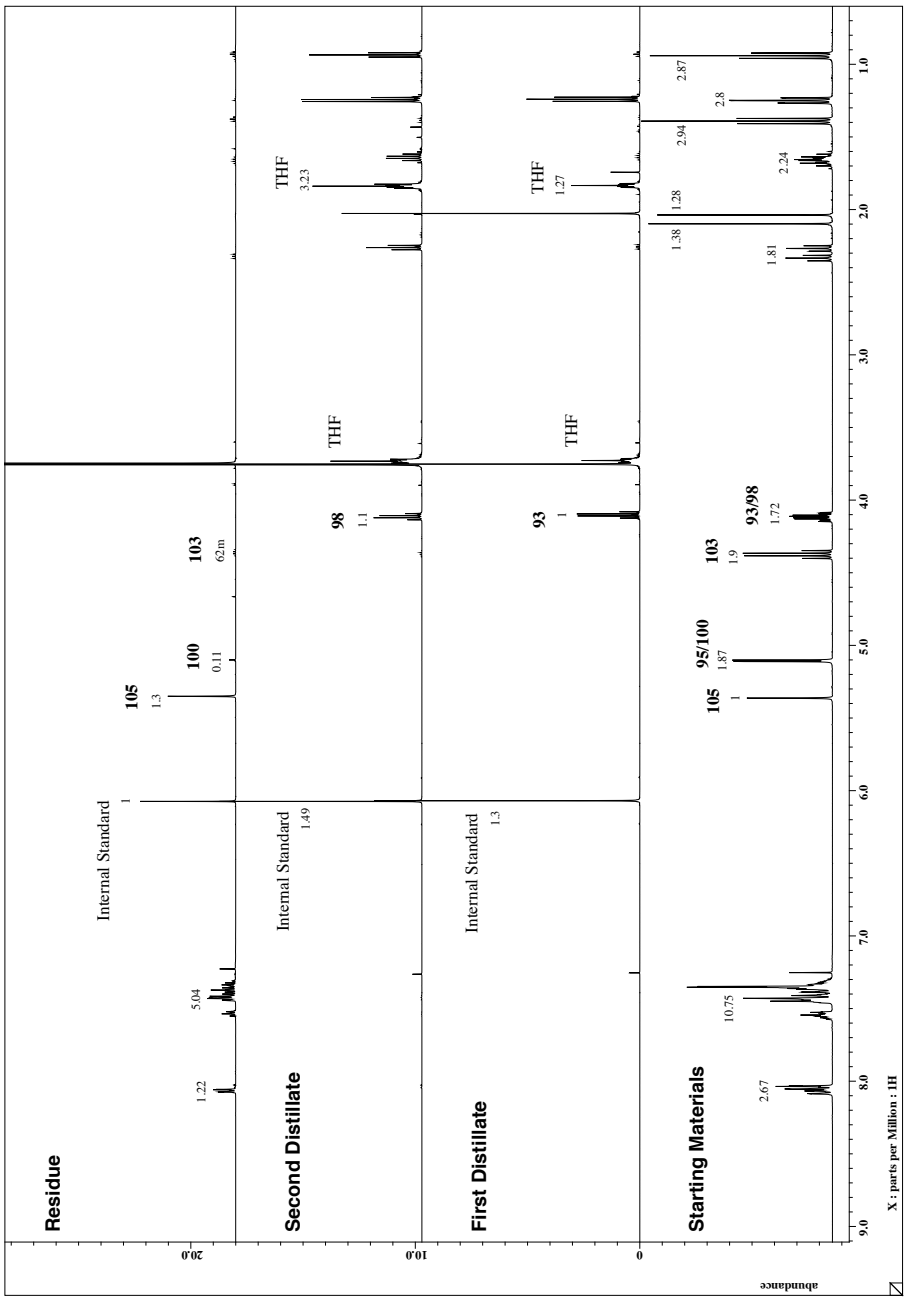

Figure 2.17 ^{1}H NMR spectra of the starting mixture (bottom) of esters **93**, **95**, **98**, **100**, **103** (2 equivalent), and **105**, and the two distillates (middle) and distillation residue (top) obtained after the reactive distillation of that mixture.

2.5 References

[1] The work described in this chapter has been previously published: Ji, Q.; Miljanić, O. Š. *J. Org. Chem.* **2013**, *78*, 12710–12716.

[2] *Origin of Life: Chemical Approach*; Herdewin, P., Kısakürek, M. V., Eds.; Wiley VCH: Weinheim, Germany, **2008**.

[3] (a) *Dynamic Combinatorial Chemistry*; Reek, J. N. H., Otto, S., Eds.; Wiley-VCH: Weinheim, Germany, **1996**. (b) Corbett, P. T.; Leclaire, J.; Vial, L.; West, K. R.; Wietor, J.-L.; Sanders, J. K. M.; Otto, S. *Chem. Rev.* **2006**, *106*, 3652–3711. (c) Rowan, S. J.; Cantrill, S. J.; Cousins, G. R. L.; Sanders, J. K. M.; Stoddart, J. F. *Angew. Chem., Int. Ed.* **2002**, *41*, 898–952. (d) Ludlow, R. F.; Otto, S. *Chem. Soc. Rev.* **2008**, *37*, 101–108.

[4] (a) Safont-Sempere, M. M.; Fernandez, G.; Würthner, F. *Chem. Rev.* **2011**, *111*, 5784–5814. (b) Osowska, K.; Miljanić, O. Š. *Synlett* **2011**, 1643–1648. (c) Ghosh, S.; Isaacs, L. in *Dynamic Combinatorial Chemistry in Drug Discovery, Bioorganic Chemistry, and Materials Science*; Miller, B. L., Ed.; Wiley: Hoboken, NJ, **2010**; pp 155–168. (d) Northrop, B. H.; Zheng, Y.-R.; Chi, K.-W.; Stang, P. J. *Acc. Chem. Res.* **2009**, *42*, 1554–1563. (e) Nitschke, J. R. *Acc. Chem. Res.* **2007**, *40*, 103–112.

[5] Osowska, K.; Miljanić, O. Š. *Angew. Chem., Int. Ed.* **2011**, *50*, 8345–8349.

[6] Osowska, K.; Miljanić, O. Š. *J. Am. Chem. Soc.* **2011**, *133*, 724–726.

[7] Lirag, R. C.; Osowska, K.; Miljanić, O. Š. *Org. Biomol. Chem.* **2012**, *10*, 4847–4850.

[8] (a) Kaiser, G.; Sanders, J. K. M. *Chem. Commun.* **2000**, 1763–1764. (b) Rowan, S. J.; Reynolds, D. J.; Sanders, J. K. M. *J. Org. Chem.* **1999**, *64*, 5804–5814. (c) Amatore, C.; Jutand, A.; Meyer, G.; Mottier, L. *Chem. Eur. J.* **1999**, *5*, 466–473. (d) Rowan, S. J.; Hamilton, D. G.; Brady, P. A.; Sanders, J. K. M. *J. Am. Chem. Soc.* **1997**, *119*, 2578–2579. (e) Brady, P. A.; Sanders, J. K. M. *J. Chem. Soc., Perkin Trans. 1* **1997**, 3237–3253. (f) Rowan, S. J.; Brady, P. A.; Sanders, J. K. M. *Angew. Chem., Int. Ed. Engl.* **1996**, *35*, 2143–2145. (g) Brady, P. A.; Bonar-Law, R. P.; Rowan, S. J.; Suckling, C. J.; Sanders, J. K. M. *Chem. Commun.* **1996**, 319–320.

[9] (a) Harmsen, G. J. *Chem. Eng. Process* **2007**, *46*, 774–780. (b) *Reactive Distillation: Status and Future Directions*; Sundmacher, K.; Kienle, A., Eds.; Wiley-VCH: Weinheim, Germany, **2003**.

[10] For previous applications of dynamic combinatorial chemistry in the controlled release of volatile chemicals, see: (a) Herrmann, A. *Chem. Eur. J.* **2012**, *18*, 8568–8577. (b) Buchs, B.; Fieber, W.; Vigouroux-Elie, F.; Sreenivasachary, N.; Lehn, J.-M.; Herrmann, A. *Org. Biomol. Chem.* **2011**, *9*, 2906–2919. (c) Buchs, B.;

Godin, G.; Trachsel, A.; de Saint Laumer, J.-Y.; Lehn, J.-M.; Herrmann, A. *Eur. J. Org. Chem.* **2011**, 681–695.

[11] For methyl acetate, see: (a) Agreda, V. H.; Partin, L. R. U.S. Patent 4435595, **1984**. (b) Popken, T.; Steinigeweg, S.; Gmehling, J. *Ind. Eng. Chem. Res.* **2001**, *40*, 1566–1574. For butyl acetate, see: (c) Hanika, J.; Kolena, J.; Smejkal, Q. *Chem. Eng. Sci.* **1999**, *54*, 5205–5209. (d) Zhicai, Y.; Xianbao, C.; Jing, G. *Chem. Eng. Sci.* **1998**, *53*, 2081–2088.

[12] (a) Kiss, A. A. *Fuel Process. Technol.* **2011**, *92*, 1288–1296. (b) Dimian, A. C.; Bildea, C. S.; Omota, F.; Kiss, A. A. *Comput. Chem. Eng.* **2009**, *33*, 743–750. (c) Omota, F.; Dimian, A. C.; Bliek, A. *Chem. Eng. Sci.* **2003**, *58*, 3159–3174.

[13] Lyuben, W. L.; Yu, C.-C. *Reactive Distillation Design and Control*; Wiley-AIChE: Weinheim, Germany, **2008**, pp 545–561.

[14] The volatilities of individual esters will determine the order in which they will be distilled out from the DCL. There is no explicit correlation between the volatility of a given ester and its constituent acids and alcohols. However, in this study, we found that esters formed from low boiling point alcohols and acids always had lower boiling points than those formed from alcohols and acids of higher boiling points. This behavior is probably a consequence of a sufficiently large difference

in the molecular masses and boiling points of the chosen carboxylic acids and alcohols. The reader is advised that this may not be a general rule.

[15] Freely available at www.miljanicgroup.com/IterativeSelfSorting.xlsx. Last accessed on October 15, **2013**.

[16] (a) Kissling, R. M.; Gagné, M. R. *Org. Lett.* **2000**, *2*, 4209–4212. (b) Stanton, M. G.; Allen, C. B.; Kissling, R. M.; Lincoln, A. L.; Gagné, M. R. *J. Am. Chem. Soc.* **1998**, *120*, 5981–5989.

[17] It should be noted that ester libraries presented in Schemes 2.1–2.4 were not prepared through a random esterification of the corresponding alcohols and carboxylic acids. Instead, the commercial samples of the requisite esters (dried over CaH_2) were mixed in exactly equimolar ratios and then subjected to reactive distillation. The purpose of this strategy was (a) to ensure the most random ester distribution possible, that is, to prevent any potential biasing of the library during the esterification process, and (b) to avoid possible losses of highly volatile esters during the high-temperature esterification.

[18] This hypothesis was indirectly confirmed through an experiment in which ester **95** alone was exposed to a stoichiometric amount of NaO*t*-Bu and then subjected to distillation. *t*-Butyl acetate could be clearly identified in the distillate, although in low yield (∼10%).

[19] Schnurrenberger, P.; Züger, M. F.; Seebach, D. *Helv. Chim. Acta* **1982**, *65*, 1197–1201.

[20] Some of the formed amount of **99** could have resulted from the extraction of butoxy groups from the titanium catalyst. There is no obvious way of telling whether the butoxy groups came from the catalyst, but the maximum amount $Ti(OBu)_4$ could have contributed would be 4 times its catalytic amount; in that worst-case scenario, the lowered "real" yield of **99** would have to be corrected to 81%. Similar argument can be applied to the yields of butyl esters in the [4×4] experiment.

[21] Of course, as soon as the acyl exchange catalyst is added to this mixture, the excess amount of **103** probably gets redistributed among other esters that share a component with it, that is, **93**, **98**, and **105**. The same argument applies to the [2×2] library that results after the first distillation step; the 2 equivalent amount of **105** (marked with an * in Scheme 2.4) is only one of the several possible distributions of the excess of **105**'s components.

[22] Tasic, L.; Abraham, R. J.; Rittner, R. *Magn. Reson. Chem.* **2002,** *40*, 449–454.

[23] Liu, X.; Wu, J.; Shang, Z. *Synth. Commun.* **2012,** *42*, 75–83.

[24] Salome, C.; Kohn, H. *Tetrahedron* **2009,** *65*, 456–460.

[25] Poeylaut-Palena, A. A.; Testero, S. A.; Mata, E. G. *Chem. Commun.* **2011,** *47*, 1565–1567.

[26] Cronin, L.; Manoni, F.; O'Connor, C. J.; Connon, S. J. *Angew. Chem. Int. Ed.* **2010,** *49*, 3045–3048.

[27] Das, A.; Chaudhuri, R.; Liu, R. S. *Chem. Commun.* **2009,** *27,* 4046–4048.

[28] Gowrisankar, S.; Neumann, H.; Beller, M. *Angew. Chem. Int. Ed.* **2011,** *50,* 5139–5143.

[29] Mantri, K.; Komura, K.; Sugi, Y. *Synthesis* **2005,** *12,* 1939–1944.

Chapter Three Scent Transmutation: A New Way to Teach on Chemical Equilibrium, Distillation, and Dynamic Combinatorial Chemistry[1]

3.1 Introduction

Chemical equilibrium is one of the key concepts in all of chemistry and is being taught in undergraduate curricula throughout the world. The behavior of equilibrated mixtures that are disturbed from equilibrium is governed by the well-known Le Châtelier's principle, which states that "a system always kicks back",[2] that is, an equilibrium shifts to replenish the mixture components that were removed by the disturbing stimulus. Le Châtelier's principle is viewed as relatively intuitive; at the same time, its immense practical and industrial importance may not be fully appreciated by undergraduate students, as curricula spend little to no time establishing connections between basic physicochemical principles and industrial processes.

Our group has had a long-standing interest in reactive distillation, which is both a very direct application of the Le Châtelier's principle and a widely used process in chemical industry. In a reactive distillation, a chemical reactor doubles as a distillation setup, as the product is continuously being distilled away from the equilibrating reaction mixture. As the volatile product is being removed, the remainder of the mixture shuffles to replenish it, until the starting materials are completely exhausted and the pure

product(s) are isolated in high yields. Reactive distillation yielded some of the chemical industry's biggest savings over the past three decades in terms of construction, energy, and raw material cost. Many compounds are industrially produced by reactive distillation, including esters, ethers, and some alkylated aromatic hydrocarbons.[3] Here, we present a series of reactive distillation experiments that illustrate this process using fragrant compounds. This simple and appealing set of experiments is highly instructive and they could easily be adapted to the undergraduate lab curriculum, where they could be utilized to teach the concepts of chemical equilibrium, Le Châtelier's principle, and reactive distillation.

Consider a hypothetical library of four esters (Scheme 3.1), constructed by random transesterification of an equimolar mixture of two carboxylic acids and two alcohols. When this mixture is exposed to $Ti(OBu)_4$ catalyst, an acyl exchange,[4] that is, the swapping of acyl and alkoxy substituents between the esters, will ensue. Because the acyl exchange reaction is reversible, the four esters will freely transfer material among themselves, and a dynamic equilibrium will eventually be established. Such an equilibrating collection of esters is called a DCL.[5] Through the reversible acyl exchange, the DCL is capable of adapting to external stimuli by changing its composition. Subjecting a DCL to distillation, either at atmospheric or lowered pressure, removes the most volatile ester (shown in Scheme 3.1 as the red–red combination), typically formed from the alcohol and the carboxylic acid of lower molecular masses. As this volatile ester is removed, the remainder of the mixture reequilibrates to produce more of it, and this process continues until essentially all of the volatile alkoxy and the volatile acyl groups

are removed as the distillate. At the same time, the distillation residue is vastly enriched in the least volatile compound (blue–blue combination), at the expense of the two esters of intermediate volatility. In essence, the most and the least volatile esters are amplified, while the crossover esters of moderate volatility are sacrificed. This process can be iteratively repeated in more complex libraries;[6a] our group has shown that ester libraries[6b] with as many as 16 members can be reduced in complexity to just four final products during the course of a reactive distillation. In related dynamic imine libraries, even greater simplification was possible:[6c] a starting DCL with 25 imine constituents could be reduced to just five final products.

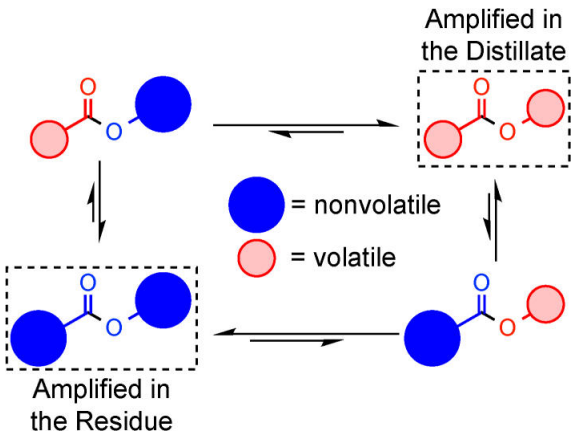

Scheme 3.1 Ester transmutation transforms two moderate volatility esters into the highly volatile ester that is distilled away (shown in red) and the low-volatility ester that remains in the distillation residue (shown in blue).

Perhaps an even more interesting case occurs if the distillation does not start with a four ester mixture, but instead uses the two "wrong" esters, that is, the two crossover red–blue combinations from Scheme 3.1, which have intermediate volatility. An outcome

of a reactive distillation in this case is essentially an ester transmutation experiment, in which two moderate-volatility esters quantitatively give rise to two different compounds, a highly volatile and a nonvolatile ester, and the high yields of this reaction are driven by fractional vacuum distillation.

As many esters are pleasantly smelling (and essentially nontoxic) compounds[7] and some are even approved as food additives by the US Food and Drug Administration (FDA),[8] we envisioned that an ester transmutation experiment could also proceed with a dramatic change in odors from the mixture of two starting esters to the two final products. Such an experiment would allow the change in the chemical composition to literally be smelled during the course of the reaction. To create such a *scent transmutation* experiment, all that was needed was a judicious choice of starting esters, so that they have easily identifiable aromas different from those of the product esters.

In this chapter, we describe the use of the $Ti(OBu)_4$-catalyzed transesterification in the synthesis of two ester products with different organoleptic properties from the two starting esters. We also demonstrate how the yields of the resulting products can be quantified by nuclear magnetic resonance (NMR) spectroscopy and gas chromatography (GC). This experiment illustrates several important experimental techniques and theoretical concepts: (1) fractional distillation, both at atmospheric and lowered pressure; (2) chemical equilibrium, exemplified by the $Ti(OBu)_4$-catalyzed ester exchange; (3) ester organoleptic properties, and (4) the use of internal standard methods to quantify product yields using NMR spectroscopy and GC. This series of experiments would be

particularly suitable for organic chemistry students in their third and fourth years, who have already been exposed to the theory of esterification reactions.

3.2 Results and Discussion

The six scent transmutation experiments shown in Scheme 3.2 have been standardized. All of them employ commercially available and FDA-approved ester starting materials. The first five experiments (Scheme 3.2A–E) were performed under a reduced pressure, which can be achieved using a small vacuum pump, such as those used for rotary evaporators. The last experiment (Scheme 3.2F) utilized atmospheric pressure, but this distillation took significantly longer to complete.

The very first experiment (Scheme 3.2A) will be used to illustrate the principles that guide all other reactive distillations presented here. The two starting esters were octyl acetate (**96**) and ethyl octanoate (**106**), with distinct aromas of apricot and melon, respectively. Equimolar amounts of these two esters were placed into a round-bottom distillation flask and exposed to 1.5 mol% of $Ti(OBu)_4$ as the catalyst. The mixture was placed under vacuum and heating commenced. We found that the progress of reactive distillation was better followed by monitoring the temperature of the external heating oil bath, rather than the temperature of the vapors (as would be the case in a standard distillation). If the oil bath temperature is kept between 90 and 110 °C, only ethyl acetate (**93**) will distill out of the reaction mixture. After the distillation of this material was

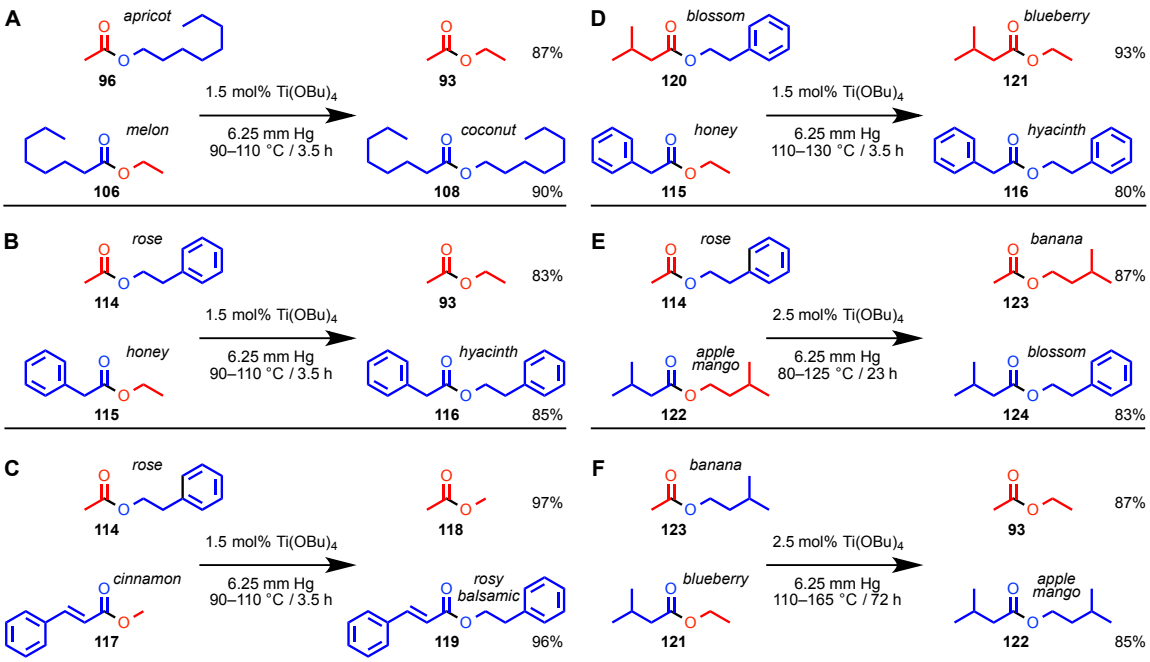

Scheme 3.2 Ester Transmutation Experiments Performed in this Study (organoleptic properties of selected compounds are given next to their structures).

complete (in approx. 3.5 h), the heating was stopped and the distillation setup was disassembled. Octyl octanoate (**108**) was the dominant component of the distillation residue.

The two product compounds could be qualitatively identified by their smell. Ethyl acetate has an aroma that some liken to pineapple or pears, but it is also so frequently used in everyday life that describing its aroma as "nail polish remover" is probably more accessible to the undergraduate student population. Octyl octanoate (**108**), in contrast, has a heavy odor of coconut and is clearly distinct from the two starting materials.[9]

Following the qualitative identification of distillation products, their yields were quantified by a combination of NMR spectroscopy and GC. NMR quantification was performed in chloroform-*d*, using 1,3,5-trimethoxybenzene as the internal standard (with two diagnostic singlets at δ 6.04 and 3.73 ppm). Known (i.e., weighed) amounts of the distillate and the distillation residue were placed into two separate NMR tubes and then known (but not necessarily identical) amounts of the internal standard were added into each NMR tube. The tubes were filled with chloroform-*d* and the corresponding spectra were taken. From the relative integrations of the peaks associated with the internal standard and those associated with each of the esters, molar amounts of each ester in the entire distillate (or distillation residue) could be readily calculated (see Experimental Section further details). While both the distillate and the distillation residue consisted mostly of a single ester, these fractions also contained small amounts of other possible esters that could be quantified using NMR spectroscopy. If the multiple products present in the distillate or distillation residue differed in at least one peak in their NMR spectra, they could have been accurately quantified using NMR spectroscopy alone. As an example, the reaction shown in Scheme 3.2C resulted in a distillation residue which had diagnostic peaks at 7.67 ppm (doublet) and 3.82 ppm (singlet). While the former peak corresponded to a mixture of two possible cinnamates (**117** and **119**), the later was representative of only methyl cinnamate (**117**), and so the amount of pure **119** could have been deduced by subtracting the integral values of the two peaks. However, in cases where the overlap of the peaks was too extensive to permit full quantification, GC was used as the alternative quantification method.

Gas chromatographic quantification utilized dodecane as the internal standard. Since the relative integration in gas chromatography depends on the compound's identity, correlation factors had to be elucidated for each individual ester. Specifically, a known amount of dodecane was mixed with five different known amounts of each of the corresponding esters. These mixtures were then injected into the gas chromatograph and the corresponding integrations of dodecane and the ester were compared to establish a correlation factor, which was averaged over five measurements at different concentrations (see Experimental Section for details). With gas chromatography, yields of esters could be determined even in cases where NMR spectroscopy proved problematic because of significant overlap among the peaks.

If this procedure were to be used as a basis of a future laboratory experiment, some common problems should be anticipated during its execution. None of them presents a safety risk or jeopardizes the learning outcomes, but some advice on how to best handle such issues is appropriate. The first common problem could be the low yield of the distillate, often coupled with a highly impure distillation residue. This issue would suggest that the reactive distillation did not proceed to completion. The remainder of the experiment can still proceed as planned: the distillate should have clear olfactory properties that should allow its identification, although the residue will present a mixture of three odors and its qualification may prove ambiguous. The quantification part of the experiment can proceed without any problems. In fact, running a shorter (and incomplete) reactive distillation may be a practical way to fit this experiment into a shorter time slots, in situations where, for example, class scheduling may present some restrictions. Another

potential problem may be the occurrence of impure distillate and/or distillation residue. This would suggest that the distillation was too fast, removing not only the most volatile but also one (or both) of the "crossover" esters of intermediate volatility. The solution here is obvious: lower the temperature of the oil bath. However, while qualification of odors in this case is very likely to fail, quantification can still proceed without significant modifications to the procedure. Finally, it may be challenging for students, and even more experienced chemists, to accurately describe odors of individual esters.[9]

For the full separation during the course of reactive distillation, the experiments shown in Scheme 3.2A–D require 3.5 h, and those in Scheme 3.2E–F require more than 20 h. The last two experiments are significantly longer than the typical organic laboratory period in US universities (~4 h). Thus, only the first four reactive distillations would be suitable for adaptation into hands-on experiments; the last two could be performed in the form of demonstrations, if needed.

3.3 Conclusions and Outlook

In summary, the scent transmutation protocol presented in this article constitutes a simple way to simultaneously teach students about several experimental techniques and fundamental concepts. First, it teaches how to perform vacuum distillation, a skill that many incoming graduate students in Chemistry PhD programs appear to lack. Second, it demonstrates the pleasant olfactory properties of many esters and highlights the fact that

these are used in the flavoring of foods. From a fundamental perspective, this procedure reinforces the concepts of equilibrium, Le Châtelier's principle, and the law of mass action. Additionally, it demonstrates how these principles can yield dynamic combinatorial libraries capable of adapting to external pressures through changes in their chemical composition. Finally, we hope that the industrially relevant process of reactive distillation can be brought closer to undergraduate students and hopefully encourage them to look for further connections between the principles they learn in classrooms and industrial processes that yield products that surround them.

3.4 Experimental Section

3.4.1 General Methods

NMR spectra were obtained on a JEOL ECA-500 spectrometer, with working frequency of 500 MHz for ^{1}H nuclei and 125 MHz for ^{13}C nuclei. ^{1}H NMR chemical shifts are reported in ppm units relative to the residual signal of the solvent ($CDCl_3$: 7.25 ppm). All NMR spectra were recorded at 25°C, and ^{13}C NMR spectra were recorded with simultaneous decoupling of ^{1}H nuclei. Compound 1,3,5-trimethoxybenzene (Alfa Aesar, 99%) was utilized as the internal standard for the calculations of yields of different esters on the basis of integration of ^{1}H NMR spectra of distillates and distillation residues. Gas chromatography was performed using GC-2010 Shimadzu gas chromatograph. The temperature program that was used for all characterizations started with (1) constant

temperature of 50 °C for 1 min, followed by (2) monotonous temperature increase from 50 to 270 °C within 4 min, and finally (3) constant temperature of 270 °C for 10 min. Dodecane (Alfa Aesar, 99%) was utilized as an internal standard for the calculation of yields based on the integration of gas chromatograms.

Three methods were used for the reactive distillation of ester mixtures. The first method was employed for the first four distillations (Scheme 3.2A–D in the introduction); the second method was used for the fifth distillation (Scheme 3.2E in the introduction), while the third method was utilized for the last of the reactive distillations (Scheme 3.2F in the introduction).

Method 1

Two intermediate volatility esters (30.0 mmol of each) were placed into an oven-dried 100-mL two-neck round bottom flask equipped with a magnetic stir bar. The flask was flushed with nitrogen and connected to a 100-mm long vacuum-jacketed Vigreux column topped with a short-path distillation head. A round bottom receiving flask was connected to the distillation head and the entire setup connected to a vacuum pump. Then, 1.5 mol% of $Ti(OBu)_4$ was added to the distillation flask through the second unutilized neck. The second neck was stoppered, the vacuum pump was turned on, and the oil bath was heated to the requisite temperature (see individual experiments for details). The reaction flask was lowered into the oil bath and heated for 3.5 h. The vacuum pump was turned off and the gas inlet adaptor on the side arm was carefully opened. The distillation

apparatus was disconnected and the amounts of the residue and the distillate were separately weighed.

Method 2

Two intermediate volatility esters (30.0 mmol of each) were placed into an oven-dried 100-mL two-neck round bottom flask equipped with a magnetic stir bar. The flask was flushed with nitrogen and then connected to a 100-mm long vacuum-jacketed Vigreux column topped with a short-path distillation head. A round bottom receiving flask was also connected to the distillation head and the entire setup connected to a vacuum pump. Then, 2.5 mol% of $Ti(OBu)_4$ was added to the distillation flask through the second unutilized neck. The second neck was stoppered and the flask was lowered into the oil bath. The vacuum pump and the hot plate were turned on and the oil bath was heated to 80 °C. Temperature of the oil bath was increased by 5 °C every one hour from until 125 °C, and was then maintained at 125 °C for 14 h. The reaction was stopped after 23 h. The vacuum pump was turned off and the gas inlet adaptor on the side arm was carefully opened. The distillation apparatus was disconnected and the amounts of the residue and the distillate were separately weighed.

Method 3

Two intermediate volatility esters (30.0 mmol of each) were placed into an oven-dried 50-mL two-neck round bottom flask equipped with a magnetic stir bar. The flask was flushed with nitrogen and then connected to a short-path distillation head. A 25-mL

round bottom receiving flask was connected to the distillation head. Then, 2.5 mol% of $Ti(OBu)_4$ was added to the distillation flask through the second unutilized neck. The second neck was stoppered, the reaction flask lowered into the oil bath, and the heating commenced. The oil bath was heated to 110 °C first, and then its temperature was increased by 5 °C every two hours, until the temperature reached 130 °C. The oil bath was maintained at 130 °C for 12 h. Then, temperature was again increased by 5 °C every 2 h until it reached 155 °C, where it was again maintained for 12 h. Finally, temperature was increased to 165 °C over 2 h. The reaction was stopped after 46 h of additional heating. The heating was disconnected, distillation apparatus disassembled, and the amounts of the residue and the distillate were separately weighed.

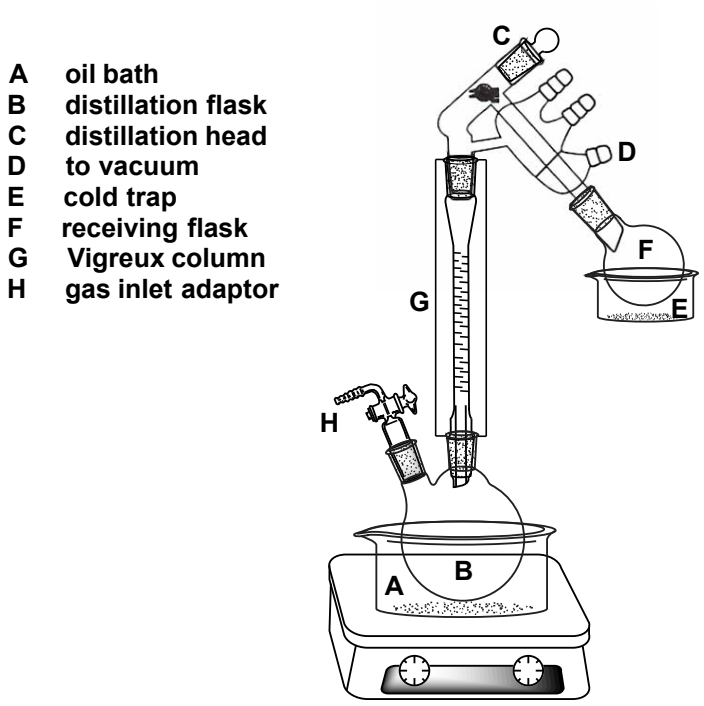

Figure 3.1 General setup used for the scent transmutation reactions.

3.4.2 Ethyl Acetate (93) and Octyl Octanoate (108)

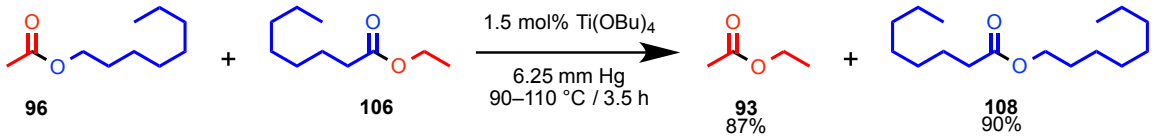

Distillate was isolated in the amount of 2.31 g, with compound **93** as the principal component. Compound **93**: ^{1}H NMR ($CDCl_3$): 4.10 (q, ^{3}J=6.8 Hz, 2H), 2.00 (s, 3H), 1.23 (t, ^{3}J=6.8 Hz, 3H) ppm. ^{13}C NMR ($CDCl_3$): 171.2, 60.4, 21.1, 14.2 ppm. Spectral data agree with a literature report.[10]

Distillation residue was isolated in the amount of 6.90 g, with compound **108** as the principal component. Compound **108**: ^{1}H NMR ($CDCl_3$): 4.04 (t, ^{3}J=6.8 Hz, 2H), 2.27 (t, ^{3}J=7.5 Hz, 2H), 1.63–1.57 (m, 4H), 1.34–1.23 (m, 18H), 0.87 (t, ^{3}J=7.5 Hz, 6H) ppm. ^{13}C NMR ($CDCl_3$): 174.08, 64.47, 34.49, 31.87, 31.76, 29.30, 29.28, 29.20, 29.02, 28.74, 26.02, 25.11, 22.73, 22.68, 14.16, 14.14 ppm. Spectral data agree with a previous literature report.[11]

*Calculation of the Yield of **93** Based on the Integration of ^{1}H NMR Spectra*

Internal standard 1,3,5-trimethoxybenzene (52.9 mg, 0.311 mmol) was added to a 602 mg aliquot of the distillate. From their relative integrals in the ^{1}H NMR spectrum (Figure 3.2), the number of moles of **93** was calculated to be 0.311 mmol × 12.08 ÷ (2/3) = 5.635 mmol. Thus, the total number of moles of **93** in the distillate was 5.635 mmol × 2.80 g ÷ 0.602 g = 26.2 mmol, corresponding to the yield of **93** of 26.2 mmol ÷ 30.0

mmol × 100% = 87%. Minor fractions were not quantified because of the extensive overlap of their ^{1}H NMR spectral peaks.

Yield of **108** was calculated from gas chromatography data, as described below.

*Calculation of the Yield of **108** Based on the Integration of GC Peaks*

For the purpose of quantification of yield of **108**, we determined a response factor (F) for this ester with respect to dodecane, which was used as GC internal standard. The area of ester signal / mass of ester = F × area of standard signal / mass of standard. That is, $a_e / m_e = F \times a_s / m_s$. Therefore, a_e and m_e of a pure sample of **108** and a_s and m_s of GC internal standard (dodecane) were used to calculate F value. Five independent determinations of the F value were performed (0.787, 0.792, 0.760, 0.799, 0.803), yielding an average F = 0.788. This value was then used to calculate the amount of **108** in the distillation residue of this reactive distillation (Figure 3.3). A 39.5 mg aliquot of the distillation residue was added to a glass vial, followed by addition of dodecane (19.3 mg) and THF (3 mL) as the solvent. The mixture was subjected to gas chromatography using the temperature program described in the General Methods section. From the integration, mass of **108** could be calculated as $m_e = (a_e \times m_s) / (a_s \times F)$ = (15921215 × 19.3 mg) / (11439130 × 0.788) = 34.1 mg. The total mass of **108** in the distillation residue was 34.1 mg × 8.0 g ÷ 39.5 mg = 6.90 g. The yield of **108** is 6.90 g ÷ 256.42 g mol^{-1} ÷ 30.0 mmol × 100% = 90%.

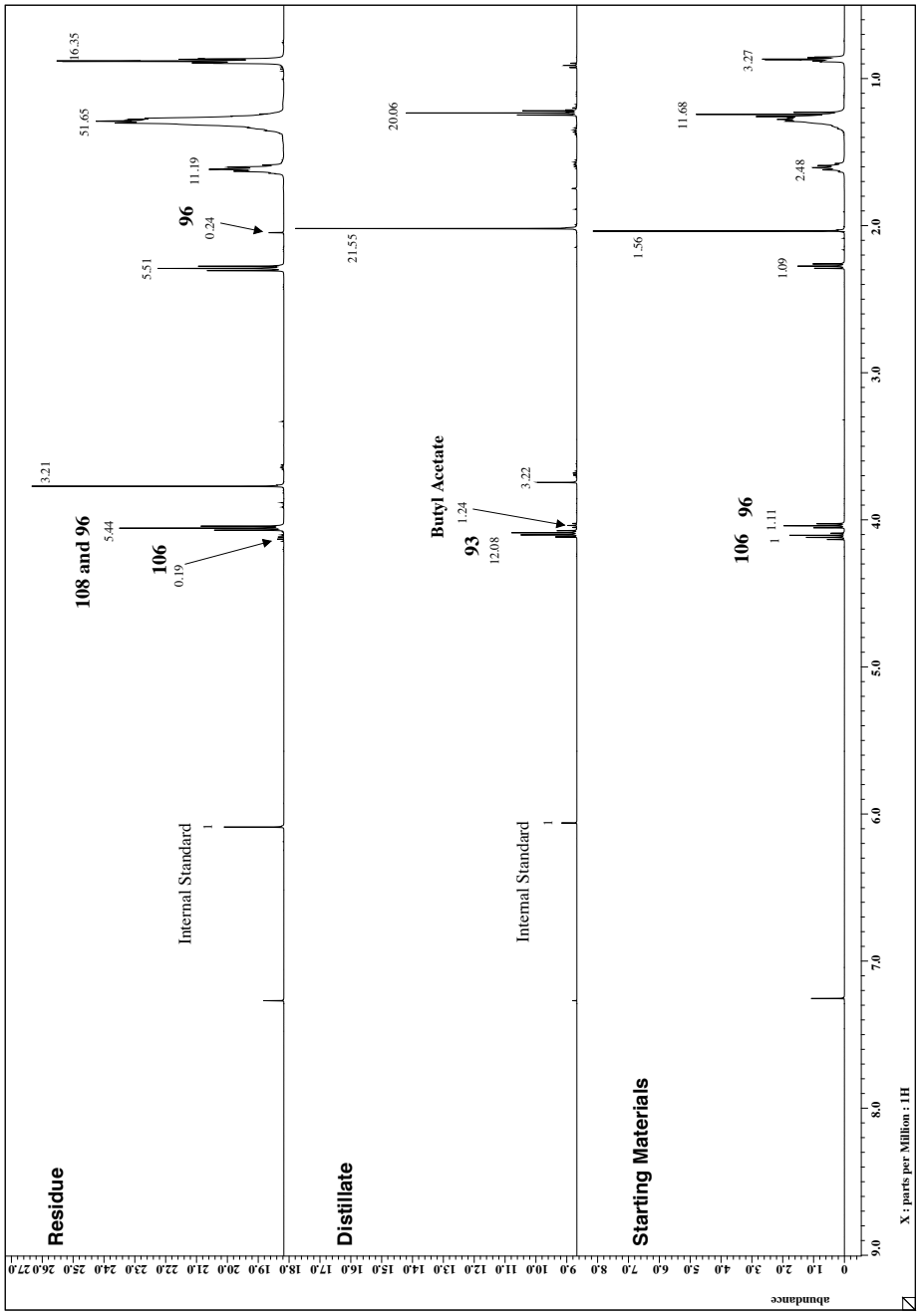

Figure 3.2 ^{1}H NMR spectra of the starting mixture (bottom) of esters **96** and **106**, and the distillate (middle) and distillation residue (top) after the scent transmutation of that mixture.

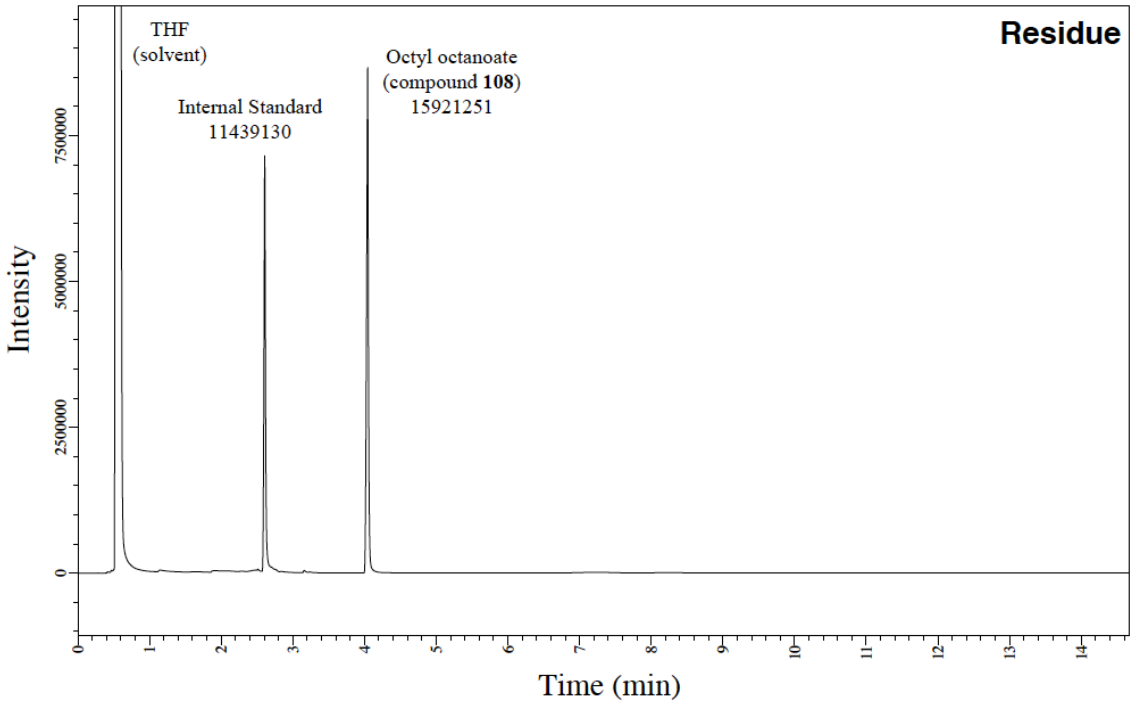

Figure 3.3 Gas chromatogram of the distillation residue from the scent transmutation of an equimolar mixture of **96** and **106**, with internal standard (dodecane) added for calibration. THF was used as the solvent.

3.4.3 Ethyl Acetate (93) and Phenylethyl Phenylacetate (116)

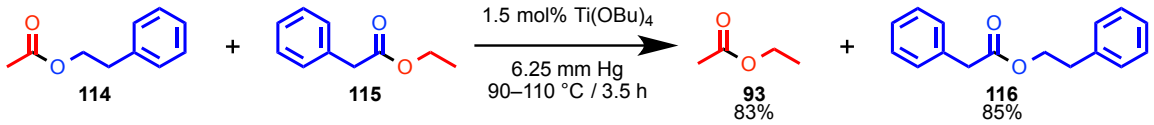

Distillate was isolated in the amount of 2.19 g, with compound **93** as the principal component. Compound **93**: ^{1}H NMR ($CDCl_3$): 4.10 (t, ^{3}J=7.5 Hz, 2H), 2.02 (s, 3H), 1.23 (t, ^{3}J=7.5 Hz, 3H) ppm. ^{13}C NMR ($CDCl_3$): 171.16, 60.41, 21.05, 14.21 ppm. Spectral data agree with a literature report.[10]

Distillation residue was isolated in the amount of 6.10 g, with compound **116** as the principal component. Compound **116**: ^{1}H NMR ($CDCl_3$): 7.33–7.14 (m, 10H), 4.31 (t, ^{3}J=7.5 Hz, 2H), 3.60 (s, 2H), 2.92 (t, ^{3}J=6.9 Hz, 2H) ppm. ^{13}C NMR ($CDCl_3$): 171.62, 137.87, 134.12, 129.42, 129.06, 128.69, 128.60, 127.19, 126.66, 65.47, 41.56, 35.16 ppm. Spectral data agree with a previous literature report.[10]

*Calculation of the Yield of **93** Based on the Integration of ^{1}H NMR Spectra*

Internal standard 1,3,5-trimethoxybenzene (61.9 mg, 0.364 mmol) was added to a 576 mg aliquot of the first distillate. From their relative integrals in the ^{1}H NMR spectrum (Figure 3.4), the number of moles of **93** was calculated to be 0.364 mmol × 9.36 ÷ (2/3) = 5.111 mmol. Thus, the total number of moles of **93** in the first distillate was 5.111 mmol × 2.80 g ÷ 0.576 g = 24.845 mmol, corresponding to the yield of **93** of 24.845 mmol ÷ 30.0 mmol × 100% = 83%.

Yield of **116** was calculated from gas chromatography data, as described below.

*Calculation of the Yield of **116** Based on the Integration of GC Peaks*

For the purpose of quantification of yield of **116**, we determined a response factor (F) for this ester with respect to dodecane, which was used as GC internal standard. The area of ester signal / mass of ester = F × area of standard signal / mass of standard. That is, $a_e / m_e = F \times a_s / m_s$. Therefore, a_e and m_e of a pure sample of **116** and a_s and m_s of GC internal standard (dodecane) were used to calculate F value. Five independent determinations of the F value were performed (0.867, 0.874, 0.862, 0.863, 0.864), yielding an average F = 0.866. This value was then used to calculate the amount of **116** in the distillation residue of this reactive distillation (Figure 3.5). A 50.5 mg aliquot of the distillation residue was added to a glass vial, followed by addition of dodecane (19.6 mg) and THF (3 mL) as the solvent. The mixture was subjected to gas chromatography using the temperature program described in the General Methods section. From the integration, mass of **116** could be calculated as $m_e = (a_e \times m_s) / (a_s \times F)$ = (20291213 × 19.6 mg) / (11103612 × 0.866) = 41.4 mg. The total mass of **116** in the distillation residue was 41.4 mg × 7.5 g ÷ 50.5 mg = 6.10 g. The yield of **116** is 6.10 g ÷ 240.30 g mol^{-1} ÷ 30.0 mmol × 100% = 85%.

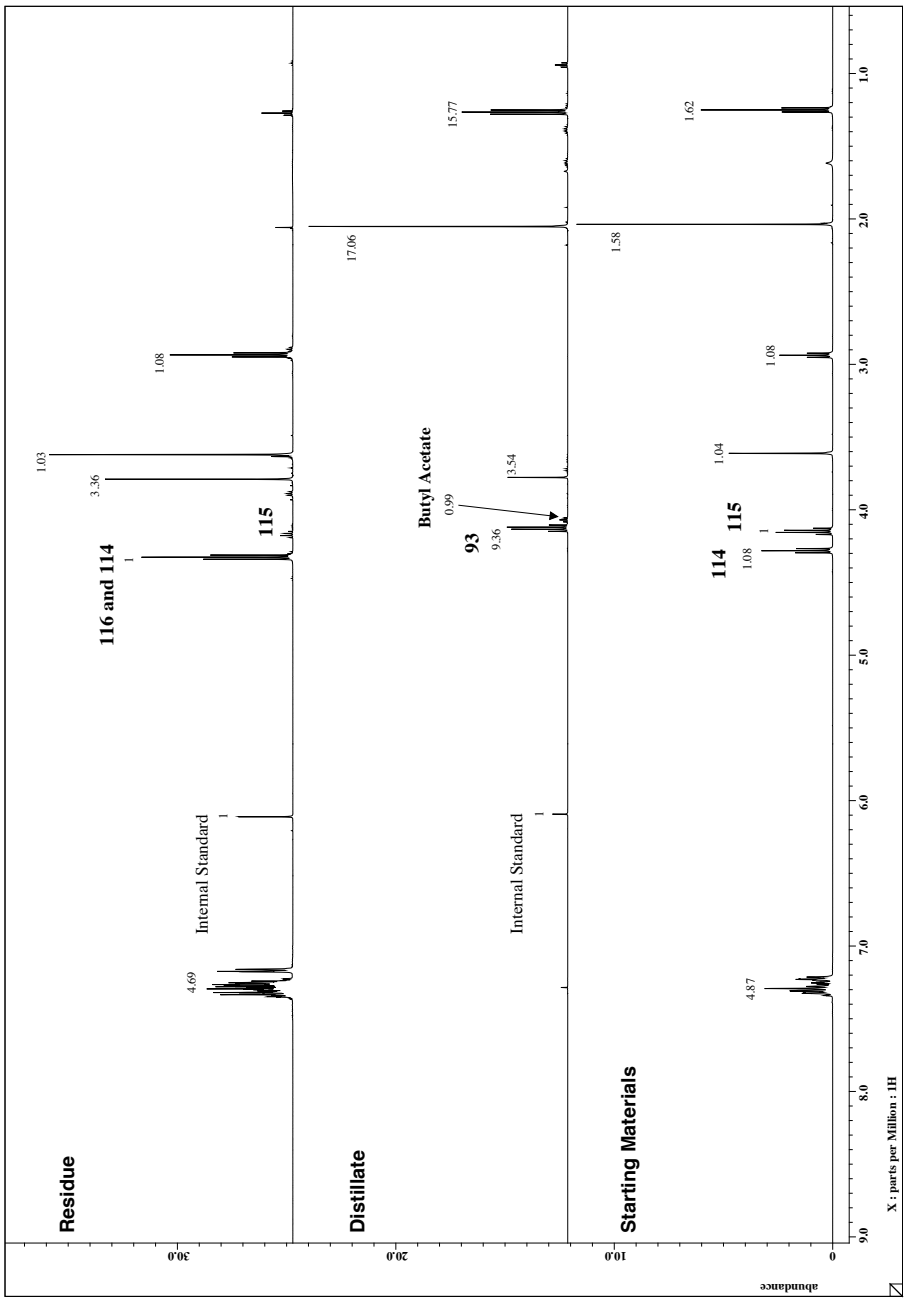

Figure 3.4 ^{1}H NMR spectra of the starting mixture (bottom) of esters **114** and **115**, and the distillate (middle) and distillation residue (top) after the scent transmutation of that mixture.

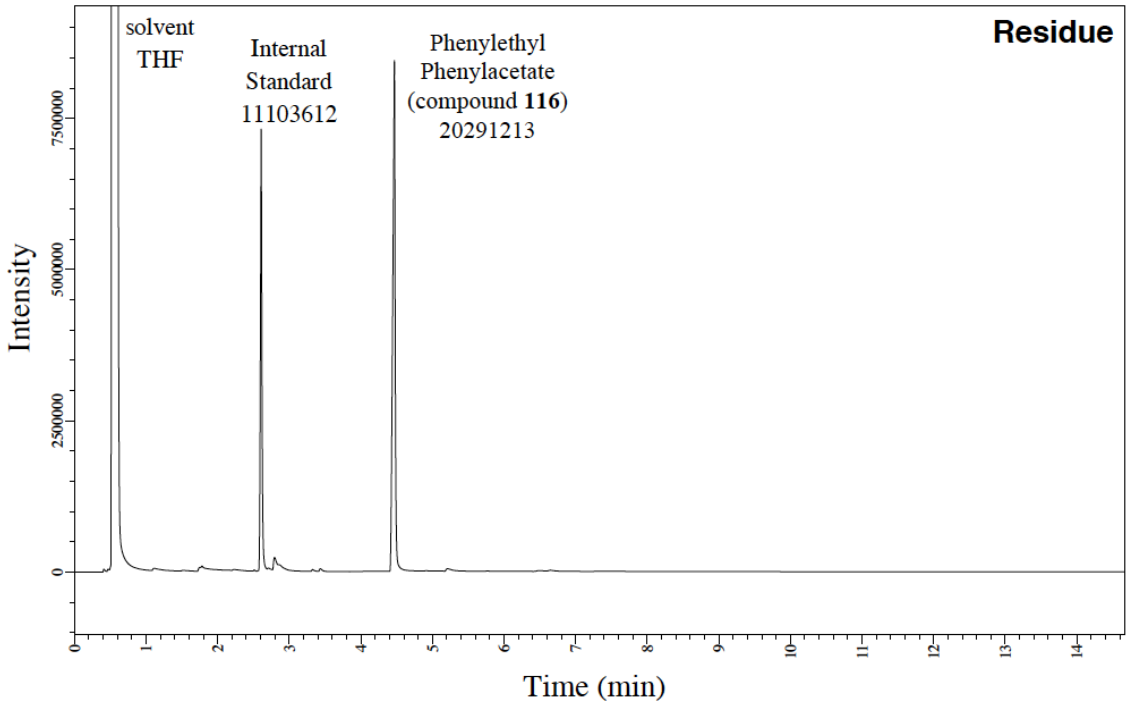

Figure 3.5 Gas chromatogram of the distillation residue from the scent transmutation of an equimolar mixture of **114** and **115**, with internal standard (dodecane) added for calibration. THF was used as the solvent.

3.4.4 Methyl Acetate (118) and Phenylethyl Cinnamate (119)

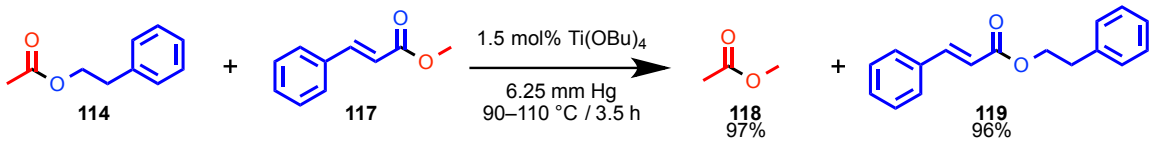

Distillate was isolated in the amount of 2.16 g, with compound **118** as the principal component. Compound **118**: ^{1}H NMR ($CDCl_3$): 3.63 (s, 3H), 2.02 (s, 3H) ppm. ^{13}C NMR ($CDCl_3$): 171.48, 51.54, 20.61 ppm. Spectral data agree with a previous literature report.[12]

Distillate was isolated in the amount of 7.29 g, with compound **119** as the principal component. Compound **119**: ^{1}H NMR ($CDCl_3$): 7.67 (d, ^{3}J=16.1 1H), 7.53–7.24 (m, 10H), 6.45 (d, ^{3}J=16.1 1H), 4.43 (t, ^{3}J=7.5 Hz, 2H), 3.03 (t, ^{3}J=6.9 Hz, 2H) ppm. ^{13}C NMR ($CDCl_3$): 167.01, 144.99, 138.01, 134.50, 130.43, 129.08, 129.01, 128.66, 128.22, 126.71, 118.16, 65.15, 35.33 ppm. Spectral data agree with a previous literature report.[13]

*Calculation of the Yields of **118** and **119** Based on the Integration of ^{1}H NMR Spectra*

Internal standard 1,3,5-trimethoxybenzene (45.8 mg, 0.270 mmol) was added to a 672 mg aliquot of the distillate. From their relative integrals in the ^{1}H NMR spectrum (Figure 3.6), the number of moles of **118** was calculated to be 0.270 mmol × 31.5 ÷ 1 = 8.51 mmol. Thus, the total number of moles of **118** in the first distillate was 8.51 mmol × 2.30 g ÷ 0.672 g = 29.1 mmol, corresponding to the yield of **118** of 29.1 mmol ÷ 30.0 mmol × 100% = 97%.

Internal standard 1,3,5-trimethoxybenzene (47.8 mg, 0.281 mmol) was added to an 818 mg aliquot of the residue. From their relative integrals in the ^{1}H NMR spectrum (Figure 3.6), the number of moles of **119** was calculated to be 0.281 mmol × (4.21 – 1.02 ÷ 3) ÷ (1/3) = 3.038 mmol. Thus, the total number of moles of **119** in the first distillate was 3.038 mmol × 7.8 g ÷ 0.819 g = 28.9 mmol, corresponding to the yield of **119** of 28.9 mmol ÷ 30.0 mmol × 100% = 96%.

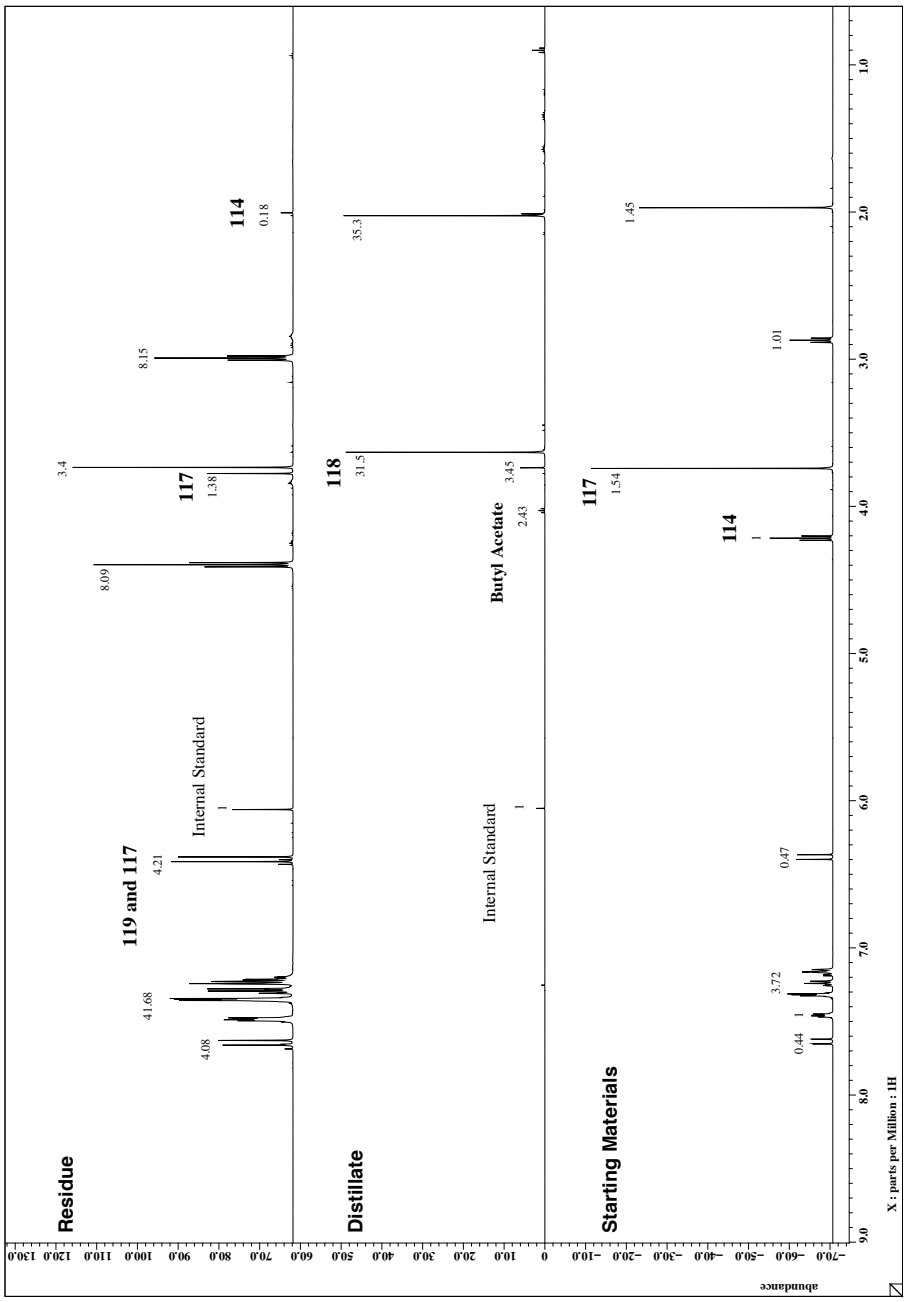

Figure 3.6 ^{1}H NMR spectra of the starting mixture (bottom) of esters **114** and **117**, and the distillate (middle) and distillation residue (top) after the scent transmutation of that mixture.

3.4.5 Ethyl Isovalerate (121) and Phenylethyl Phenylacetate (116)

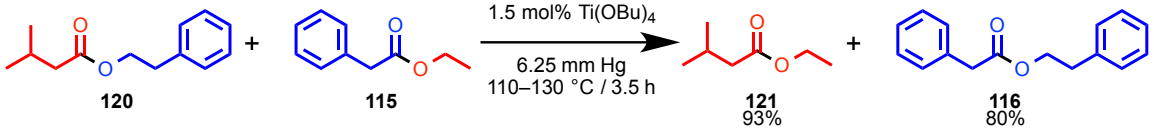

Distillate was isolated in the amount of 3.61 g, with compound **121** as the principal component. Compound **121**: ^{1}H NMR ($CDCl_3$): 4.11 (q, ^{3}J=7.4 Hz, 2 H), 2.16 (d, J=6.8 Hz, 3 H), 2.11–2.05 (m, 1 H), 1.23 (t, ^{3}J=7.5 Hz, 3 H), 0.94 (d, ^{3}J=6.3 Hz, 6 H) ppm. ^{13}C NMR ($CDCl_3$): 173.22, 60.10, 43.53, 25.76, 22.42, 14.32 ppm. Spectral data agree with a previous literature report.[14]

Distillation residue was isolated in the amount of 5.75 g, with compound **116** as the principal component. Compound **116**: ^{1}H NMR ($CDCl_3$): 7.33–7.15 (m, 10H), 4.32 (t, ^{3}J=7.5 Hz, 2H), 3.61 (s, 2H), 2.93 (t, ^{3}J=6.9 Hz, 2H) ppm. ^{13}C NMR ($CDCl_3$): 171.62, 137.87, 134.12, 129.42, 129.06, 128.69, 128.60, 127.19, 126.66, 65.47, 41.56, 35.16 ppm. Spectral data agree with a previous literature report.[10]

*Calculation of the of Yield of **121** Based on the Integration of ^{1}H NMR Spectra*

Internal standard 1,3,5-trimethoxybenzene (73.6 mg, 0.433 mmol) was added to a 651 mg aliquot of the distillate. From their relative integrals in the ^{1}H NMR spectrum (Figure 3.7), the number of moles of **121** was calculated to be 0.433 mmol × 7.32 ÷ (2/3) = 4.754 mmol. Thus, the total number of moles of **121** in the first distillate was 4.754 mmol × 3.8 g ÷ 0.651 g = 27.750 mmol, corresponding to the yield of **121** of 27.750 mmol ÷ 30.0 mmol × 100% = 93%.

*Calculation of the Yield of **116** Based on the Integration of GC Peaks*

For the purpose of quantification of yields of **116**, we determined response factors (*F*) for this ester with respect to dodecane as the GC internal standard. The area of ester signal / mass of ester = *F* × area of standard signal / mass of standard. That is, $a_e / m_e = F \times a_s / m_s$. Therefore, a_e and m_e of a pure samples of **116** and a_s and m_s of GC internal standard (dodecane) were used to calculate *F* value. Five independent determinations of the *F* value were performed for **116** (0.867, 0.874, 0.862, 0.863, 0.864), yielding an average *F* = 0.866 for **116**. This value was then used to calculate the amounts of **116** in the distillate and distillation residue of this reactive distillation (Figures 3.8). A 48.0 mg aliquot of the distillation residue was added to a glass vial, followed by addition of dodecane (20.0 mg) and THF (3 mL) as the solvent. The mixture was subjected to gas chromatography using the temperature program described in the General Methods section. From the integration, mass of **116** could be calculated as $m_e = (a_e \times m_s) / (a_s \times F)$ = (18483051 × 20.0 mg) / (12233856 × 0.866) = 34.9 mg. The total mass of **116** in the distillation residue was 34.9 mg × 7.9 g ÷ 48.0 mg = 5.75 g. The yield of **116** is 5.75 g ÷ 240.30 g mol^{-1} ÷ 30.0 mmol × 100% = 80%.

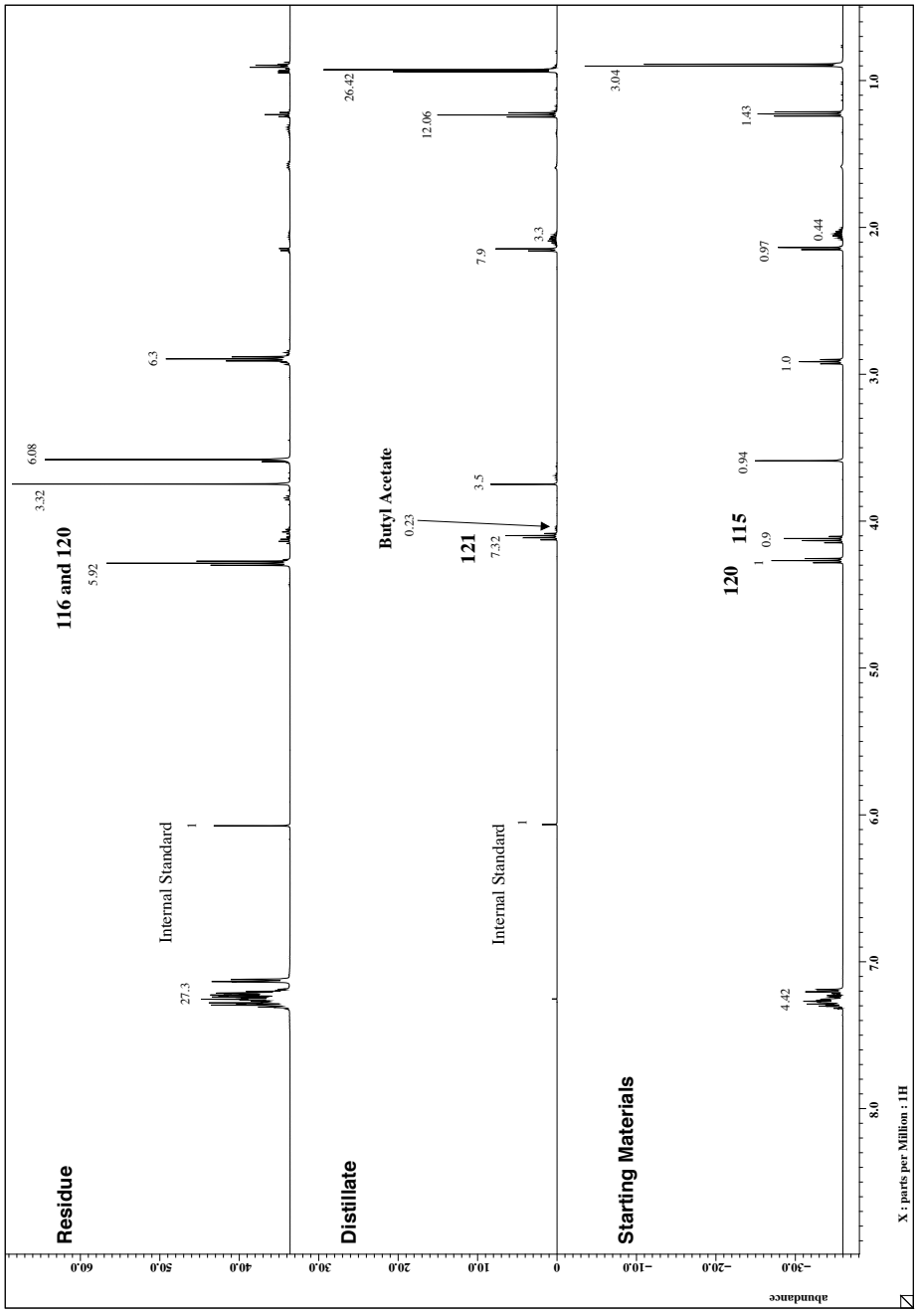

Figure 3.7 ^{1}H NMR spectra of the starting mixture (bottom) of esters **120** and **115**, and the distillate (middle) and distillation residue (top) after the scent transmutation.

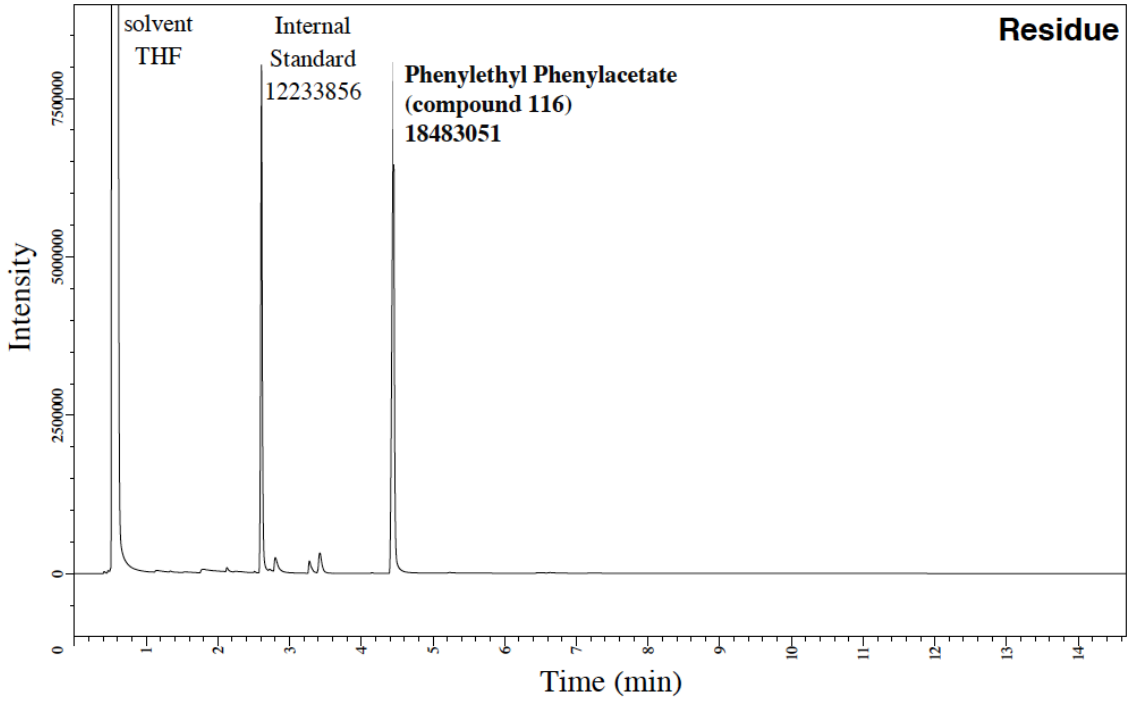

Figure 3.8 Gas chromatogram of the distillation residue from the scent transmutation of an equimolar mixture of **120** and **115**, with internal standard (dodecane) added for calibration. THF was used as the solvent.

3.4.6 Isoamyl Acetate (123) and Phenylethyl Isovalerate (124)

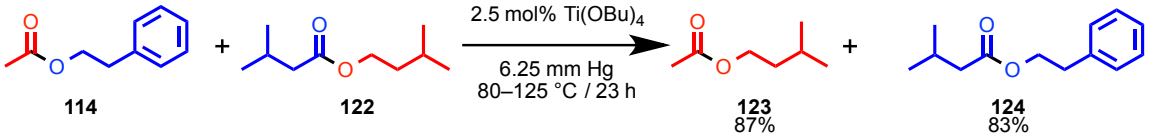

Distillate was isolated in the amount of 1.70 g, with compound **123** as the principal component. Compound **123**: ^{1}H NMR ($CDCl_3$): 4.06 (t, ^{3}J=6.9 Hz, 2H), 2.01 (s, 3H), 1.70–1.62 (m, 1H), 1.51 (dd, ^{3}J=6.9 Hz, 2H), 0.90 (d, ^{3}J=6.9 Hz, 6H) ppm. ^{13}C NMR ($CDCl_3$): 171.27, 63.17, 37.34, 25.07, 22.48, 21.05 ppm. Spectral data agree with a previous literature report.[14]

Distillation residue was isolated in the amount of 2.60 g, with compound **124** as the principal component. Compound **124**: ^{1}H NMR ($CDCl_3$): 7.32–7.21 (m, 5H), 4.29 (t, ^{3}J=7.5 Hz, 2H), 2.94 (t, ^{3}J=6.9 Hz, 2H), 2.16 (d, 2H), 2.10–2.04 (m, 1H), 0.91 (d, 6H) ppm. ^{13}C NMR ($CDCl_3$): 173.18, 138.00, 129.00, 128.57, 126.63, 64.73, 43.52, 35.27, 25.76, 22.49 ppm. Spectral data agree with a previous literature report.[15]

*Calculation of the Yields of **123** and **124** based on the Integration of GC Peaks*

For the purpose of quantification of yields of **123** and **124**, we determined response factors (F) for these esters with respect to dodecane as the GC internal standard. The area of ester signal / mass of ester = F × area of standard signal / mass of standard. That is, $a_e / m_e = F \times a_s / m_s$. Therefore, a_e and m_e of a pure samples of **123** and **124** and a_s and m_s of GC internal standard (dodecane) were used to calculate F value. Five independent determinations of the F value were performed for **123** (0.615, 0.613, 0.611,

0.621, 0.619), yielding an average $F = 0.616$ for **123**. Five independent determinations of the F value were performed for **124** (0.787, 0.802, 0.811, 0.815, 0.814), yielding an average $F = 0.806$ for **124**. This value was then used to calculate the amounts of **123** and **124** in the distillate and distillation residue of this reactive distillation (Figures 3.9 and 3.10, respectively). A 42.3 mg aliquot of the distillate was added to a glass vial, followed by addition of dodecane (30.1 mg) and THF (3 mL) as the solvent. The mixture was subjected to gas chromatography using the temperature program described in the General Methods section. From the integration, mass of **123** could be calculated as $m_e = (a_e \times m_s) / (a_s \times F) = (12375559 \times 30.1 \text{ mg}) / (16936985 \times 0.616) = 35.7$ mg. The total mass of **123** in the distillation residue was 35.7 mg × 2.01 g ÷ 42.3 mg = 1.70 g. The yield of **123** is 1.70 g ÷ 130.18 g mol^{-1} ÷ 15.0 mmol × 100% = 87%.

A 44.2 mg aliquot of the distillation residue was added to a glass vial, followed by addition of dodecane (30.7 mg) and THF (3 mL) as the solvent. The mixture was subjected to gas chromatography using the temperature program described in the General Methods section. From the integration, mass of **124** could be calculated as $m_e = (a_e \times m_s) / (a_s \times F) = (16178325 \times 30.7 \text{ mg}) / (17836124 \times 0.806) = 34.5$ mg. The total mass of **124** in the distillation residue was 34.5 mg × 3.3 g ÷ 44.2 mg = 2.58 g. The yield of **124** is 2.58 g ÷ 206.28 g mol^{-1} ÷ 15.0 mmol × 100% = 83%.

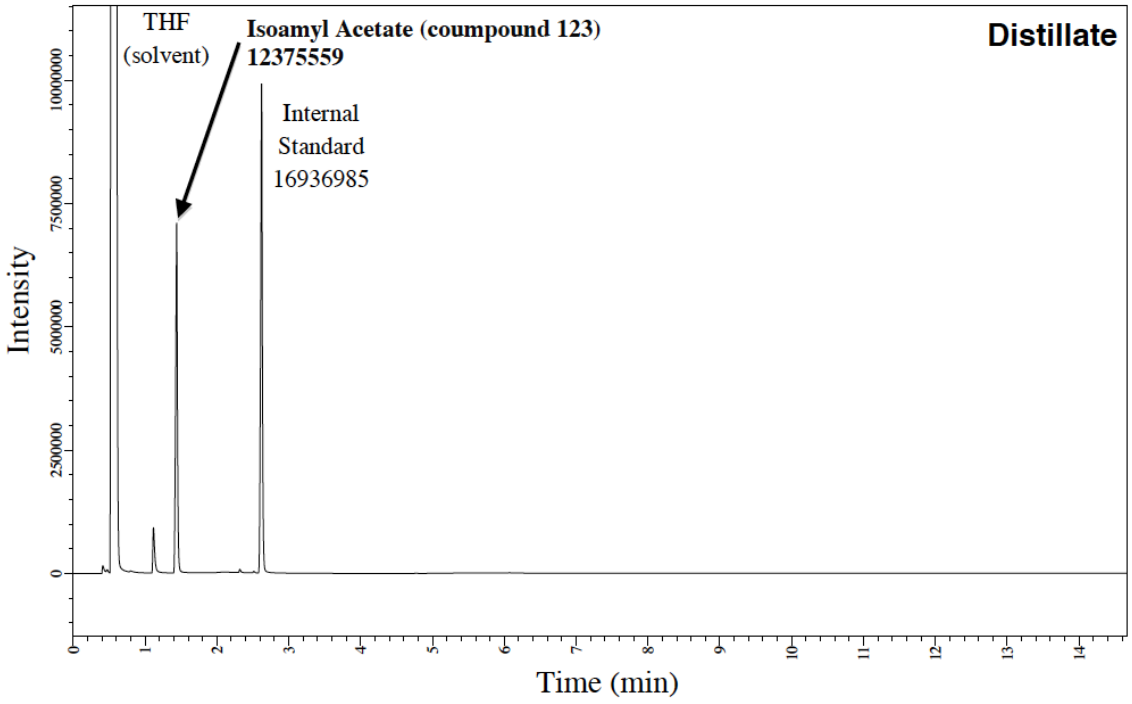

Figure 3.9 Gas chromatogram of the distillation distillate from the scent transmutation of an equimolar mixture of **114** and **122**, with internal standard (dodecane) added for calibration. THF was used as the solvent.

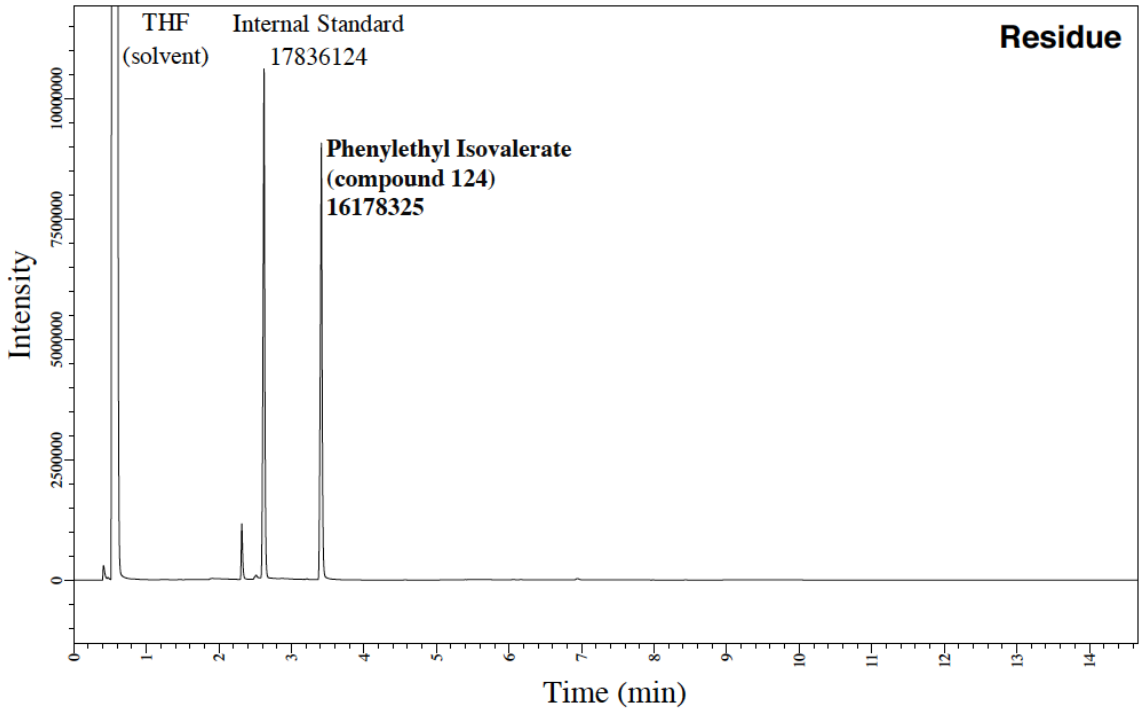

Figure 3.10 Gas chromatogram of the distillation residue from the scent transmutation of an equimolar mixture of **114** and **122**, with internal standard (dodecane) added for calibration. THF was used as the solvent.

3.4.7 Ethyl Acetate (93) and Isoamyl Isovalerate (122)

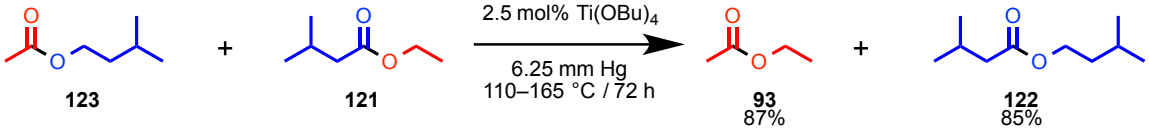

Distillate was isolated in the amount of 2.46 g, with compound **93** as the principal component. Compound **93**: ^{1}H NMR ($CDCl_3$): 4.09 (q, ^{3}J=6.8 Hz, 2H), 2.00 (s, 3H), 1.22 (t, ^{3}J=6.8 Hz, 3H) ppm. ^{13}C NMR ($CDCl_3$): 171.16, 60.40, 21.03, 14.20 ppm. Spectral data agree with a literature report.[10]

Distillate was isolated in the amount of 4.40 g, with compound **122** as the principal component. Compound **122**: ^{1}H NMR ($CDCl_3$): 4.08 (t, ^{3}J=6.8 Hz, 2H), 2.17 (d, J=6.9 Hz, 2H), 2.11–2.07 (m, 1H), 1.70–1.65 (m, 2H), 1.51 (dd, J=6.8 Hz, 1H), 0.94 (d, J=6.8 Hz, 6H), 0.91 (d, J=6.8 Hz, 6H) ppm. ^{13}C NMR ($CDCl_3$): 173.34, 62.86, 43.60, 37.44, 25.80, 25.12, 22.51, 22.46 ppm. Spectral data agree with a previous literature report.[10]

*Calculation of the Yield of **93** Based on the Integration of ^{1}H NMR Spectra*

Internal standard 1,3,5-trimethoxybenzene (51.1 mg, 0.301 mmol) was added to a 407 mg aliquot of the distillate. From their relative integrals in the ^{1}H NMR spectrum (Figure 3.11), the number of moles of **93** was calculated to be at least 0.301 mmol × [9.2 – (0.76 ÷ 3)] ÷ (2/3) = 4.04 mmol. Thus, the total number of moles of **93** in the distillate was 4.04 mmol × 2.62 g ÷ 0.407 g = 26.1 mmol, corresponding to the yield of **93** of 26.1

mmol ÷ 30.0 mmol × 100% = 87%. Minor fractions were not quantified because of the extensive overlap of their ^{1}H NMR spectral peaks.

*Calculation of the Yield of **122** based on the Integration of GC Peaks*

For the purpose of quantification of yields of **122**, we determined response factors (*F*) for these esters with respect to dodecane as the GC internal standard. The area of ester signal / mass of ester = *F* × area of standard signal / mass of standard. That is, a_e / m_e = *F* × a_s / m_s. Therefore, a_e and m_e of a pure samples of **122** and a_s and m_s of GC internal standard (dodecane) were used to calculate *F* value. Five independent determinations of the *F* value were performed for **122** (0.709, 0.717, 0.708, 0.713, 0.713), yielding an average *F* = 0.712 for **122**. This value was then used to calculate the amounts of **122** in the distillate and distillation residue of this reactive distillation (Figures 3.12). A 484 mg aliquot of the distillation residue was added to a glass vial, followed by addition of dodecane (31.6 mg) and THF (3 mL) as the solvent. The mixture was subjected to gas chromatography using the temperature program described in the General Methods section. From the integration, mass of **116** could be calculated as m_e = (a_e × m_s) / (a_s × *F*) = (14947710 × 31.6 mg) / (17726517 × 0.712) = 37.4 mg. The total mass of **122** in the distillation residue was 37.4 mg × 5.7 g ÷ 48.4 mg = 4.40 g. The yield of **116** is 4.40 g ÷ 172.26 g mol^{-1} ÷ 30.0 mmol × 100% = 85%.

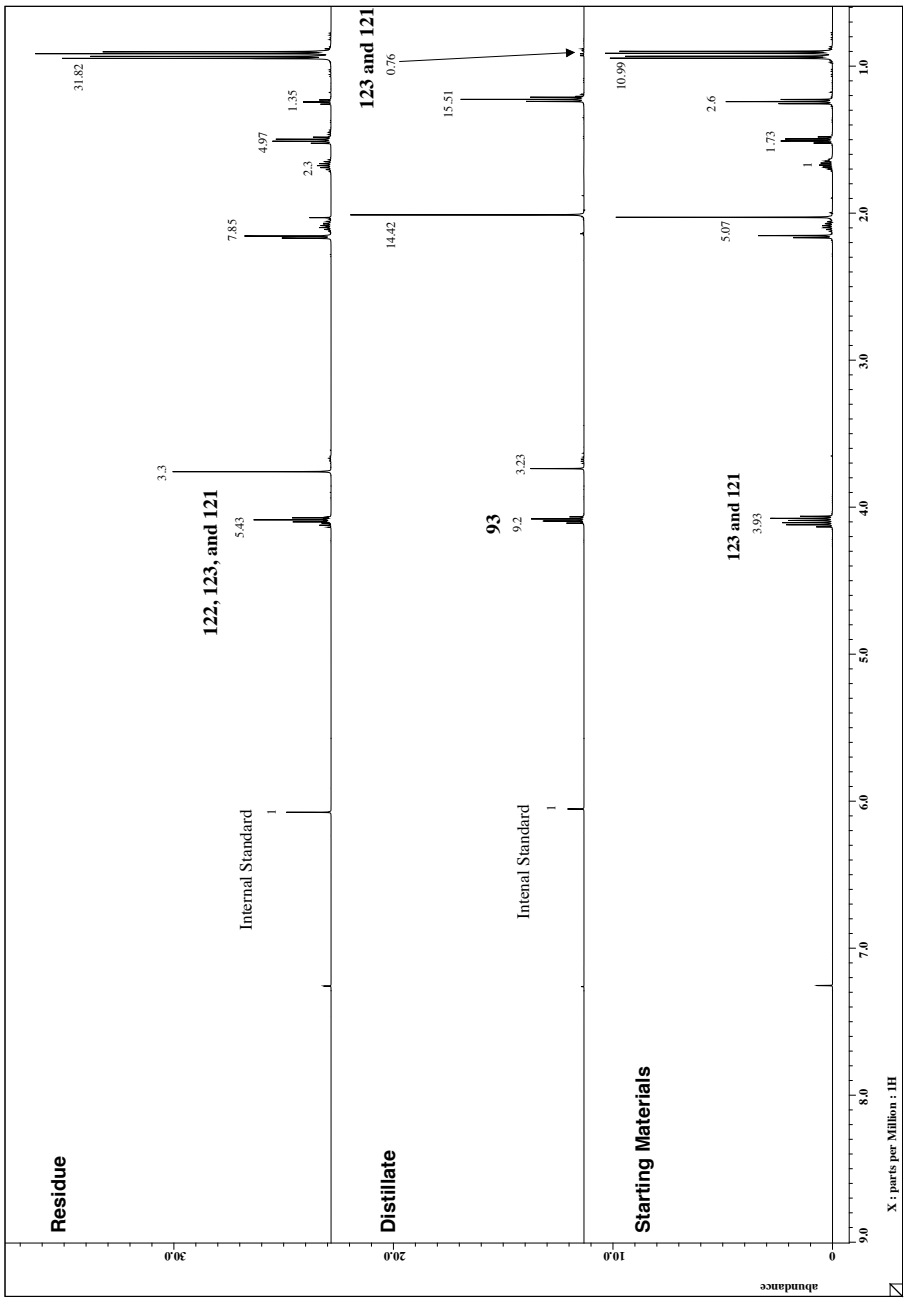

Figure 3.11 ^{1}H NMR spectra of the starting mixture (bottom) of esters **123** and **121**, and the distillate (middle) and distillation residue (top) after the scent transmutation of that mixture.

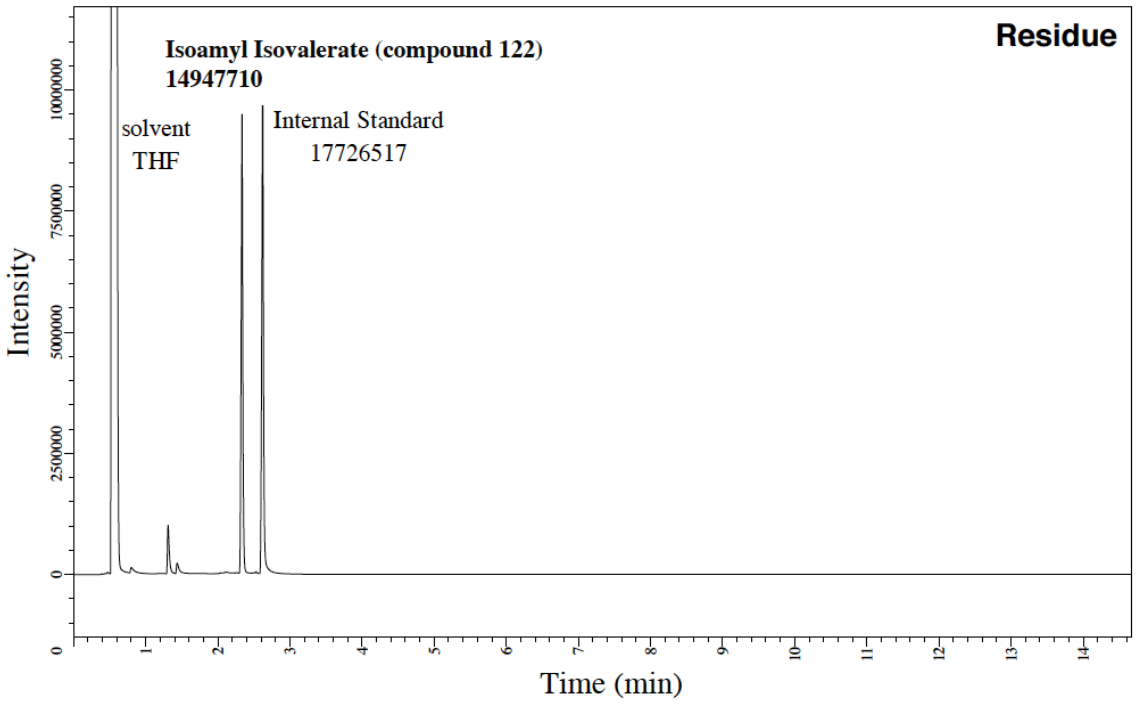

Figure 3.12 Gas chromatogram of the distillation residue from the scent transmutation of an equimolar mixture of **123** and **121**, with internal standard (dodecane) added for calibration. THF was used as the solvent.

3.5 References

[1] The work described in this chapter has been previously published: Ji. Q.; El-Hamdi, N. S.; Miljanić, O. Š. *J. Chem. Educ.* **2014**, *91*, 830–833.

[2] Gall, J. *The Systems Bible*; General Systemantics Press: Walker, MN, **2002**.

[3] Lyuben, W. L.; Yu, C.-C. *Reactive Distillation Design and Control*; Wiley-AIChE: Weinheim, **2008**, pp 545–561.

[4] Schnurrenberger, P.; Züger, M. F.; Seebach, D. *Helv. Chim. Acta* **1982**, *65*, 1197–1201.

[5] For recent reviews of dynamic combinatorial chemistry, see: (a) Li, J.; Nowak, P.; Otto, S. *J. Am. Chem. Soc.* **2013**, *135*, 9222–9239. (b) *Dynamic Combinatorial Chemistry*; Reek, J. N. H.; Otto, S., Eds.; Wiley-VCH: Weinheim, **2010**. (c) Corbett, P. T.; Leclaire, J.; Vial, L.; West, K. R.; Wietor, J.-L.; Sanders, J. K. M; Otto, S. *Chem. Rev.* **2006**, *106*, 3652–3711. For educational experiments utilizing concepts of DCC, see also: (d) Angelin, M.; Larsson, R.; Vongvilai, P.; Ramström, O. *J. Chem. Educ.* **2010**, *87*, 1248–1251. (e) Pentecost, C. D.; Tangchaivang, N.; Cantrill, S. J.; Chichak, K. S.; Peters, A. J.; Stoddart, J. F. *J. Chem. Educ.* **2007**, *84*, 856–859.

[6] (a) Ji, Q.; Lirag, R. C.; Miljanić, O. Š. *Chem. Soc. Rev.* **2014**, *43*, 1873–1884. (b) Ji, Q.; Miljanić, O. Š. *J. Org. Chem.* **2013**, *78*, 12710–12716. (c) Osowska, K.; Miljanić, O. Š. *Angew. Chem. Int. Ed.* **2011**, *50*, 8345–8349.

[7] Surburg, H.; Panten, J. *Common Fragrance and Flavor Materials*; Wiley-VCH: Weinheim, **2006**.

[8] See: Code of Federal Regulations, Title 21, Volume 3 (revised April 1, 2013), part 172: Food Additives Permitted for Direct Addition to Food for Human Consumption. Available online at: http://www.accessdata.fda.gov/scripts/cdrh/cfdocs/cfcfr/CFRSearch.cfm?CFRPart=172&showFR=1. (accessed Mar 2014).

[9] It may be useful to provide the reader with cursory instructions on how to use appropriate terms to describe odor. For example, "balsamic" is a term best suited for heavy and sweet odors: cocoa, vanilla, or cinnamon. "floral" or "flowery" is the generic term for odors of various flowers; and "fruity" is the generic term for various fruits. In reactions presented in Scheme 3.2A and 3.2F, identification of scent transmutation products should not be too challenging, as all odors are associated with fruits, and each of the four components is quite distinct from the others. In reactions presented in Scheme 3.2B–E, the two starting materials should be easily discriminated; the distillate of each reaction is also very distinguishable from the two starting materials. For instance, the distillate of reaction shown in Scheme 3.2B is ethyl acetate (**93**), with a light fruity odor. In contrast, ethyl phenylacetate (**115**) brings a honey-balsamic odor that is very strong, while the odor of phenylethyl acetate (**114**) is reminiscent of a fine rose. The inconvenience resides in the odor difference between the product phenylethyl phenylacetate (**116**) and its two starting materials. This product has a very heavy sweet odor that can be described as rose or hyacinth, but also a distinctive honey note that can overlap

with either **114** or **115**. Although it is not insuperable to identify them, the reader should bear in mind the scent change is not only dependent on terminology of the odor but also relies on the threshold concentration of the target compound (defined as the lowest concentration at which a chemical compound can be distinguished with certainty from a blank under standard conditions). Similar ambiguity may be encountered in identifying the products of reactions shown in Scheme 3.2C–E.

[10] Tejel, C.; Ciriano, M. A.; Passarelli, V. *Chem. Eur. J.* **2011,** *17*, 91–95.

[11] Gowrisankar, S.; Neumann, H.; Beller, M. *Angew. Chem. Int. Ed.* **2011,** *50*, 5139–5143.

[12] Khusnutdinova, J. R.; Rath, N. P.; Mirica, L. M. *J. Am. Chem. Soc.* **2010,** *132*, 7303–7305.

[13] Zhang, B.; Feng, P.; Cui, Y. X.; Jiao, N. *Chem. Commun.* **2012,** *48*, 7280–7282.

[14] Bandres, M.; De Caro, P.; Thiebaud-Roux, S.; Borredon, M. E. *C. R. Chimie* **2011,** *14*, 636–646.

[15] Mamedov, M. K. *Russ. J. Appl. Chem.* **2006,** *79,* 408–410.

Chapter Four Cyclotribenzoin and Cyclotetrabenzoin: Synthesis and Gas Adsorption Studies[1]

4.1 Introduction

Chemistry of macrocycles has evolved into a broad research area that spans the fields of organic, inorganic, and supramolecular chemistry.[2] To list just a handful of applications, macrocycles play a role in studies of aromaticity,[3] porous materials,[4] and supramolecular binding.[2] Shape-persistent macrocycles and cages[5] have in particular been the subject of much attention as components of ordered three- (porous materials),[6] two- (assemblies at liquid-solid interfaces),[7] and one- (organic nanowires and nanofibrils)[8] dimensional functional ensembles. At the same time, macrocyclic molecules still present a synthetic challenge: macrocyclization reactions are entropically unfavorable, an obstacle that often has to be circumvented through long and indirect synthetic routes. The few macrocycle classes that are easily synthesized or obtained from nature—such as cyclodextrins[9] or cucurbituril[10]—present challenges in terms of selective derivatization. Because of these two factors, synthetic research on macrocycles is still an active area; for example, the recent dramatic ascent of pillarenes[11] happened in large part due to their facile synthesis, which—coupled with easy preparation of derivatives—presented the supramolecular chemistry community with a class of receptors that could be easily diversified. Additionally, the use of DCC[12] allowed error-correction in the preparation of thermodynamically stabilized species and opened up faster routes to

macrocycles and cages based on imine,[6h–o,8c,d] boronate ester,[6f,g] alkyne,[13] and boroxine[14] functionalities. In this chapter, we demonstrate arguably the shortest route to two macrocycle ornamented with multiple oxygen-based functional groups through benzoin condensation of isophthaldehyde (**125**) and terephthaldehyde (**126**).

Benzoin condensation (term *condensation* is purely historic, as no small molecule is eliminated in this addition reaction) was discovered by Liebig and Wöhler during their work on bitter almond oil. In recent years, this reaction has been utilized in the synthesis of pharmaceutical precursors and microporous organic polymers; enantioselective versions have also been developed. The first attempts to extend benzoin condensation to more complex dialdehyde precursors were performed early in the development of this reaction. Benzoin condensation of **126** was first examined by Grimaux in 1876 and then revisited by Oppenheimer (1886), as well as by Jones and Tinker (1955). These studies concluded that only polymeric products were formed. Isomeric **125** was also reported to yield only polymeric benzoin adducts. We report here, however, that **125** and **126** can be converted into a single macrocyclic timer and tetramer, which we propose to name *cyclotribenzoin* (**127**) and *cyclotetrabenzoin* (**129**).

4.2 Results and Discussion

4.2.1 Synthesis of Compounds 127, 128, and 129

We revisited the reaction of **125** with NaCN (Scheme 4.1), and found that the outcome of this reaction depends on the solvent and concentration of **125**. We were pleasantly surprised to observe that heating of **125** with NaCN at reflux in 1:1 mixtures of H_2O with either MeOH, EtOH, or *t*-BuOH resulted in the predominant formation of trimer **127**. This trimer conveniently precipitated from the solution if the starting concentration of **125** was 0.5 M. At higher concentrations of **125**, mixtures of **127** with other noncyclic oligomers and insoluble (presumed) polymers were obtained, and similar results were observed if the reaction mixtures were not heated. Alcoholic solvents appear essential for the success of this reaction, as switching to 1,4-dioxane/H_2O solvent combination completely suppressed the reaction, while the use of ethylene glycol as solvent led to the formation of mixtures. Ultimately, reaction in EtOH/H_2O mixture was chosen as the most convenient and was optimized to produce **127** in 41% yield after recrystallization from 2-methoxyethanol. While this yield is moderate, one-step synthesis and low cost of isophthaldehyde mean that **127** can easily be prepared on multigram scale (up to 80 mmol scale).

To circumvent the problems associated with the poor solubility of **127** in common organic solvents, we converted it into a *t*-butyldimethylsilyl (TBDMS) derivative **128** by treatment with TBDMS–Cl in CH_2Cl_2 (Scheme 4.1). As anticipated, this derivative is significantly more soluble in most organic solvents. This increased solubility allowed us

to probe its conformational flexibility using variable-temperature NMR spectroscopy. Upon cooling to −85 °C in CD_2Cl_2, no decoalescence of peaks was observed, although some shifting of peak positions was observed—possibly suggesting aggregation or changes in intermolecular hydrogen bonding configurations.

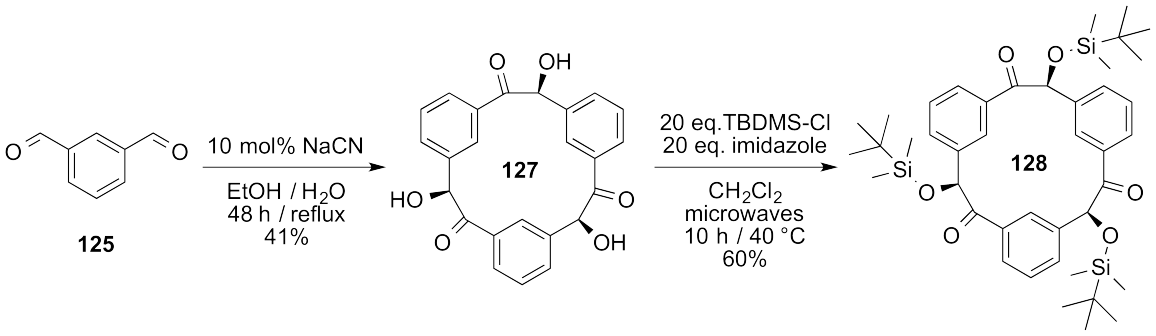

Scheme 4.1 Synthesis of cyclotribenzoin **127** and its silylated derivative **128**. Both enantiomers of **127** and **128** are produced.

Exposure of **126** to NaCN in a 1:1 mixture of EtOH and H_2O (Scheme 4.2) resulted in a complex mixture of benzoin condensation products in solution, as well as in the formation of some insoluble materials (which we again presumed to be polymeric). Mass spectrometry suggested the presence of a tetramer of **126** in the soluble fraction, and we suspected that the tetrameric compound could be **129** (or its diastereomers). Unfortunately, we could not optimize this reaction to exclusively yield **129**, and the high polarity of the obtained products made their separation by column chromatography impractical. Switching the reaction solvent to a 1:1 mixture of 2-methoxyethanol and H_2O, and lowering the concentration of **126** to 0.167 M, resulted, however, in the formation of a precipitate consisting almost entirely of the tetramer. Recrystallization

from DMSO/MeOH produced pure **129** in 21% yield, and allowed us to confirm its structure using standard spectroscopic tools.

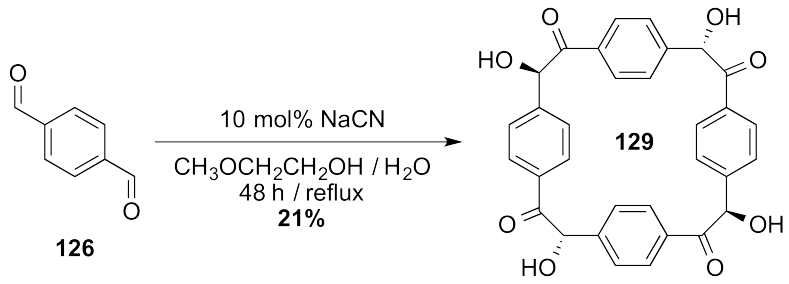

Scheme 4.2 Synthesis of cyclotetrabenzoin **129**.

4.2.2 X-Ray Crystal Structure Analysis of Compound 127

Compound **127** is a white powder, soluble in DMSO, 2-methoxyethanol, THF, 1,4-dioxane, nitrobenzene, and DMF. It is insoluble in H_2O, acetone, MeCN, EtOAc, MeOH, EtOH, Et_2O, as well as in hydrocarbon and chlorinated hydrocarbon solvents. Diffraction-quality single crystals of macrocycle **127** were grown by vapor diffusion of $CHCl_3$ into its solution in THF.[15] It crystallizes in the *R*3 space group, with three molecules of **127** and three molecules of THF per unit cell. The THF molecules are disordered over three orientations.

From its crystal structure, several structural features of cyclotribenzoin could be noticed. First, all three stereocenters have the same orientation (*S* in Figure 4.1), and **127**

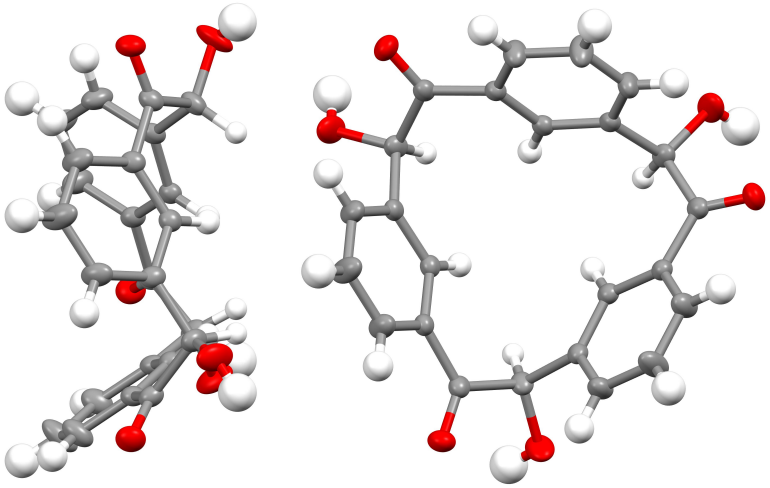

Figure 4.1 X-ray crystal structure of **127**. On the left, a side view showing convergent positioning of six C–H bonds in a conical structure. On the right, a top down view of the macrocycle. Disordered THF molecules were removed for clarity. Thermal ellipsoids shown at 50% probability. Element colors: C—gray, O—red, H—white.

crystallizes as a racemic twin, with the minor component having an occupancy of ~32%, which suggests that both enantiomers are present. Secondly, the molecule adopts a conical shape, where three aromatic rings define a cup-like cavity, orienting the six oxygen-based functionalities (three C=O and three O–H groups) away from it. It appears that this conical shape relieves all of the potential strain in the molecule, as all carbon atoms in **127** have bonding angles within ±2° of their idealized geometries. Finally, six C–H bonds—three coming from the arene rings and three from the C–H groups in the immediate neighborhood of the hydroxy groups—all appear to point to a single spot. This convergent positioning suggests that perhaps **127** and its derivatives could be used as receptors for anions based on [C–H···anion] interactions.[16]

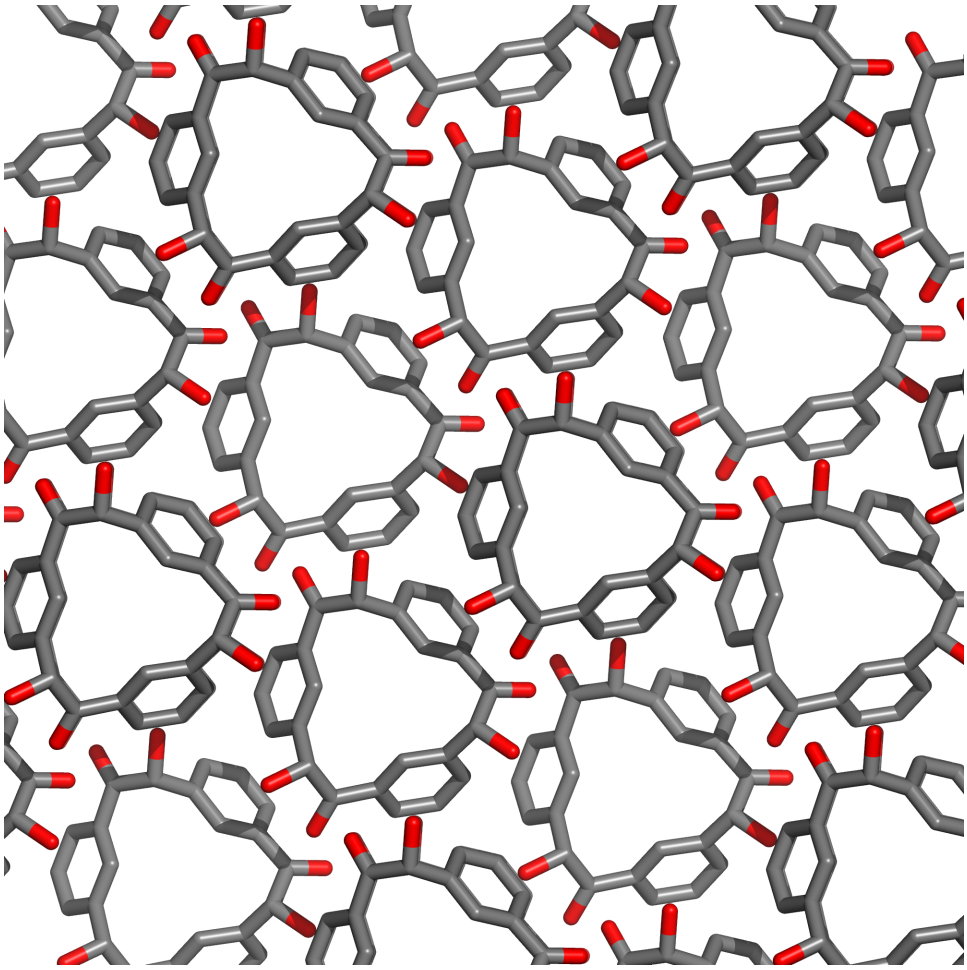

Figure 4.2 Segment of a crystal packing diagram of **127**, viewed along the crystallographic *c* axis. Hydrogen atoms and disordered THF molecules were removed for clarity. Element colors: C—gray, O—red, H—white.

Crystal packing diagram of **127** is shown in Figure 4.2. Within the *a*–*b* crystallographic plane, molecules of **127** orient parallel to each other. Along the *c* axis, they similarly stack in a parallel orientation. Each molecule of **127** establishes twelve short [C–H···O] contacts (H···O distances between 2.50 and 2.60 Å) with twelve of its neighbors. Specifically, on each benzene ring of **127**, the hydrogen positioned *ortho*

relative to the carbonyl group establishes a short contact with a carbonyl oxygen from a neighboring molecule. Similarly, the hydrogen positioned *meta* to the carbonyl group has contact with the hydroxyl oxygen atoms from three neighboring molecules. As this relationship is reciprocal, C=O and O–H groups from the "other side" of **127** establish short contacts with C–H groups from six additional molecules of **127**.

4.2.3 X-Ray Crystal Structure Analysis of Compound 129

Compound **129** is an off-white powder, soluble in DMSO and slightly soluble in 1,4-dioxane. It is insoluble in H_2O, acetone, MeCN, EtOAc, MeOH, EtOH, Et_2O, 2-methoxyethanol, THF, as well as in hydrocarbon and chlorinated hydrocarbon solvents.

Single crystals of **129** suitable for X-ray diffraction analysis were grown by slow vapor diffusion of MeOH into a dilute DMSO solution of **129**. Compound **129** crystalizes in the tetragonal space group with $P\bar{4}2_1c$ two molecules in the unit cell. The four stereocenters of **129** have *R*, *S*, *R*, *S* configurations. Curiously, the molecule is achiral—even though it lacks symmetry planes—on account of the existence of an S_4 axis that passes through the central cavity. The molecule adopts a roughly square shape (Figure 4.3 left), with four benzene rings acting as the sides of the square. A central cavity is clearly discernible: it has dimensions of 6.9×6.9 Å, defined as the distances between the centroids of two pairs of benzene rings on the opposite sides of the cyclotetrabenzoin molecule. Some twisting is observable in the planes of these benzene rings (Figure 4.3

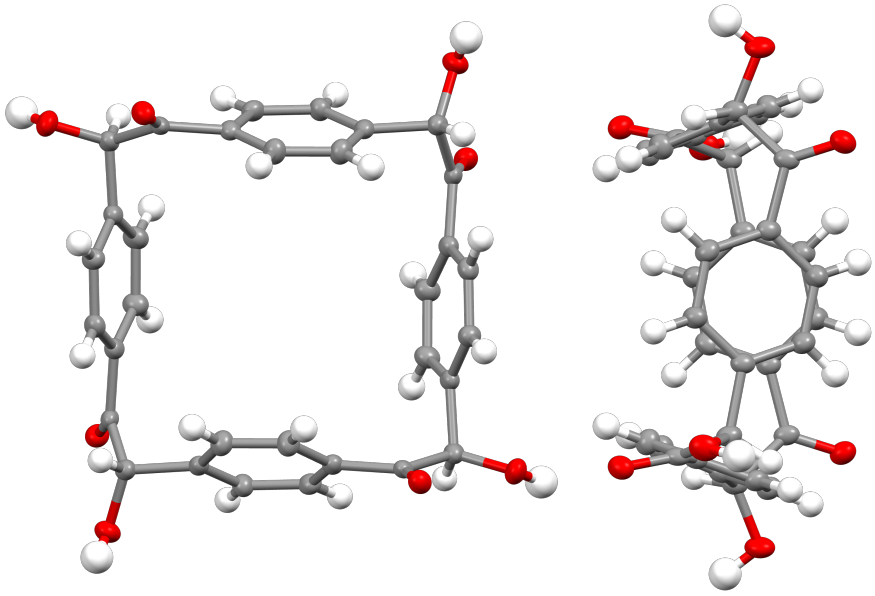

Figure 4.3 X-ray crystal structure of **129**. A top-down view of the tetramer, showing all α-hydroxyketone functional groups pointing away from the macrocycle cavity (left). A side view showing the twisted orientation of the benzene rings on the opposite sides of the square tetramer (right). Thermal ellipsoids shown at 50% probability. Element colors: C—gray, O—red, H—white.

right), as they define a 40.8 ° angle with the benzene ring on the opposite side. From this perspective, it is also visible that the four α-hydroxyketone functionalities point away from the central cavity, a feature that plays a crucial role in the crystal packing of **129** (vide infra, Figure 4.4). The molecule is not strained, as all carbon atoms in **129** have bonding angles within ±2° of their idealized geometries.

The crystal packing diagram of **129** is shown in Figure 4.4. In the solid state, the key intermolecular interaction is a bifurcating hydrogen bond established between the

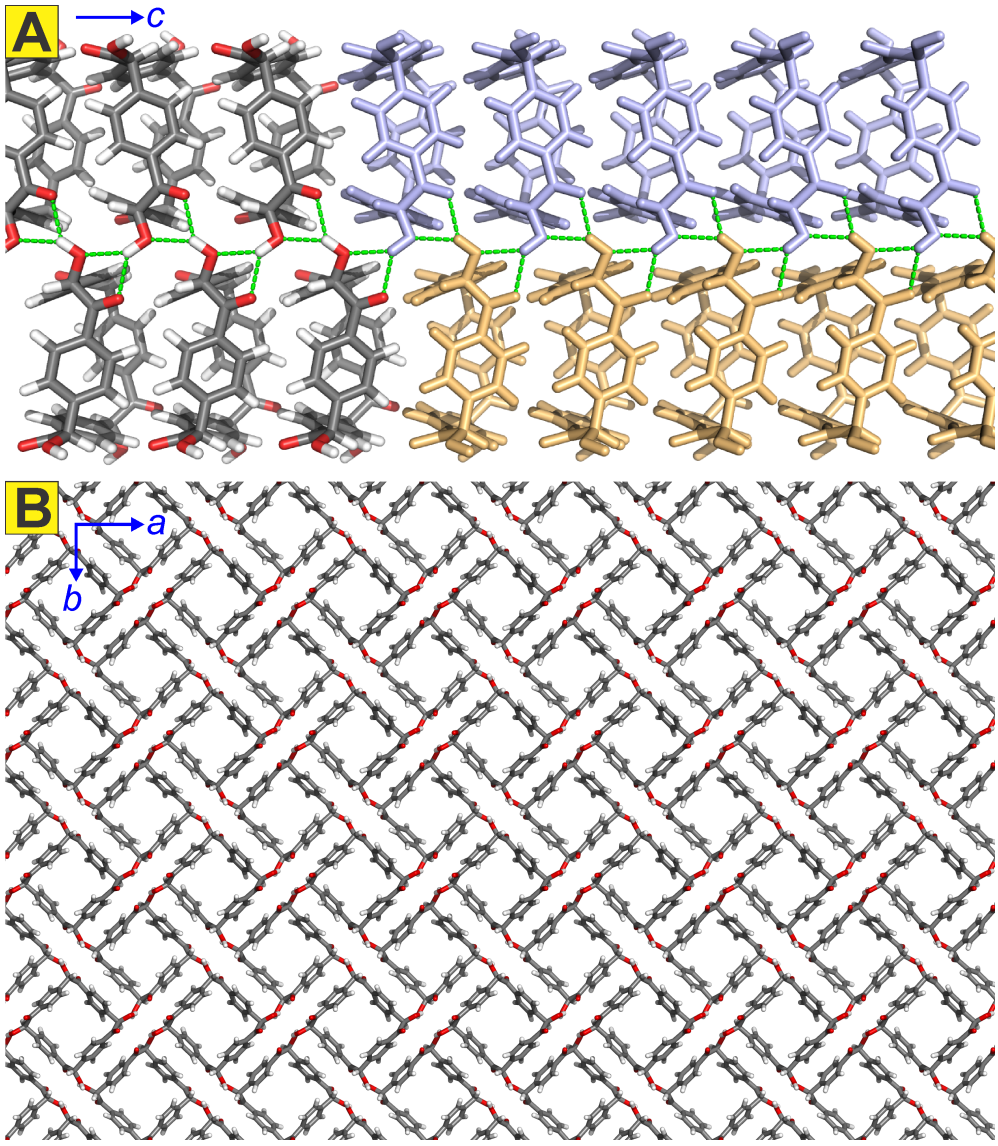

Figure 4.4 Crystal packing of **129**. **A**: Two parallel columns of molecules of **129** establish an infinite tape of hydrogen bonds, highlighted in green. Molecules on the left are colored by element, those on the right are colored to highlight separate nanotubes. **B**: Segment of the extended crystal structure of **129**, viewed along the crystallographic *c* axis. This view of the structure shows the arrays of hydrogen bonded nanotubes, and the intrinsic pores of **129**. Element colors: C—gray, O—red, H—white.

benzoin O–**H** hydrogen and oxygens from both the carbonyl (C=**O**; O···H distance 2.11 Å)[17] and hydroxyl groups (**O**–H; O···H distance 2.16 Å) in the neighboring molecule of **129**. Each macrocycle acts as both a hydrogen bond donor and acceptor, resulting in an infinite "tape" of hydrogen bonds along the crystallographic *c* axis (highlighted in green in Figure 4.4A). This relationship is repeated four times on all four sides of the macrocycle. When viewed along the crystallographic *c* axis, this arrangement results in a remarkably ordered square grid (Figure 4.4B), wherein individual molecules of **129** are stacked perfectly on top of each other, resulting in square-shaped nanotubes. These nanotubes are then bundled through hydrogen bonds established between edge benzoin functionalities. Notably, the strong [O–H···O] hydrogen bonds are established between molecules from adjacent nanotubes. Molecules within each individual nanotube engage in comparatively weaker [C–H···O] interactions between the benzoin carbonyl group (C=O) oxygen atoms and hydrogen atoms from the aromatic ring as well as the α-protons of benzoin functionality (with H···O distances between 2.40 and 3.00 Å). Single crystal X-ray diffraction also determined that no solvent molecules were present in the cavity.

The extended structure of **129** (Figure 4.4B) is unique and important from several viewpoints. First, it is a rare example of an intrinsically porous organic molecule, organized into a crystal structure with 10% void volume.[18] Secondly, its highly polar outside groups and nonpolar internal cavities could serve as interesting platforms for transport of species through crystals and membranes. Third, its infinitely hydrogen-bonded nanotubular subunits may play a role in the development of novel ferroelectric materials.[19] Finally, it is aesthetically pleasing, as its square-grid structure resembles that

of a well-planned city—in fact, it superimposes remarkably well onto the satellite image of Eixample, a district of Barcelona known for its visionary urban plan designed by Ildefons Cerdà (Figure 4.5).[20,21]

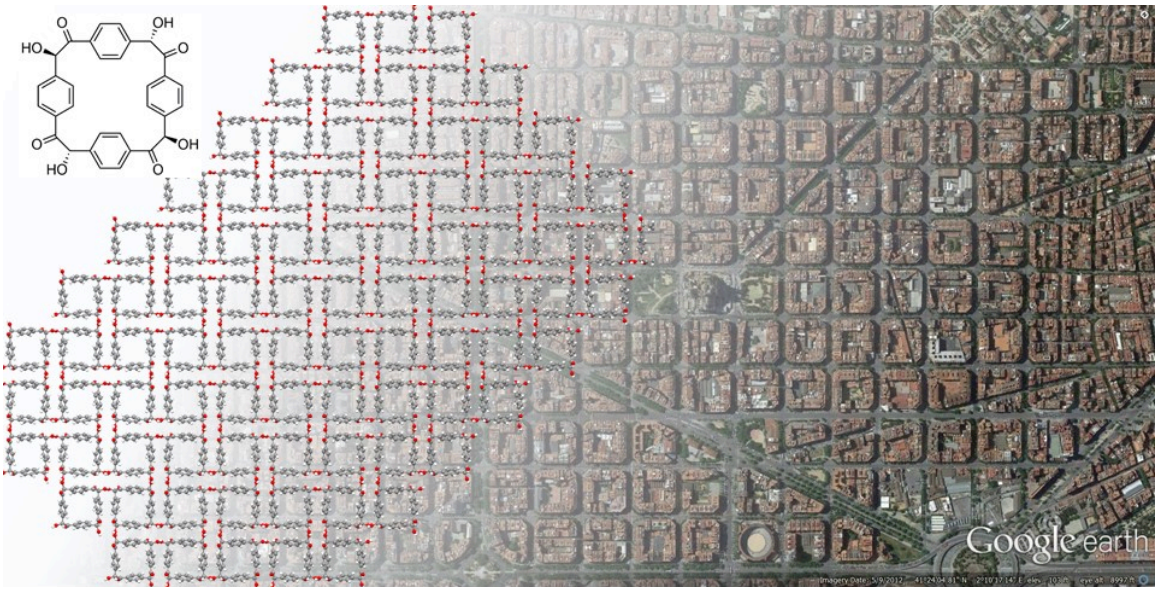

Figure 4.5 The crystal structure packing of compound **129** superimposes the satellite image of Eixample.

Macrocycle **129** is microcrystalline after recrystallization; the powder X-ray diffraction (PXRD) pattern of the as-synthesized **129** (Figure 4.7, bottom) is in excellent agreement with the PXRD pattern simulated from the single crystal X-ray data (Figure 4.7, top).

4.2.4 Thermogravimetric Analysis of Compound 129

The thermal stability of compound **129** was evaluated using thermogravimetric analysis (TGA) under N_2, with a heating rate of 2 °C min^{-1}. The TGA trace (Figure 4.6) shows no weight loss until approx. 250 °C. Between 250 and 320 °C, a small (<4%) weight loss is observed; this is followed by a rapid loss of approx. 14% of the original weight in the 320–360 °C range, and a relatively featureless TGA trace above 360 °C, likely indicative of full decomposition. As it is synthesized under aqueous conditions, cyclotetrabenzoin is obviously also stable to water.[22]

4.2.5 Gas Adsorption Analysis of Compound 129

Gas sorption of **129** was probed using N_2 as the guest (degassing conditions: 160 ºC, 15 h, under 10 μmHg). Based on the isotherm (Figure 4.8), the Brunauer-Emmett-Teller (BET) and Langmuir surface areas of **129** were determined to be 42 and 52 m^2g^{-1}, respectively. The isotherm can be categorized as a hybrid between type I isotherm—characteristic for microporous systems, and a small contribution from type II isotherm.[6m,23]

4.3 Conclusions and Outlook

In conclusion, cyclotribenzoin and cyclotetrabenzoin may be progenitors for an entire class of easily synthesized, shape-persistent, intrinsically porous all-organic

macrocycles. Its extensively oxygenated rim allows the molecule to engage in strong hydrogen bonds, which on one hand plays a role in its assembly in the solid state, and on the other could be utilized to bind discrete molecular guests. While cyclotetrabenzoin's surface area is small, its chemical and thermal stability are superior to the previously reported intrinsically porous organic cages based on imine, boronate esters, and boroxine functional groups. Our present focus is on building an isoreticular series of analogs of **127** and **129** by switching the central *p*-phenylene motif of terephthaldehyde for longer biphenylene- or triphenylene-based precursors. Results of these studies will be reported in due course.

4.4 Experimental Section

4.4.1 General Methods

NMR spectra were obtained on JEOL ECX-400, ECA-500, and ECA 600 spectrometers, with working frequencies (for ^{1}H and ^{13}C nuclei) of 400, 500, and 600 MHz, respectively. ^{1}H and ^{13}C NMR chemical shifts are reported in ppm units relative to the residual signals of the solvents (^{1}H: $CDCl_3$, 7.26 ppm and DMSO-d_6, 2.50 ppm; ^{13}C: DMSO-d_6, 39.5 ppm). All NMR spectra were recorded at 25 °C. Infrared spectra were recorded on a Perkin-Elmer Spectrum 100 FT-IR spectrophotometer using Pike MIRacle Micrometer pressure clamp. UV-Vis spectra were recorded on a Perkin-Elmer Lambda 25 UV-Vis spectrophotometer. TGA were carried out on a TA Instruments TGA 2050

thermogravimetric analyzer at a temperature ramping rate of 2 °C/min under the flow of N_2 gas. PXRD data were collected at 25 °C on a Phillips X'pert Pro diffractometer. Single crystal XRD measurement was performed on a Bruker DUO platform diffractometer equipped with a 4K CCD APEX II detector and an Incoatec 30 Watt Cu microsource with compact multilayer optics (Compound **127**). Single crystal XRD data was collected at ChemMatCARS beamline at Advanced Photon Source in Argonne National Laboratory (Compound **129**). Simulated PXRD patterns were calculated with the Mercury software employing the structure model from the single crystal data obtained.

4.4.2 Synthesis of Compound 127, 128, and 129

*4.4.2.1 Synthesis of Compound **127***

Isophthaldehyde (**125**, 684 mg, 5.10 mmol), EtOH (5 mL), and deionized H_2O (5 mL) were added to a round bottom flask equipped with a stirring bar, and the mixture was heated at reflux under nitrogen until all of **125** dissolved. At that time, NaCN (25 mg, 0.51 mmol) was added into the round bottom flask, and continued heating for 48 h. The precipitate obtained was filtered and then washed with deionized H_2O (10 mL), EtOH (10 mL), and Et_2O (10 mL). After recrystallization from 2-methoxyethanol, pure **127** was obtained (280 mg, 41%) as a white solid. Mp 245 °C (decomposition). UV/Vis (THF): λ_{max} (log ε) = 248 (4.29), 288 (3.46) nm. IR (neat): 3456 (w, $\tilde{\upsilon}_{O-H}$), 3070 (w, $\tilde{\upsilon}_{C-H}$), 2925 (w, $\tilde{\upsilon}_{C-H}$), 1682 (s, $\tilde{\upsilon}_{C=O}$), 1583 (s), 1432 (s), 1395 (s), 1274 (m), 1182 (m), 1083 (m), 796

(s), 743 (s), 692 (s) cm^{-1}. ^{1}H NMR (DMSO-d_6, 400 MHz): δ 8.78 (s, 3H), 7.63 (d, $^{3}J_{H–H}$ = 7.8 Hz, 3H), 7.45 (d, $^{3}J_{H–H}$ = 7.8 Hz, 3H), 7.35 (dd, $^{3}J_{H–H}$ = 7.8 and 7.3 Hz, 3H), 6.42 (d, $^{3}J_{H–H}$ = 5.5 Hz, 3H), 6.01 (d, $^{3}J_{H–H}$ = 5.5 Hz, 3H) ppm. ^{13}C NMR (DMSO-d_6, 100 MHz): δ 198.4, 140.8, 134.9, 132.4, 130.2, 130.0, 128.2, 74.7 ppm. LRMS (ESI/$[M–H]^–$): calcd for $C_{24}H_{18}O_6$ 401.11, found 401.13.

Single crystal growth method: crude product (10 mg) was dissolved in THF (10 mL) under heating. The resulting solution was cooled to 20 °C and filtered. The filtrate was added to five small vials (size: 0.8 mL) in different volumes from 0.1 to 0.5 mL separately. These vials were then placed inside a larger scintillation vial (size: 20 mL) containing $CHCl_3$ (4 mL) as the diffusing solvent. The vial was closed and kept at 20 °C for seven days, Colorless crystals were obtained.

*4.4.2.2 Synthesis of Compound **128***

Compound **127** (128 mg, 0.32 mmol), imidazole (1.30 g, 19.1 mmol), and dry CH_2Cl_2 (15 mL) were added to a thick-walled 20 mL microwave vial. The mixture was stirred under nitrogen for 10 min. The reagent *t*-butyldimethylsilyl chloride (2.90 g, 19.1 mmol) was then added to the mixture. The vial was sealed, and then placed into a Biotage microwave reactor, where it was heated for 10 h at 40 °C. The reaction mixture was diluted with $CHCl_3$ (50 mL), washed with H_2O (50 mL), and the organic layer was separated and dried over anhydrous $MgSO_4$. After removal of solvent, the crude product

was isolated as light yellow oil. Pure compound **128** was obtained after recrystallization from pentane at −78 °C (142 mg, 60%). Mp 167 °C. UV–Vis (THF): λ_{max} (log ε) = 286 (3.61), 326 (3.18) nm. IR (neat): 3070 (w, $\tilde{\upsilon}_{C-H}$), 2929 (w, $\tilde{\upsilon}_{C-H}$), 1713 (s, $\tilde{\upsilon}_{C=O}$), 1674 (s), 1581 (s), 1471 (s), 1362 (s), 1257 (m), 1120 (m), 1028 (m), 862 (m), 781 (s), 735 (s), 698 (s) cm^{-1}. ^1H NMR ($CDCl_3$, 500 MHz): δ 7.88 (s, 3H), 7.72 (d, $^3J_{H-H}$ = 8.0 Hz, 3H), 7.73 (d, $^3J_{H-H}$ = 7.6 Hz, 3H), 7.33 (dd, $^3J_{H-H}$ = 8.0 and 7.4 Hz, 3H), 5.82 (s, 3H), 0.87 (s, 27H), 0.09 (s, 9H), 0.08 (s, 9H). ^{13}C NMR ($CDCl_3$, 125 MHz): δ 198.3, 139.2, 135.7, 131.6, 129.5, 128.9, 127.0, 79.4, 25.9, 18.5, −4.6, −4.7. LRMS (ESI/[M+Na^+]): calcd for $C_{42}H_{60}O_6Si_3$ 767.36, found 767.38, and (ESI/[2M+Na^+]): calcd 1511.73, found 1511.09.

*4.4.2.3 Synthesis of Compound **129***

Terephthaldehyde (**126**, 6.80 g, 50.0 mmol), 2-methoxyethanol (150 mL), and deionized H_2O (150 mL) were added to the 500 mL round bottom flask equipped with a stirring bar, and the mixture was heated under nitrogen until all **126** dissolved. At that point, NaCN (253 mg, 5.00 mmol) was added into the round bottom flask, and the heating was continued for 48 h. The obtained precipitate was subjected to a hot filtration and then washed with deionized H_2O (200 mL), MeOH (200 mL), and Et_2O (200 mL). After dried in *vacuo*, crude product (2.70 g, 40%) was obtained. Recrystallization from DMSO and hot MeOH, pure **129** was obtained (1.40 g, 21%) as an off-white solid. Mp 299–300 °C (decomposition); ^1H NMR ([D]$_6$DMSO, 600.2 MHz): δ = 7.83 (d, J = 8.4 Hz, 2H), 7.34 (d, J = 8.4 Hz, 2H), 6.22 (d, J = 5.4 Hz, 2H), 5.91 ppm (d, J = 4.8 Hz, 2H); ^{13}C NMR ([D]$_6$DMSO, 125.8 MHz): δ = 197.40, 144.59, 132.95, 129.44, 127.12, 76.36 ppm;

UV–Vis (DMSO): λ_{max} (log ε) = 261 (4.68), 318 (3.28) nm; FTIR (KBr pellet): $\tilde{\nu}$ = 3456 (s, br), 3057 (w), 2937 (w), 1930 (w), 1807 (w), 1679 (s), 1606 (s), 1413 (m), 1255 (s), 1188 (m), 1122 (m), 1095 (s), 1018 (w), 981 (s), 841 (s), 818 (s), 744 (s), 704 (s) cm^{-1}; CI–HRMS: *m/z* calcd for $C_{32}H_{24}O_8$: 536.1471; found $[M + H]^+$: 537.1548.

Recrystallization method: crude product (2.70 g) was added DMSO (400 mL); the mixture was stirred under N_2 at 50 °C for 12 h. The resulting solution was filtered and transferred to a 1 L round bottom flask; boiling MeOH (500 mL) was then carefully layered on top of the mother solution. After it was cooled to 20 °C, the round bottom flask was sealed with septa and filled with N_2. After 7 days, the precipitates were filtered and washed with MeOH (100 mL) and ether (100 mL).

Single crystal growth method: crude product (40 mg) was dissolved in DMSO (20 mL) under heating. The resulting solution was cooled to 20 °C and filtered. The filtrate was added to five small vials (size: 0.8 mL) in different volumes from 0.1 to 0.5 mL separately. These vials were then placed inside a larger scintillation vial (size: 20 mL) containing MeOH (4 mL) as the diffusing solvent. The vial was closed and kept at 20 °C for two weeks, Colorless needle shaped crystals were obtained.

4.4.3 Thermogravimetric Analysis of Compound 129

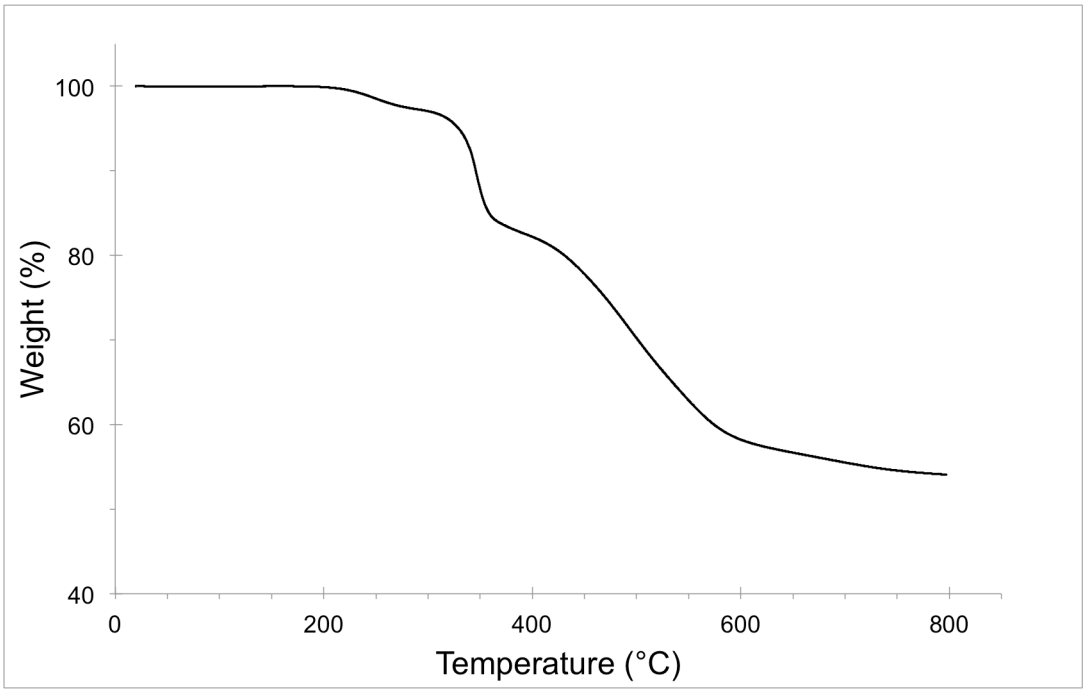

Figure 4.6 TGA of compound **129**.

4.4.4 Powder X-Ray Diffraction Patterns of Compound 129

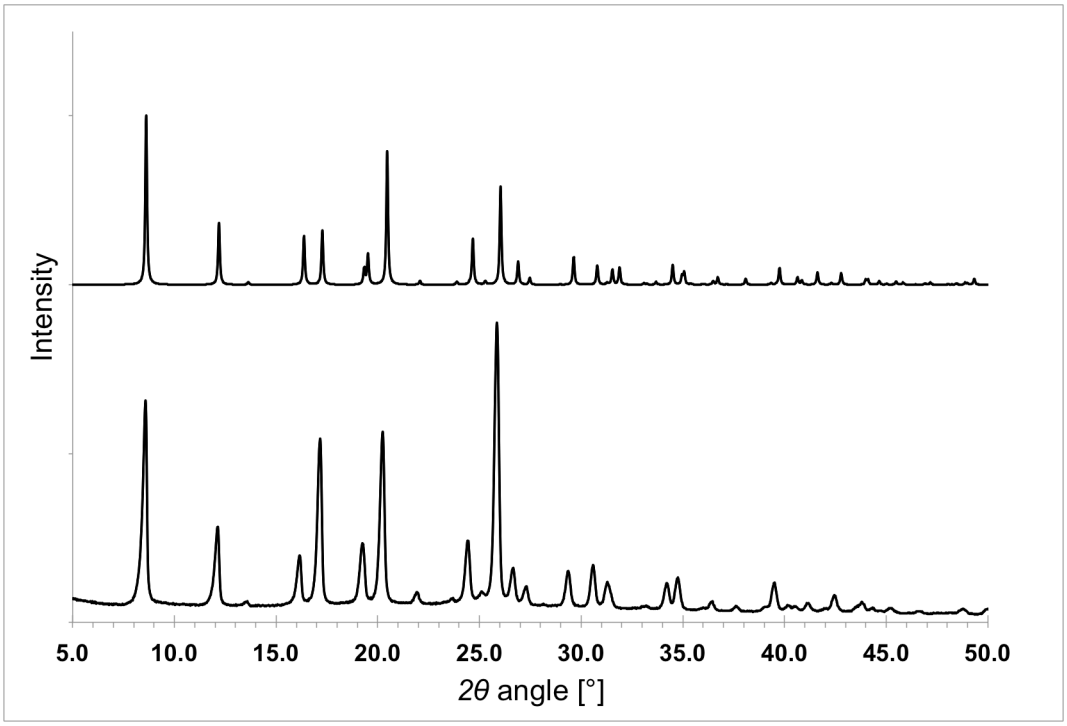

Figure 4.7 Comparison of PXRD patterns of compound **129**: simulated from single-crystal X-ray data (top) and measured from a freshly recrystallized sample of **126** (bottom).

4.4.5 Gas Adsorption Isotherm of Compound 129

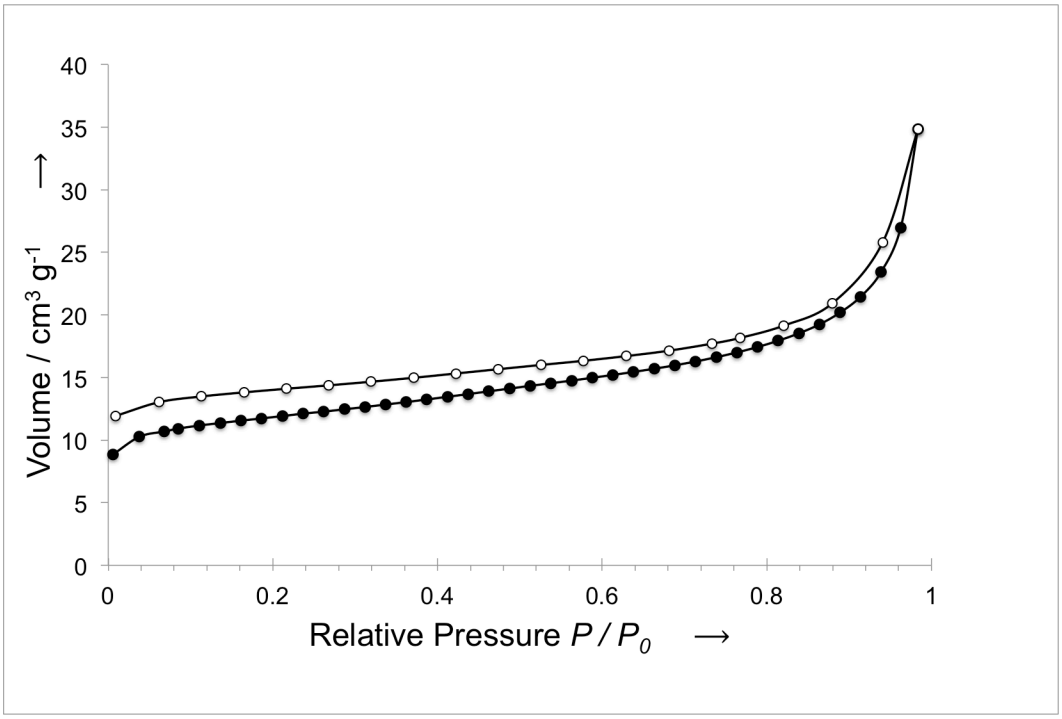

Figure 4.8 Adsorption (●) and desorption (○) of N_2 gas within the pores of **129**, measured at 77 K.

4.4.6 Crystal Data for Compound 127

Table 4.1 Crystallographic Data of Compound **127**.

Empirical formula	$C_{28.32}H_{26.64}O_{7.08}$
Formula weight	480.26
Temperature	123(2) K
Wavelength	0.71073 Å

Crystal system	Hexagonal
Space group	$R3$
Unit cell dimensions	a = 14.650(2) Å α = 90°
	b = 14.650(2) Å β = 90°
	c = 9.2986(16) Å γ = 120°
Volume	1728.3(5) Å^3
Z	3
Density (calculated)	1.384 Mg/m^3
Absorption coefficient	0.099 mm^{-1}
F(000)	760
Crystal size	0.28×0.25×0.24 mm^3
θ range for data collection	2.72° to 30.50°
Index ranges	$-20 \leq h \leq 20$, $-19 \leq k \leq 20$, $-12 \leq l \leq 12$
Reflections (collected)	7063
Reflections (unique)	2262 [R(int) = 0.0162]
Completeness to θ = 30.50	98.6 %
Absorption correction	Empirical
Max. and min. transmission	0.9765 and 0.9727
Refinement method	Full-matrix least-squares on F^2
Data / restraints / parameters	2262 / 7 / 117
Goodness-of-fit on F^2	1.034
Final R indices [$I > 2\sigma(I)$]	R_1 = 0.0500, wR_2 = 0.1411

R indices (all data)	$R_1 = 0.0503$, w$R_2 = 0.1415$
Largest diff. peak and hole	0.605 and -0.276 e / Å^3

4.4.7 Crystal Data for Compound 129

Table 4.2 Crystallographic Data of Compound **129**.

Empirical formula	$C_{32}H_{24}O_8$	
Formula weight	536.51	
Temperature	100(2) K	
Wavelength	0.40651 Å	
Crystal system	Tetragonal	
Space group	$P\bar{4}2_1c$	
Unit cell dimensions	a = 14.507(3) Å	$\alpha = 90°$
	b = 14.507(3) Å	$\beta = 90°$
	c = 5.8300(10) Å	$\gamma = 90°$
Volume	1226.9(5) Å^3	
Z	2	
Density (calculated)	1.452 Mg/m^3	
Absorption coefficient	0.046 mm^{-1}	
F(000)	560	
Crystal size	0.10×0.01×0.01 mm^3	

θ range for data collection	1.795° to 17.318°
Index ranges	$-21 \leq h \leq 21, -21 \leq k \leq 21, -8 \leq l \leq 8$
Reflections collected	24222
Independent reflections	2018 [R(int) = 0.1760]
Completeness to θ = 14.117°	98.2 %
Absorption correction	None
Refinement method	Full-matrix least-squares on F^2
Data / restraints / parameters	2018 / 0 / 94
Goodness-of-fit on F^2	1.051
Final R indices [$I > 2\sigma(I)$]	R_1 = 0.0562, wR_2 = 0.1162
R indices (all data)	R_1 = 0.0908, wR_2 = 0.1308
Absolute structure parameter	0.4(10)
Extinction coefficient	N/A
Largest diff. peak and hole	0.280 and -0.211 e / Å^3

4.5 References

[1] (a) Ji, Q.; Loi, H. D.; Miljanić, O. Š. *Synlett*, **2015**, *26*, 1625–1627. (b) Ji, Q.; Le, H. T. M.; Wang, X.; Chen, Y.-S.; Makarenko, T.; Jacobson A. J.; Miljanić, O. Š. **2015**, submitted.

[2] *Macrocycles: Construction, Chemistry and Nanotechnology Applications*; Davis, F.; Higson, S.; Wiley: Chichester, **2011**.

[3] (a) Eickmeier, C.; Junga, H.; Matzger, A. J.; Scherhag, F.; Shim, M.; Vollhardt, K. P. C. *Angew. Chem., Int. Ed. Engl.* **1997**, *36*, 2103–2108. (b) Diederich, F.; Staab, H. A. *Angew. Chem., Int. Ed. Engl.* **1978**, *17*, 372–374. (c) Ajami, D.; Oeckler, O.; Simon, A.; Herges, R. *Nature* **2003**, *426*, 819–821.

[4] (a) Venkataramen, D.; Lee, S.; Zhang, J.; Moore, J. S. *Nature* **1994**, *371*, 591–593. (b) Li, Q.; Zhang, W.; Miljanić, O. Š.; Sue, C.-H.; Zhao, Y.-L.; Liu, L.; Knobler, C. B.; Stoddart, J. F.; Yaghi, O. M. *Science* **2009**, *325*, 855–859. (c) Chen, T.-H.; Popov, I.; Chuang, Y.-C.; Chen, Y.-S.; Miljanić, O. Š. *Chem. Commun.* **2015**, *51*, 6340–6342.

[5] For reviews, see: (a) Zhang, W.; Moore, J. S. *Angew. Chem. Int. Ed.* **2006**, *45*, 4416–4439. (b) MacLachlan, M. J. *Pure Appl. Chem.* **2006**, *78*, 873–888. (c) S. Hoger, *Chem. Eur. J.* **2004**, *10*, 1320–1329. (d) Zhao, D.; Moore, J. S. *Chem. Commun.* **2003**, 807–818. (e) Moore, J. S. *Acc. Chem. Res.* **1997**, *30*, 402–413. (f) Smith, M. K.; Miljanić, O. Š. *Org. Biomol. Chem.* **2015**, *13*, 7841–7845.

[6] For reviews, see: (a) Zhang, G.; Mastalerz, M. *Chem. Soc. Rev.* **2014,** *43,* 1934–1947. (b) Mastalerz, M. *Synlett* **2013***, 24,* 781–786. (c) Mastalerz, M. *Angew. Chem. Int. Ed.* **2010**, *49*, 5042–5053. For notable examples, see: (d) Chen, T.-H.;

Popov, I.; Chuang, Y.-C.; Chen, Y.-S.; Miljanić, O. Š. *Chem. Commun*. **2015,** *51*, 6340–6342. (e) Yang, H.; Du, Y.; Wan, S.; Trahan, G. D.; Jin, Y.; Zhang, W. *Chem. Sci.* **2015**, *6*, 4049–4053. (f) Zhang, G.; Presly, O.; White, F.; Oppel, I. M.; Mastalerz, M. *Angew. Chem. Int. Ed.* **2014**, *53*, 5126–5130. (g) Zhang, G.; Presly, O.; White, F.; Oppel, I. M.; Mastalerz, M. *Angew. Chem. Int. Ed.* **2014,** *53,* 1516–1520. (h) Elbert, S. M.; Rominger, F.; Mastalerz, M. *Chem. Eur. J.* **2014**, *20*, 16707–16720. (i) Mitra, T.; Jelfs, K. E.; Schmidtmann, M.; Ahmed, A.; Chong, S. Y.; Adams, D. J.; Cooper, A. I. *Nature Chem.* **2013,** *5,* 276–281. (j) Schneider, M. W.; Hauswald, H.-J. S.; Stoll, R.; Mastalerz, M. *Chem. Commun.* **2012**, *48*, 9861–9863. (k) Schneider, M. W.; Oppel, I. M.; Mastalerz, M. *Chem. Eur. J.* **2012**, *18*, 4156–4160. (l) Jones, J. T. A.; Hasell, T.; Wu, X.; Bacsa, J.; Jelfs, K. E.; Schmidtmann, M.; Chong, S. Y.; Adams, D. J.; Trewin, A.; Schiffmann, F.; Cora, F.; Slater, B.; Steiner, A.; Day, G. M.; Cooper, A. I. *Nature* **2011**, *474*, 367–371. (m) Mastalerz, M.; Schneider, M. W.; Oppel, I. M.; Presly, O. *Angew. Chem. Int. Ed.* **2011**, *50*, 1046–1051. (n) Jiang, S.; Jones, J. T. A.; Hasell, T.; Blythe, C. E.; Adams, D. J.; Trewin, A.; Cooper, A. I. *Nature Commun.* **2011**, *2*, doi:10.1038/ncomms1207; (o) Mastalerz, M. *Chem. Commun.* **2008**, 4756–4758. (p) Venkataraman, D.; Lee, S.; Zhang, J. S.; Moore, J. S. *Nature,* **1994,** *371,* 591–593. See also: (q) Finke, A. D.; Gross, D. E.; Han, A.; Moore, J. S. *J. Am. Chem. Soc.* **2011,** *133,* 14063–14070.

[7] (a) Tahara, K.; Gotoda, J.; Carroll, C. N.; Hirose, K.; De Feyter, S.; Tobe, Y. *Chem. Eur. J.* **2015**, *21*, 6806–6816. (b) Tahara, K.; Inukai, K.; Adisoejoso, J.; Yamaga, H.; Balandina, T.; Blunt, M. O.; De Feyter, S.; Tobe, Y. *Angew. Chem. Int. Ed.* **2013**, *52*, 8373–8376. (c) Tahara, K.; Yamaga, H.; Ghijsens, E.; Inukai, K.; Adisoejoso, J.; Blunt, M. O.; De Feyter, S.; Tobe, Y. *Nature Chem.* **2011**, *3*, 714–719. (d) Chen, T.; Pan, G.-B.; Wettach, H.; Fritzsche, M.; Höger, S.; Wan, L.-J.; Yang, H.-B.; Northrop, B. H.; Stang, P. J. *J. Am. Chem. Soc.* **2010**, *132*, 1328–1333. (e) Adisoejoso, J.; Tahara, K.; Okuhata, S.; Lei, S.; Tobe, Y.; De Feyter, S. *Angew. Chem. Int. Ed.* **2009**, *48*, 7353–7357. (f) Lei, S.; Tahara, K.; De Schryver, F. C.; Van der Auweraer, M.; Tobe, Y.; De Feyter, S. *Angew. Chem. Int. Ed.* **2008**, *47*, 2964–2968. (g) Tahara, K.; Lei, S.; Mamdouh, W.; Yamaguchi, Y.; Ichikawa, T.; Uji-I, H.; Sonoda, M.; Hirose, K.; De Schryver, F. C.; De Feyter, S.; Tobe, Y. *J. Am. Chem. Soc.* **2008**, *130*, 6666–6667. (h) Höger, S.; Bonrad, K.; Mourran, A.; Beginn, U.; Möller, M. *J. Am. Chem. Soc.* **2001**, *123*, 5651–5659. (i) Mena-Osteritz, E.; Bäuerle, P. *Adv. Mater.* **2001***, 13*, 243–246.

[8] (a) Zang, L.; Che, Y.; Moore, J. S. *Acc. Chem. Res.* **2008**, *41*, 1596–1608. (b) Balakrishnan, K.; Datar, A.; Zhang, W.; Yang, X.; Naddo, T.; Huang, J.; Zuo, J.; Yen, M.; Moore, J. S.; Zang, L. *J. Am. Chem. Soc.* **2006**, *128*, 6576–6577. (c) Hui, J. K.-H.; Frischmann, P. D.; Tso, C.-H.; Michal, C. A.; MacLachlan, M. J. *Chem. Eur. J.* **2010**, *16*, 2453–2460. (d) Gallant, A. J.; MacLachlan, M. J. *Angew. Chem. Int. Ed.* **2003**, *42*, 5307–5310.

[9] (a) Crini, G. *Chem. Rev.* **2014**, *114*, 10940–10975. (b) del Valle, E. M. M. *Process Biochem.* **2004**, *39*, 1033–1046.

[10] (a) Lee, J. W.; Samal, S.; Selvapalam, N.; Kim, H.-J.; Kim, K. *Acc. Chem. Res.* **2003**, *36*, 621–630. (b) Masson, E.; Ling, X.; Joseph, R.; Kyeremeh-Mensah, L.; Lu, X. *RSC Adv.* **2012**, *2*, 1213–1247.

[11] (a) Xue, M.; Yong, Y.; Chi, X.; Zhang, Z.; Huang, F. *Acc. Chem. Res.* **2012**, *45*, 1294–1308. (b) Ogoshi, T.; Kanai, S.; Fujinami, S.; Yamagishi, T.-a.; Nakamoto, Y. *J. Am. Chem. Soc.* **2008**, *130*, 5022–5023.

[12] (a) Reek, J. N. H.; Otto, S. *Dynamic Combinatorial Chemistry*, Wiley-VCH, Weinheim, **2010**. (b) Corbett, P. T.; Leclaire, J.; Vial, L.; West, K. R.; Wietor, J.-L.; Sanders, J. K. M.; Otto, S. *Chem. Rev.* **2006**, *106*, 3652–3711. (c) Rowan, S. J.; Cantrill, S. J.; Cousins, G. R. L.; Sanders, J. K. M.; Stoddart, J. F. *Angew. Chem. Int. Ed.* **2002**, *41*, 898–952.

[13] (a) Wang, Q.; Yu, C.; Long, H.; Du, Y.; Jin, Y.; Zhang, W. *Angew. Chem. Int. Ed.* **2015**, *54*, 7550–7554. (b) Wang, Q.; Zhang, C.; Noll, B. C.; Long, H.; Jin, Y.; Zhang, W. *Angew. Chem. Int. Ed.* **2014**, *53*, 10663–10667. (c) Zhang, C.; Wang, Q.; Long, H.; Zhang, W.; *J. Am. Chem. Soc.* **2011**, *133*, 20995–21001. (d) Zhang, W.; Moore, J. S. *J. Am. Chem. Soc.* **2004**, *126*, 12796. (e) Jin, Y.; Wang, Q.; Taynton, P.; Zhang, W. *Acc. Chem. Res.* **2014**, *47*, 1575–1586.

[14] (a) Ono, K.; Johmoto, K.; Yasuda, N.; Uekusa, H.; Fujii, S.; Kiguchi, M.; Iwasawa, N. *J. Am. Chem. Soc.* **2015**, *137*, 7015–7018. (b) Chen, T.-H.; Kaveevivitchai, W.; Bui, N.; Miljanić, O. Š. *Chem. Commun.* **2012**, *48*, 2855–2857.

[15] Crystallographic information file (CIF) for compound **3** has been deposited with Cambridge Structural Database under deposition code CCDC 1055400.

[16] Hua, Y.; Flood, A. H. *Chem. Soc. Rev.* **2010**, *39*, 1262–1271, and the references therein.

[17] All O–H bond lengths have been normalized to neutron-diffraction determined internuclear distance of 0.993 Å. See: Steiner, T. *Angew. Chem. Int. Ed.* **2002**, *41*, 48–76.

[18] PLATON (C) 1980−2011 A. L. Spek, Utrecht University, Padualaan 8, 3584 CH, Utrecht, The Netherlands.

[19] Tayi, A. S.; Kaeser, A.; Matsumoto, M.; Aida, T.; Stupp, S. *Nature Chem.* **2015**, *7*, 281–294.

[20] Ramoneda, J. *Cerdà and the Barcelona of the Future: Reality versus Project*. CCCB: Barcelona, 2009.

[21] Satellite image of Eixample district of Barcelona was obtained using Google Earth, © Google Inc.

[22] For hydrolytically stable cages obtained by reduction of imine-based cages, see: (a) Liu, M.; Little, M. A.; Jelfs, K. E.; Jones, J. T. A.; Schmidtmann, M.; Chong, S. Y.; Hasell, T.; Cooper, A. I. *J. Am. Chem. Soc.* **2014**, *136*, 7583–7586; (b) Jin, Y.; Voss, B. A.; Noble, R. D.; Zhang, W. *Angew. Chem. Int. Ed.* **2010**, *49*, 6348–6351.

[23] Sing, K. S. W.; Everett, D. H.; Haul, R. A. W.; Moscou, L.; Pierotti, R. A.; Rouquérol, J.; Siemieniewska, T. *Pure Appl. Chem.* **1985,** *57,* 603–619.